2010

Identifying historic storm surges and calculating storm surge return periods for the Gulf of Mexico coast

Hal Needham
Louisiana State University and Agricultural and Mechanical College, hneedh1@lsu.edu

IDENTIFYING HISTORIC STORM SURGES AND CALCULATING STORM SURGE RETURN PERIODS FOR THE GULF OF MEXICO COAST

A Thesis

Submitted to the Graduate Faculty of the
Louisiana State University and
Agricultural and Mechanical College
in partial fulfillment of the
requirements for the degree of
Master of Science

in

The Department of Geography and Anthropology

by
Hal Needham
B.S., Pennsylvania State University, 1997
May 2010

ACKNOWLEDGEMENTS

I thank God for giving me the opportunity to study at LSU, as well as perseverance in this research. I also thank my wonderful wife, Kari, for her support and encouragement throughout this process, especially when I felt discouraged. I thank my parents and sister for their interest in my research and encouragement to pursue grad school. I am also thankful for our family in Louisiana, who were supportive and helpful throughout this season of life.

I am also grateful for each member of my faculty committee. I am thankful for Dr. Keim, who took a chance on me when I walked into his office very late in the application period. This work would not have been possible apart from his involvement and guidance throughout this entire process. I am thankful for Dr. Brown's words of encouragement and research perspective when I needed advice. And I am grateful, as well, for the advice provided by Dr. Elsner, especially regarding the correlation tests.

It has also been a joy to work alongside the faculty, staff and students involved in climate research at LSU. I do not have enough room to thank everyone directly, but I especially remember all the help I received from David S. and Ricardo N. when I was technologically deficient!

I would also like to thank the kind people along the Gulf Coast with whom I interacted during this research. May this work help save lives and protect properties in your lovely communities.

TABLE OF CONTENTS

LIST OF TABLES

LIST OF FIGURES

ABSTRACT

Tropical cyclone-generated storm surges inflict natural disasters that are among the most catastrophic globally. The surges observed along the U.S. Gulf of Mexico are among the highest in the world, second only to the Bay of Bengal. Storm surge activity along the U.S. Gulf Coast remains poorly understood, however, in part, due to the absence of credible research that accurately depicts the maximum height and location of historic surge events. This research addresses this gap in the scientific literature by creating a database of storm surge observations along the Gulf Coast between the years 1880 to 2009. A total of 53 sources were utilized to construct this database, including 21 government documents, 16 books and online publications, and more than 3,000 pages of newspaper from 16 daily periodicals. The database identifies 193 surge events ≥ 1.22 meters, nine of which exceed five meters. Hurricane Katrina is the largest magnitude event in the dataset, at 8.47 meters. Spatial analysis reveals enhanced surge activity along the central and western Gulf Coast, as well as the Florida Keys. Time series analyses reveal surge frequencies and magnitudes generally coincide with Atlantic Multidecadal Oscillation phases. This research also tested the correlation between surge activity and four climate teleconnections- the Southern Oscillation Index (SOI), North Atlantic Oscillation (NAO), Atlantic Multidecadal Oscillation (AMO), and solar activity. The SOI correlated the highest, followed by the NAO. Return periods associated with extreme surge levels were calculated using four quantile estimation methods- the Gumbel and Beta-P distribution methods, and the Huff-Angel and Southern Regional Climate Center (SRCC) linear regression methods. The SRCC method produced the line of best fit, estimating a 100-year basin-wide surge level of 8.1 meters, and a 2-year basin-wide return period of 2.75 meters.

CHAPTER 1. A REVIEW OF GLOBAL TROPICAL CYCLONE-GENERATED STORM SURGE CLIMATOLOGY: PROCESSES, OBSERVATIONS AND IMPACTS

1.1 Introduction

Tropical cyclone-generated storm surges create natural disasters that are among the most deadly and costly global catastrophes. Individual disasters have inflicted hundreds of thousands of fatalities (Frank and Husain 1971; Dube et al. 1997) and billions of dollars in damage (McTaggart-Cowan 2008). Unfortunately, scholarly literature is bereft of a climatological and geographical summary of this hazard. However, a global overview of maximum water levels and fatality totals in historic surge events would be valuable to people living in high risk areas, as well as to professionals in the fields of emergency management and law enforcement, insurance, construction, urban planning, health care, science and engineering. This paper addresses this void in the literature by discussing the physical processes that generate storm surges, while providing an overview of maximum global surge observations and societal impacts.

1.2 Physical Processes that Generate Storm Surge

A storm surge is defined as an increased sea-level height in association with the approach of an intense cyclone. Persistent onshore winds, in conjunction with reduced air pressure, force water levels to rise, especially in shallow water of impacted coasts. Although tropical or extratropical cyclones can theoretically produce storm surges in any ocean basin, tropical cyclones produce the most destructive surges in terms of extreme water-level heights and human impacts.

An understanding of tropical cyclone-generated storm surge climatology requires a brief examination of the physical processes that shape tropical cyclone development.

These parameters include sea surface temperatures exceeding 26 degrees C (Ali 1996; Holland 1997; Gray 1998), proximity to the Intertropical Convergence Zone (ITCZ), or regional manifestation of this global band of low pressure, such as the South Pacific Convergence Zone (SPCZ) (De Scally 2008), which is necessary to provide the atmospheric lift for cyclonic development (Ali 1996; Dube et al. 1997; De Scally 2008), and a Coriolis parameter that is sufficient to generate the dynamic potential of an area of convection (Gray 1998). Because the Coriolis parameter is a function of latitude, with higher values found at higher latitudes, tropical cyclone development is generally suppressed near the Equator, so tropical cyclones are usually generated between 5 - 25 degrees latitude on either side of the Equator (Gray 1975). Although the Coriolis parameter is more favorable for cyclonic development in higher latitudes, cooler ocean waters and detachment from the ITCZ in latitudes poleward of approximately 25 degrees latitude suppress the development of tropical cyclones. Figure 1.1 shows the most favorable regions for tropical cyclogenesis, and the average annual number of tropical cyclones observed in each ocean basin (Landsea 2007).

Once a tropical cyclone has developed, atmospheric circulation will usually steer the cyclone from the point of origin, sometimes transporting the disturbance thousands of kilometers. The atmospheric circulation of the specific ocean basin will govern the exact path of the storm. Typical circulation patterns exist for each basin, depending on several physical factors. For example, the clockwise circulation around the Bermuda and Hawaiian Highs, dominant mid-oceanic features in the North Atlantic and North Pacific

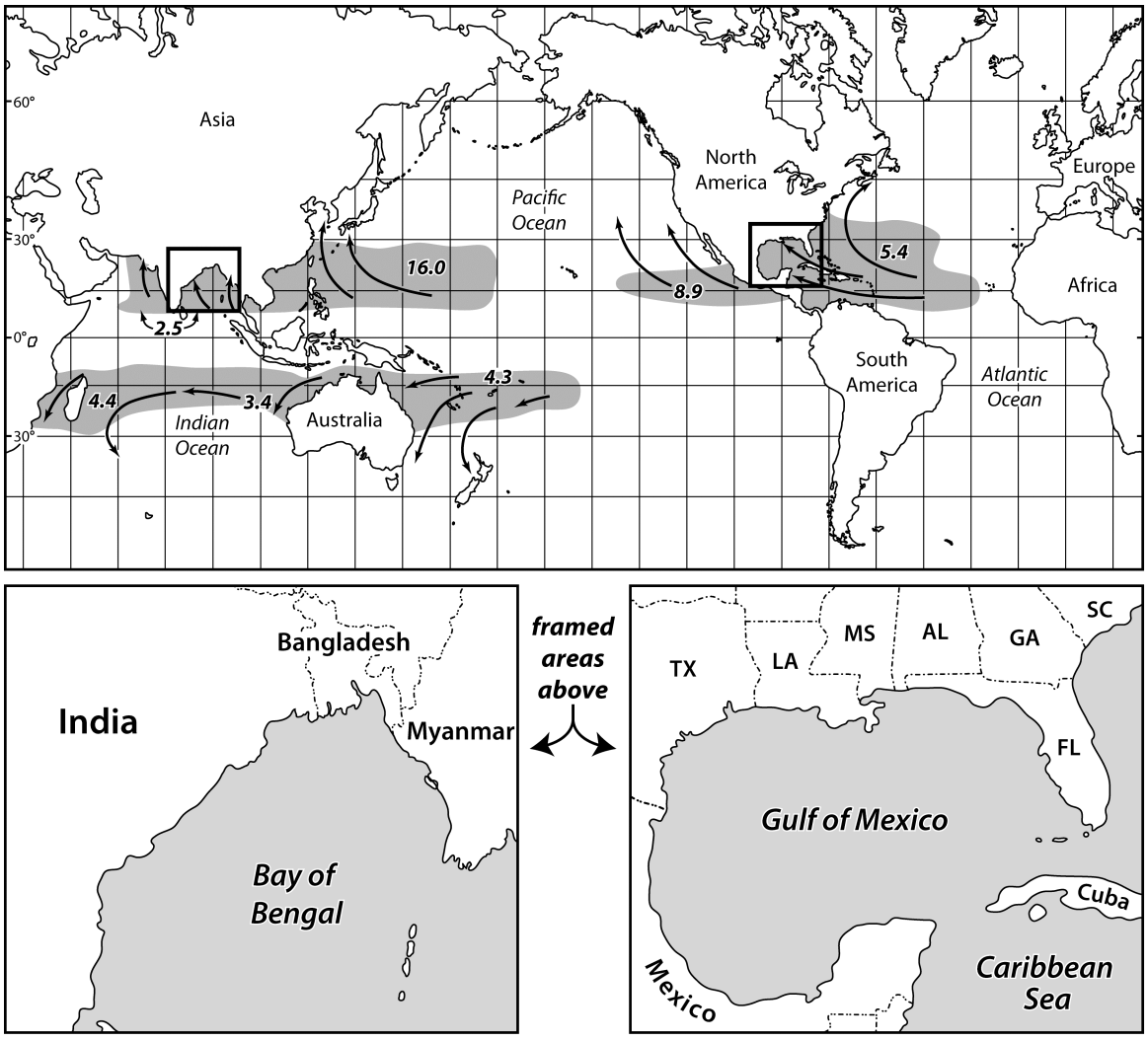

Figure 1.1: Shaded areas depict regions of frequent tropical cyclone development, arrows indicate common tropical cyclone tracks, and numeric values indicate the average annual number of tropical cyclones/ hurricanes (sustained winds of greater than 33 m/s) that develop in each ocean basin. Numeric data is taken from Landsea (2007).

Oceans, respectively, typically produce easterly trade winds between 10 and 25 degrees latitude, the region of highest tropical cyclogenesis. This typical circulation pattern causes most tropical cyclones in these basins to initially travel westward in the easterly trade winds, before making a northerly turn as they approach North America or East Asia. Figure 1.2 depicts a map of 270 August tropical cyclone tracks in the north Atlantic from 1886 – 2006.

Spatial patterns of tropical cyclone landfalls develop as the processes of tropical cyclone development and movement are considered within the context of physical geography. Exposed islands, peninsulas and capes often experience the highest landfall frequencies. Coasts that curve in a convex manner, such as the North Carolina coast, along the eastern seaboard of the United States, protrude from the continent and experience higher frequencies of tropical cyclone strikes than concave-bending coasts, such as the Georgia coast, 650 kilometers to the southwest (Keim et al. 2007).

As tropical cyclones approach a coastline, several additional factors determine the characteristics, and essentially the climatology, of the resultant storm surges. These factors include maximum sustained cyclonic winds, minimum central pressure, cyclonic size, forward movement and angle of approach to the coast, shape and bathymetry of the coastline, and presence of obstructions to flowing water.

Wind stress is the predominant factor forcing storm surge heights. A quantitative relationship exists between wind speed and water heights, as wind stress exerts a force on water proportional to the square of the wind speed (Ali 1996). Kurian et al. (2009) state that wind stress accounts for 80-85% of the generated surge.

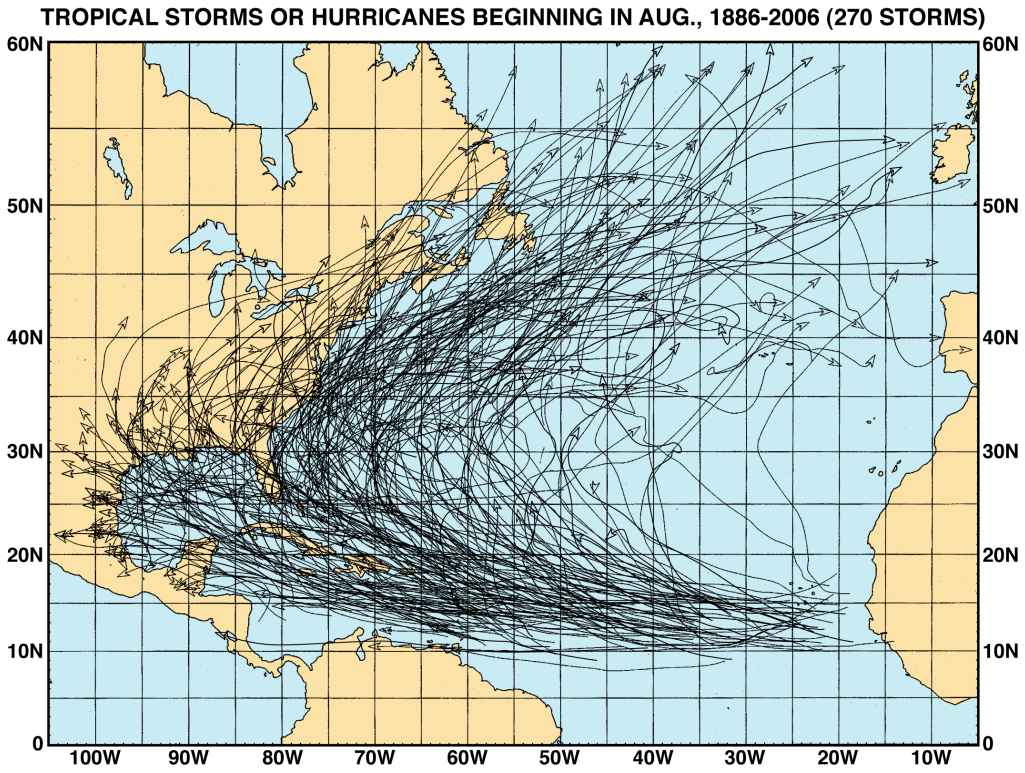

Figure 1.2: August tracks of North Atlantic Basin hurricanes, 1886-2006, from Keim and Muller (2008), adapted from Neumann et al. (1993).

Cyclonic size is an important factor that has been underestimated until recently, after very large hurricanes Katrina (2005) and Ike (2008) generated larger surges than anticipated (Irish et al. 2008). Storm size likely enabled Katrina, a category-3 storm on the Saffir-Simpson Scale at landfall, to generate significantly larger surge heights than category-5 Camille along the same coastline. Katrina's Category-5 winds, one day before landfall, enabled the storm to generate such a massive surge. It is believed that the massive size of Katrina then enabled it to maintain this enormous surge even as it weakened before striking the coastline. The relationship between storm size and surge levels has likely been underestimated because research conducted on storms from the 1950s through 1970s lacked examples of massive storms like Katrina (Irish et al. 2008).

Forward cyclonic movement is a factor which is often overlooked in surge research (Rego and Li 2009). Rego and Li (2009) resolved that faster moving cyclones generate higher peak surges, but produce less extensive inundation, than slower moving cyclones. Their model defined fast cyclones as those having a forward velocity of 5 to 12 m/s, while slow cyclones progressed at 2 to 3.5 m/s. Results indicated that faster moving cyclones increased peak surge heights by about 40%, while the additional flooded volume produced by slower moving cyclones varied by the equivalent of one category on the Saffir-Simpson scale.

Coastline shape and the presence of natural and artificial obstructions to flowing water, such as coastal forests and levees, have profound effects on storm surge, sometimes producing extreme localized water level differences (Jarvinen and Neumann 2005). The highest surges usually occur where water approaches the coast in a perpendicular direction, especially when funneled into inlets and bays. The Advanced

CIRCulation Model for Coastal Open Hydrodynamics (ADCIRC) of Hurricane Katrina's surge clearly depicts these localized differences along the Mississippi River south of New Orleans (Interagency Performance Evaluation Taskforce Report 2006). Levees along the river prohibited surge from flowing across the river from east to west, creating a surge more than three meters higher on the east side of the river than on the west, less than two kilometers away (Figure 1.3).

Shallow bathymetry enhances storm surge because deeper water currents cannot carry away excess water, and as a result, water accumulates in shallow areas (Rappaport 1995). Bays and gulfs, especially near large river deltas, therefore, generally experience larger surges than shorelines adjacent to open ocean or steeper continental shelves. For example, the extremely shallow waters near the mouth of the Mississippi River, created by extensive silt deposits, significantly enhance the surge levels of hurricanes that track near the delta. These shallow waters exacerbated the surges of Hurricanes Camille (1969) and Katrina (2005), helping these cyclones to generate the two largest storm surges in United States history. Both of these surges occurred at Pass Christian, Mississippi, on the eastern shore of Bay St. Louis. Chen et al. (2008) hypothesize that the shallow waters south of the Mississippi coast, produced by deltaic lobes from the Mississippi River, were the primary reason that the surge was extraordinarily high, and that the surge may have been four meters lower had Katrina tracked over a wide, sloping continental shelf, similar to the bathymetry south of Mobile Bay, Alabama (Figure 1.4).

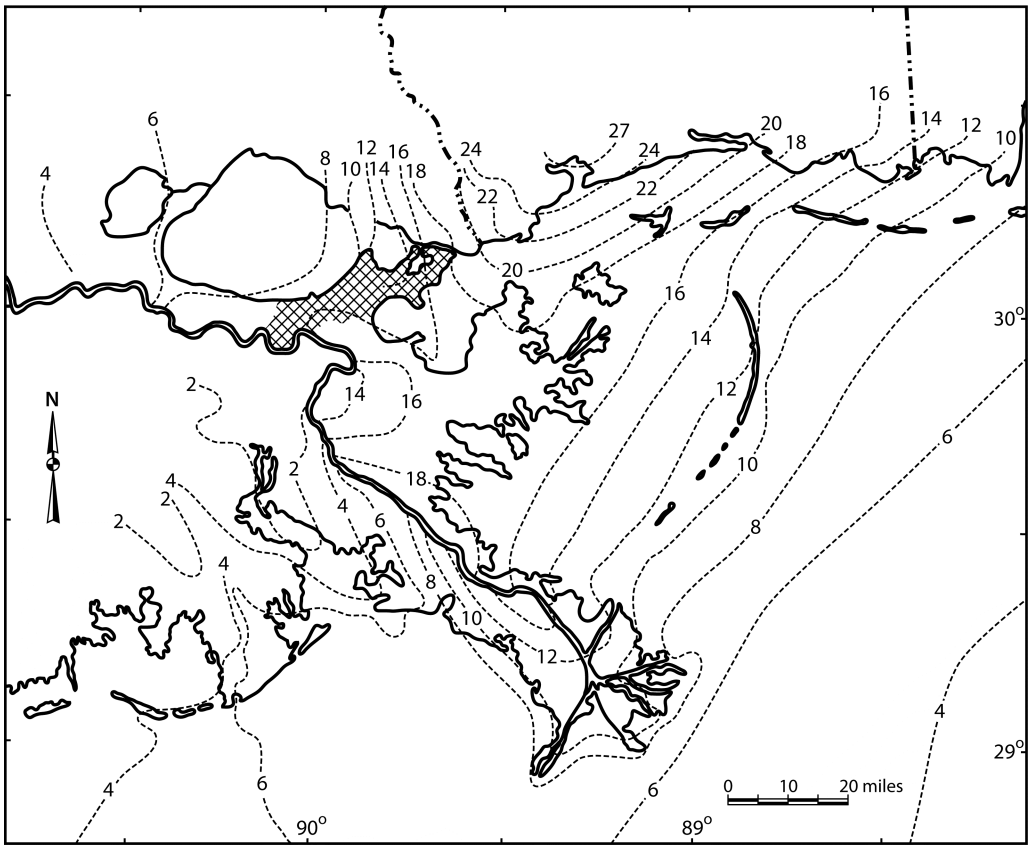

Figure 1.3: The Advanced CIRCulation Model for Coastal Open Hydrodynamics (ADCIRC) map of maximum storm surge generated by Hurricane Katrina along the Louisiana and Mississippi coasts in the Gulf of Mexico, from Keim and Muller (2009). Source: Interagency Performance Evaluation Taskforce (IPET) Report, 2006.

Notes: 1. Water levels in this figure are given in feet, NAVD88. 2. The ADCIRC surge model reveals dramatic localized difference in storm surge along the Mississippi River levee, south of New Orleans. Surge levels on the east side of the river are more than 9 feet higher than the west side of the river in some locations.

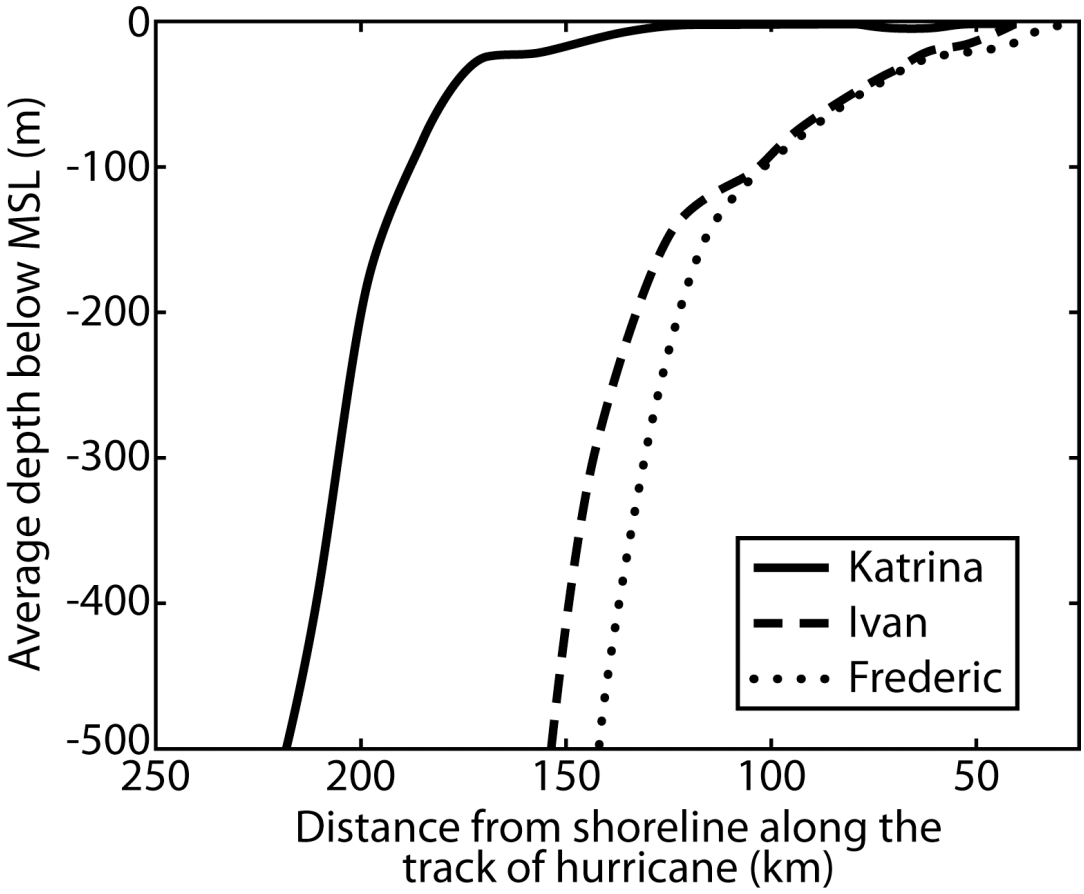

Figure 1.4: Average bathymetry, or water depth, located 90 km east of the tracks of Hurricanes Katrina, Ivan and Frederic in the Gulf of Mexico. The bottom profiles indicate that the onshore winds of Hurricane Katrina blew over much shallower water than Ivan and Frederic, as the storm approached shore. From Chen et al. (2008).

Tropical cyclone-generated storm surges sometimes inundate entire regions; widespread surge events can flood more than 1,000 kilometers of coastline (Berg 2009). Larger cyclones generally inundate more extensive areas than smaller cyclones with similar maximum wind velocities, while cyclones that track parallel or at an oblique angle to the coastline will usually flood longer stretches of shoreline than cyclones that make a perpendicular approach to the coast at landfall. The high water profiles depicted in Figures 1.5 and 1.6 reveal that Hurricane Ike inundated a much larger expanse of coastline than Hurricane Camille, even though Hurricane Ike made landfall as a Category-2 storm on the Saffir-Simpson Scale, compared with Camille's extraordinary Category-5 sustained winds and 190-mile-per-hour gusts (National Weather Bureau 1969) along the Mississippi coast. Ike's much larger geographic size and oblique path relative to the coastline enabled the cyclone to inundate a wider swath of the coast.

Generally, the portion of coastline that observes onshore winds will usually experience the greatest surge levels, with water heights increasing closer to the path of the cyclone. In contrast, the region that observes offshore winds will often experience much lower surge levels. In the northern hemisphere, onshore winds are observed to the right of the path of the cyclone, while offshore winds are experienced to the left (Figure 1.7).

In certain cases, offshore winds create negative surges, in which winds push enough water away from land that water levels fall below normal levels. This phenomenon is usually experienced when offshore winds are observed on the leeward side of a peninsula, island or isthmus. These geographic features experience the majority

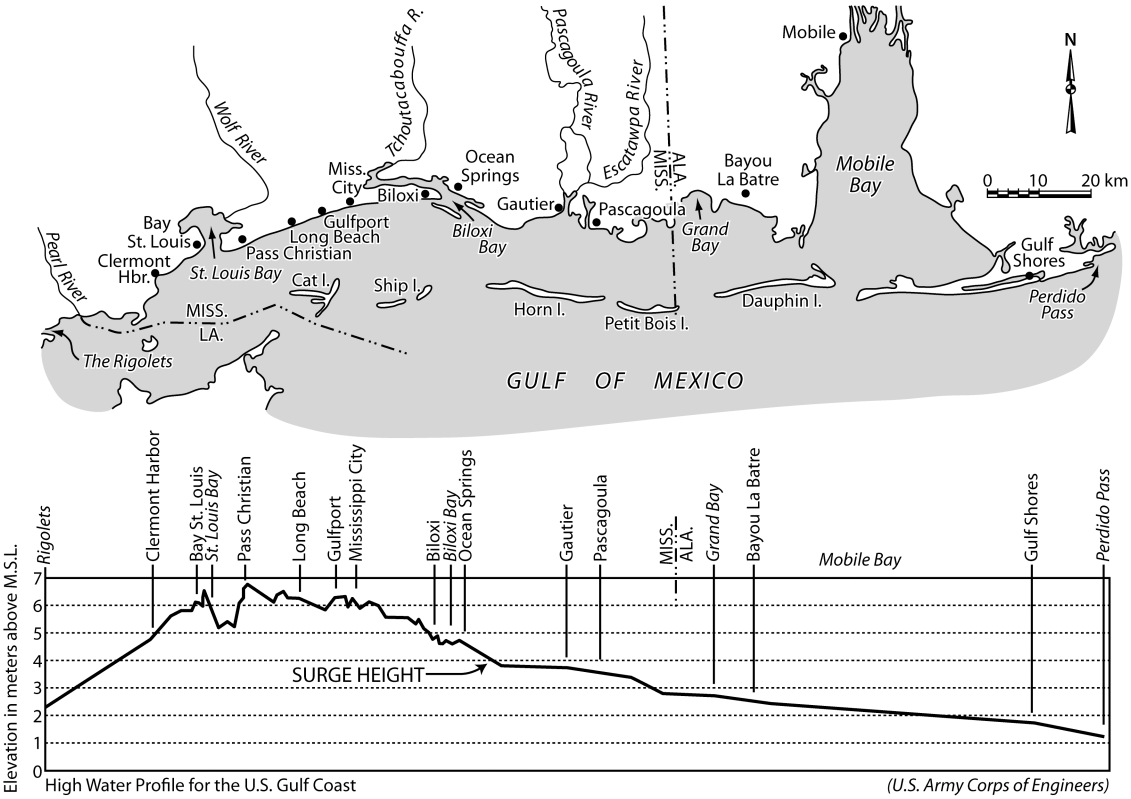

Figure 1.5: High water profile for Hurricane Camille in the northern Gulf of Mexico, from U.S. Army Corps of Engineers.

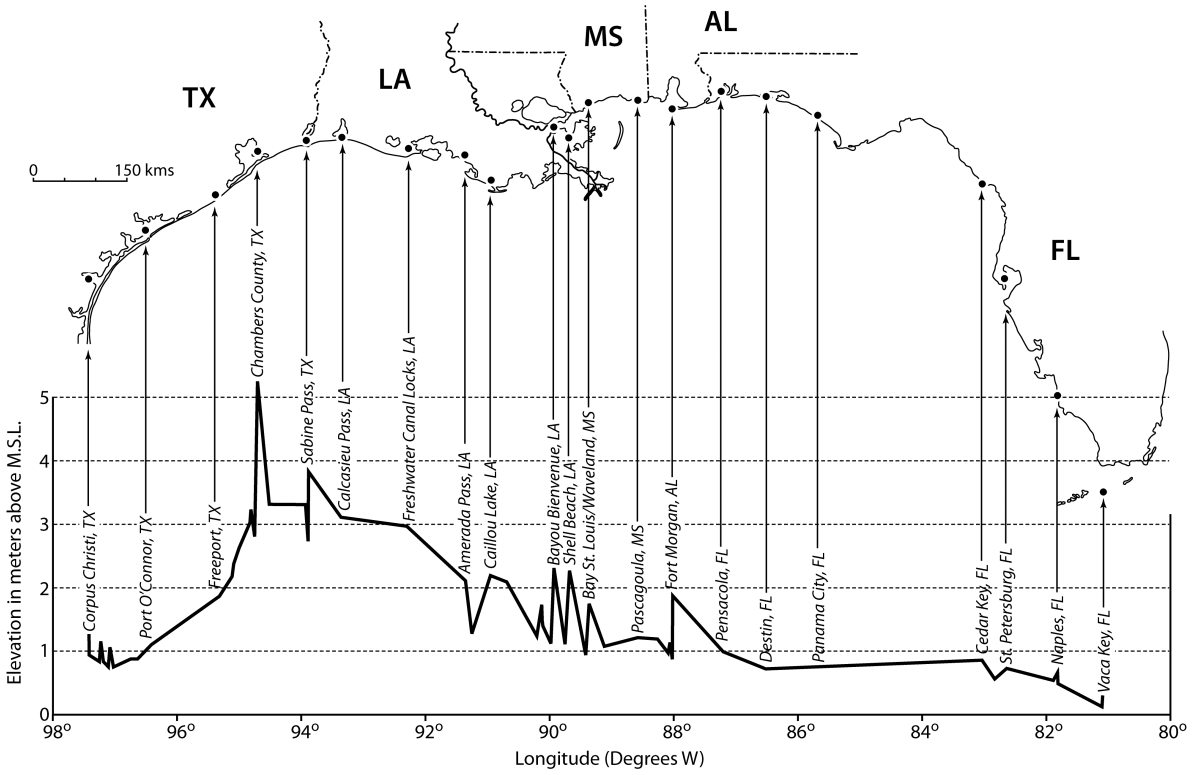

Figure 1.6: High water profile for Hurricane Ike in the Gulf of Mexico, created from selected storm surge observations provided by Berg (2009).

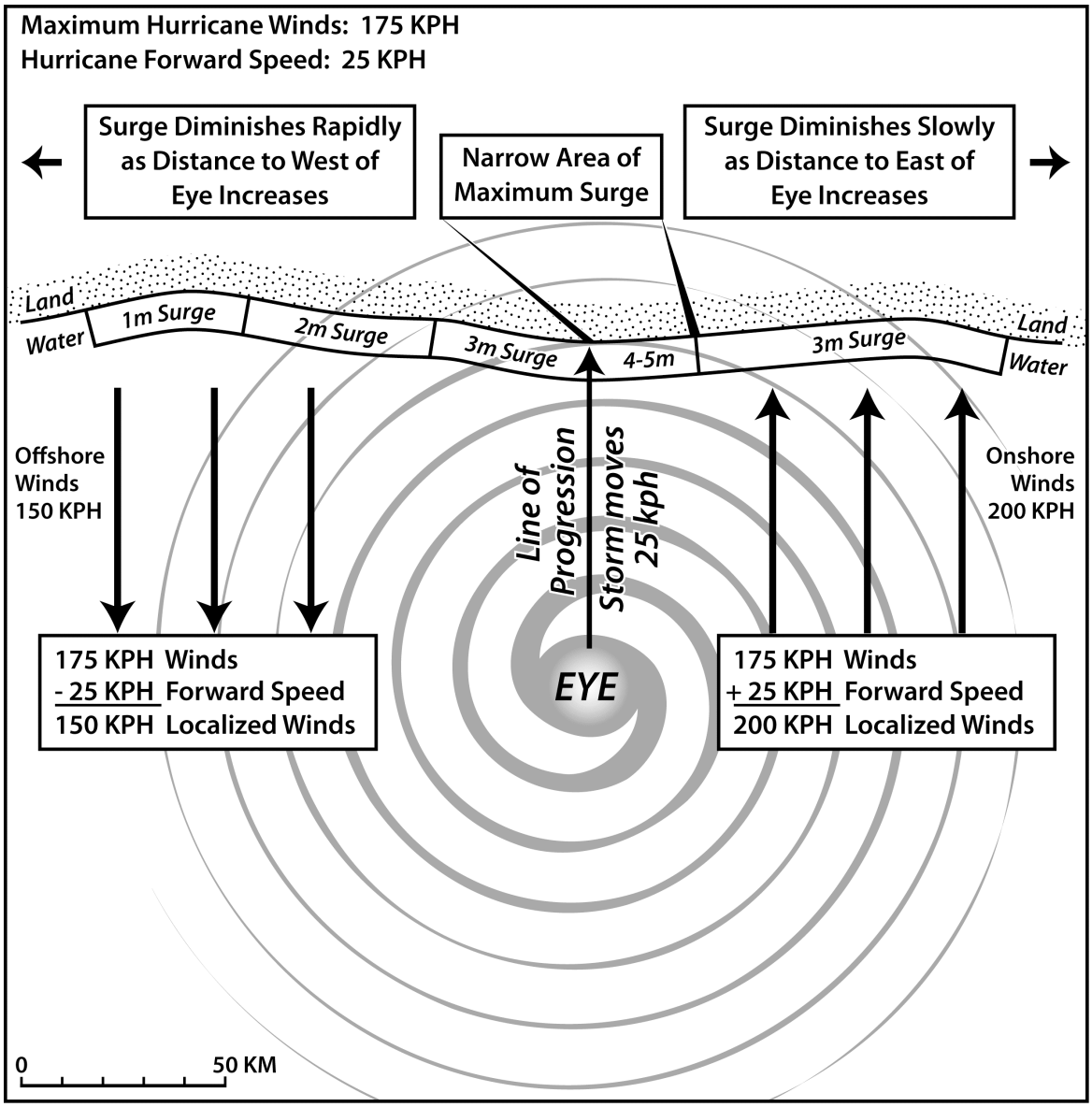

Figure 1.7: Generalized schematic of storm surge heights relative to position, path and wind speeds of a tropical cyclone.

of negative surges because they are wide enough to impede the surge that strikes the windward coastline, yet thin enough to not significantly weaken the cyclone. The west coast of Florida, for example, observes negative surges because cyclones commonly track from east to west across the peninsula, producing strong offshore winds to the north of the cyclonic path. Negative surges of minus 6.6 feet at Tampa in October 1910 (Cline 1926), minus 6.0 feet at Tampa in September 1926 (Harris 1963) and minus 4.5 feet at Cedar Key in September 2004 (Lawrence and Cobb 2005) are examples of this phenomenon. Sometimes positive surges immediately follow negative surges, such as the 3.5 foot positive surges that followed both the 1910 and 2004 negative surges at Tampa and Cedar Key, respectively (Cline 1926; Lawrence and Cobb 2005).Negative surges can damage property or infrastructure that is dependent upon the presence of water, such as marinas or industries that require water as a cooling agent. They can also endanger people, who are enticed by the novel opportunity to walk on the bed of a bay or river, unaware that a sudden change in wind direction could bury them under a torrent of rushing water. Bevan (2001, http://www.nhc.noaa.gov/2000keith.html), of the National Hurricane Center, reports that curious people did this very thing during Hurricane Keith (2000) in Belize:

"Tides of 4 ft below normal were noted on the Belize mainland coast while Keith was just offshore of the coastal islands. The National Hurricane Center also received reports that northerly winds associated with Keith had temporarily blown the water out of the Bay of Chetumal and people were walking on the exposed bay bottom. This was a potentially dangerous situation, as the water could have quickly returned had Keith moved and the winds shifted."

1.3 Surge Observations

The factors listed in the previous section produce a distinct geography of global tropical cyclogenesis. Annually, an average of 45 tropical cyclones producing maximum sustained winds of at least hurricane force, exceeding 33 m/s, develop globally (Landsea 2007) (Table 1.1). Considerable difference exists in the annual average number of these cyclones that develop in specific tropically-active ocean basins. The western North Pacific is the most prolific basin for development, producing an annual average of 16 tropical cyclones/ hurricanes (Figure 1.1). The North Atlantic Basin observes an annual average of 5.4, or about one-third as many as the western North Pacific Basin.

While a detailed analysis of tropical cyclone tracks and intensities is beyond the scope of this paper, some generalized descriptions will establish context for surge observations. In general, tropical cyclones develop between 5 and 25 degrees latitude north or south of the Equator. In the North Atlantic and North Pacific, these cyclones generally travel east-to-west before turning poleward, especially as they approach the shores of Asia or North America (Figures 1.1 and 1.2). This pattern is generally mirrored in the Southern Indian Ocean, as westward traveling cyclones often curve southwest or south before reaching Madagascar or southeast Africa. In the Northern Indian Ocean, tropical cyclones often travel north, northwest, or northeast. Various prevailing cyclone tracks occur near Australia and Oceania. Cyclones in the eastern North Pacific generally travel west or northwest, until the majority of these systems dissipate at sea, without ever making landfall. The most intense tropical cyclones have been observed in the western North Pacific, as observed in Typhoon Tip, which produced the lowest sea level pressure (870 mb) and largest circulation pattern on record (Dunnavan and Diercks 1980).

Table 1.1: Average annual number of tropical cyclones that develop in selected ocean basins, from Landsea (2007).

	Winds greater than 17 m/s (Tropical storm force winds)		Winds greater than 33 m/s (Hurricane/ Typhoon force winds)	
Basin	Average	Percentage	Average	Percentage
Atlantic	9.7	11.6	5.4	12.0
NW Pacific	25.7	30.7	16.0	35.6
N Indian	5.4	6.5	2.5	5.6
SW Indian	10.4	12.4	4.4	9.8
Aus SE Indian	6.9	8.2	3.4	7.6
Aus SW Pacific	9.0	10.8	4.3	9.6
Globally	83.7	100	44.9	100

Comparatively, Hurricane Wilma produced the lowest sea level pressure (882 hPa) in the Atlantic Basin in 2005 (McTaggart-Cowan et al. 2008). Although a relationship exists between observations of tropical cyclones and storm surges, geographical differences in these climatologies also exist. As such, we discuss storm surge observations for specific ocean basins, focusing on those basins that observe the greatest storm surge impacts: the Northern Indian Ocean, western North Atlantic, western North Pacific, and Australia and Oceania (Figure 1.1). Although the Southern Indian Ocean and Eastern Pacific Ocean also experience tropical cyclone-induced storm surges, these basins are excluded from detailed investigation, as the impacts in these regions are less pronounced.

1.3.1 Northern Indian Ocean

The greatest global storm surge levels occur in the northern Indian Ocean Basin, specifically along the shores of the Bay of Bengal in Bangladesh and India (Figure 1.1). Surge levels in the most catastrophic events range from 12 to 14 meters (Jakobsen et al. 2006). A maximum surge list for the Bay of Bengal, based on a partial list of storm surges in Bangladesh from 1876-1996, and India from 1737-1996 (Dube et al. 1997), as well as the inclusion of a 1999 surge event in India (De 2005), reveal that the greatest surges range from 7.6 meters to 13.7 meters (Table 1.2). Jakobsen et al. (2006) state that the 12.5 meter surge observed in 1876 at the Meghna Estuary was the greatest in the history of Bangladesh, and that a 10.6 meter surge in this location has a 100-year return period. The region experiences the greatest storm surges in either April-May or October-November, as tropical cyclones usually occur on either side of the summer monsoon season (Ali 1996; Jakobsen et al. 2006).

A comparison to extreme surge events in other ocean basins provides perspective on the extraordinary magnitude of these surge levels. For example, Hurricane Katrina's 8.47-meter storm surge (Knabb et al. 2006), which inundated portions of the Gulf of Mexico in the western North Atlantic, as it produced the largest documented storm surge outside the Bay of Bengal, would rank no higher than twelfth if placed in the Bay of Bengal. Perhaps even more impressive is the fact that in the past 50 years, Katrina's surge would place ninth in the Bay of Bengal, meaning eight surges higher than Katrina's have occurred in this time period, or about one event every six years.

Although these surge levels are tremendous by global comparison, even greater run-up levels in the northern Indian Ocean occurred during the 2004 Indian Ocean

Table 1.2: Highest Bay of Bengal storm surge levels, from Dube et al. (1997); De (2005).

Rank	Surge (meters)	Date(s)	Notes
1	13.7	Oct 27-Nov 1, 1876	Bangladesh
2	12.0	Oct 1737	India; 300,000 deaths
3	12.0	Oct 1864	India; 50,000 deaths
4	9.6	Sep-Oct 1, 1966	Bangladesh; 850 deaths
5	9.1	Oct 30-31, 1960	Bangladesh; 5,149 deaths
6	9.1	May 1963	Bangladesh; 11,520 deaths
7	9.1	Nov 13, 1970	Bangladesh; 300,000 deaths
8	9.1	Oct 1999	India; 9,885 deaths
9	8.8	May 6-9, 1961	Bangladesh; 11,466 deaths
10	8.8	May 27-30, 1961	Bangladesh
11	8.8	October 10-11, 1967	Bangladesh
12	8.2	April 19, 1991	Bangladesh; 140,000 deaths

Tsunami. A field report of flood observations from the Andaman and Nicobar Islands in the Northern Indian Ocean reveals a maximum run-up level of 17.26 meters at Little Andaman passenger jetty during this event (Cho et al. 2008). This is approximately 3.5 meters higher than the maximum tropical cyclone-generated storm surge event in this ocean basin, recorded in Bangladesh in 1876 (Table 1.2).

1.3.2 Gulf of Mexico

The Gulf of Mexico likely experiences the most catastrophic storm surges in the western North Atlantic Basin. The Mississippi River extends large deltaic lobes into this shallow basin that is susceptible to intense tropical cyclones, producing a similar setting to the Bay of Bengal. Maximum surges generally occur from July through October. The largest of these surges are between 6 and 9 meters, with Hurricane Katrina's 8.47-meter surge setting the modern-day record (Knabb et al. 2006).

Unfortunately, scholarly literature is void of surge rankings or statistics for the highest surge events in the Gulf of Mexico, such as a list of the highest surges or basin-wide return-period calculations of maximum water levels. As a result, we compiled the top 10 highest surges, which range from 4.88 to 8.47 meters (Table 1.3).

1.3.3 Western North Pacific

Although the western North Pacific Ocean experiences more intense typhoons than the other ocean basins, storm surge levels along the East Asian coast are moderate compared to other regions. The highest water levels in the greatest surge events along the coasts of Japan, China, Taiwan, and the Philippines range from 3 to 6 meters. The maximum surge observed on the coast of China was 5.94 meters, in the Guangdong province at the Nandu tide gage (Li et al. 2004). Although Typhoon Doug created

Table 1.3: Top 10 Gulf of Mexico tropical cyclone-induced surge levels, from 1880-2008. Compiled from the following sources: Garriott (1900), Cline (1915), McDonald (1935), Dunn et al. (1962), Sugg and Pelissier (1968), Simpson et al. (1970), Hebert (1976), National Weather Service (2003), Knabb et al. (2006), Keim and Muller (2009), Landsea et al. (2009), Berg (2009).

Rank	Surge (m)	Year	Storm Name	Maximum Surge Location
1	8.47	2005	Katrina	Pass Christian, Mississippi
2	7.50	1969	Camille	Pass Christian, Mississippi
3	6.10	1900	"Galveston"	Galveston, Texas
3	6.10	1935	"Labor Day"	Long Key, Florida
5	5.64	1961	Carla	Port Lavaca, Texas
6	5.55	1975	Eloise	Dune Allen Beach, Florida
7	5.49	1967	Beulah	South Padre Island, Texas
8	5.33	2008	Ike	Chambers County, Texas
9	5.18	1915	"New Orleans"	Southeastern Lousiana
10	4.88	1893	Cheniere Caminada	Cheniere Caminada, Louisiana
10	4.88	1919	Unnamed	Corpus Christi, Texas

widespread damage in Taiwan and generated 20-meter waves, the surge level of Lungtung Harbor was only about 3 meters (Wang et al. 2005). Likewise, the Isewan Typhoon that struck Nagoya Harbor in 1959, considered Japan's most disastrous storm surge (Makino 1992), generated a surge of slightly greater than 3 meters in the inner bays (Kawai 1999). Considering the great intensity of many of these typhoons, a possible explanation for the moderate surge levels is that deep coastal waters enable underwater currents to redistribute water, suppressing surge heights. Maximum surges generally occur from July through October.

1.3.4 Australia and Oceania

Storm surge poses a hazard to the eastern, northern, and western Australian coasts. The greatest surge heights range from 3 to 6 meters. A risk-modeling study conducted for Cairns, Australia, a coastal city vulnerable to tropical cyclones, considered the maximum probable surge to be approximately 6 meters (Zerger 2001), while a statistical study of storm surges in Hervey Bay calculated a 100-year return period of 3.11 meters (Ocean Hazards Assessment 2004). The account of a 13-meter surge generated by Typhoon Mahina in 1899, is likely distorted by misinformation or misunderstanding, perhaps due to the effects of wave run-up, as detailed geological investigation does not support such a tremendous surge event (Nott and Hayne 2000).

The islands of Oceania located farthest from the Equator experience more tropical cyclones and storm surges than those islands at lower latitudes (De Scally 2008). Storm surge observations in Oceania, however, are largely absent from scholarly literature. The relatively low, scattered population of this region may account for this absence of observations. In addition, some of the greatest surge events may have completely washed

over low-lying islands (Spennemann 1996; De Scally 2008), preventing the observation of high water marks. However, because this region lacks some of the important physical processes required to generate the largest surges, such as broad, shallow seas, it is logical that surges are smaller than in the other regions discussed. Even if the highest surges are only 2 to 4 meters, surges can completely wash over an inhabited island, as many Oceania residents live at an elevation of less than 2 meters above mean sea level (Spennemann 1996). Maximum surges generated by tropical cyclones in this region generally occur from January to March, a period of active tropical weather within the larger November- April Southern Hemisphere tropical cyclone season (De Scally 2008).

1.4 Surge Impacts

Storm surges are responsible for the highest number of fatalities in tropical cyclones globally (Ali 1996). The worst events are literally mega-catastrophes which claim hundreds of thousands of lives. In addition to casualties, surges destroy coastal infrastructure; large surges can completely scour Earth's surface, leaving nothing but debris and foundations of buildings. Salt-water intrusions from coastal flooding can dramatically change soil chemistry (Raja et al. 2009), devastating agriculture, as well as plant and animal habitats. Here, we provide an overview of these impacts by considering the effects of this hazard in the four ocean basins.

It should be noted that historical cyclone-induced fatality totals for each ocean basin do not necessarily depict the current vulnerability of these regions to this hazard. The development of technological innovations in the 20th and 21st centuries, such as wireless communications, radio, television, telephones, meteorological satellites, and, more recently, millions of personal computers networked through the World Wide Web,

have worked together to inform vulnerable coastal populations of impending disasters. Technical infrastructure has developed most rapidly in Australia, along the Gulf of Mexico, and in urban regions of East Asia. However, in certain regions, coastal population has dramatically increased during the past several decades, placing millions of additional lives at risk, and perhaps countering the benefits of technological innovations.

1.4.1 Northern Indian Ocean

Storm surge kills more people in the Northern Indian Ocean, specifically along the shores of the Bay of Bengal, than anywhere else in the world. Death tolls in the most traumatic events are staggering, claiming several hundred thousand lives in a single storm. Several factors lead to these catastrophes. Extremely large populations inhabit low-lying, water-bogged coastal zones, placing hundreds of thousands of people at risk. Because these people are among the world's poorest, many do not have the means to evacuate, while absence of technological infrastructure can keep storm warnings from reaching the masses. Bangladesh and India have experienced 15 of the 21 tropical cyclones that have generated 5,000 or more fatalities (Dube et al. 1997) (Table 1.4). From another viewpoint, 49% of the global tropical cyclone deaths in these storms occurred in Bangladesh and 22% in India (Frank and Husain 1971; Ali 1980; Ali 1996), meaning that 71% of these deaths occurred along this limited portion of coastline.

Frank and Husain (1971) and Dube et al. (1997) indicate that at least four cyclones since 1700 have claimed more than 100,000 lives in Bangladesh and India (Tables 1.4 and 1.5). The most disastrous of these events, the 1970 Bhola cyclone in Bangladesh and 1737 cyclone in India, both claimed approximately 300,000 lives, making these events

slightly more catastrophic than the 2004 tsunami, which killed nearly 228,000 people (USGS 2008).

1.4.2 Western North Atlantic

Although storm surge is the biggest killer in tropical cyclones globally, many of the highest fatality events in the Atlantic Basin are rain-induced disasters on steep terrain of the Caribbean and Central America. In 1998, for example, torrential rains from Hurricane Mitch killed more than 9,000 people in Honduras and Nicaragua (National Hurricane Center 1998). As the mountainous Greater and Lesser Antilles combine to experience about 50 percent of Atlantic basin hurricane casualties (Rappaport 1995) (Table 1.6), surely rainfall causes high numbers of cyclone fatalities in this basin.

In the United States, however, storm surges cause a substantial portion of hurricane-related deaths. The American Meteorological Society (1973) reported that coastal inundations cause 90% of hurricane fatalities. It is unclear, however, how this figure might have changed in recent decades, as improved forecasting, which has mollified the number of coastal fatalities, counters the coastal population explosion, which has nearly quadrupled the inhabitants of coastal counties and parishes along the Gulf of Mexico from 1950 to 2000 (Keim and Muller 2009) (Table 1.7).

The most disastrous surge events in the United States occur along the coast of the Gulf of Mexico. Some of the greatest fatality totals include the 1900 Galveston surge, which likely killed between 6,000 and 8,000 (Rappaport 1995); The “Cheniere Caminada” Hurricane of 1893, which killed around 2,000 people in coastal Louisiana (National Weather Service Lake Charles); and Hurricane Katrina, which caused 1833

Table 1.4: Deaths in tropical cyclones since 1700, from Dube et al. (1997).

Rank	Year	Countries	Deaths
1	1970	Bangladesh	300,000
1	1737	India	300,000
1	1886	China	300,000
4	1923	Japan	250,000
5	1876	Bangladesh	200,000
6	1897	Bangladesh	175,000
7	1991	Bangladesh	140,000
8	1833	India	50,000
8	1864	India	50,000
10	1822	Bangladesh	40,000
11	1780	Antilles (W. Indies)	22,000
12	1965	Bangladesh	19,279
13	1963	Bangladesh	11,520
14	1961	Bangladesh	11,466
15	1985	Bangladesh	11,069
16	1961	India	10,000
16	1977	India	10,000
18	1963	Cuba	7,196
19	1900	USA	6,000
20	1960	Bangladesh	5,149
21	1960	Japan	5,000
21	1973	India	5,000

Table 1.5: Deaths in tropical cyclones since 1700, from Frank and Husain (1971).

Rank	Year	Location	Deaths
1	1970	East Pakistan*	300,000
2	1737	India	300,000
3	1881	China	300,000
4	1923	Japan	250,000
5	1897	East Pakistan*	175,000
6	1876	East Pakistan*	100,000
7	1864	India	50,000
8	1833	India	50,000
9	1822	East Pakistan*	40,000
10	1780	Antilles	22,000
11	1839	India	20,000
12	1789	India	20,000
13	1965	East Pakistan*	19,279
14	1963	East Pakistan*	11,468
15	1963	Cuba-Haiti	7,196
16	1900	USA (Texas)	6,000
17	1960	East Pakistan*	5,149
18	1960	Japan	5,000

*Note: East Pakistan is now Bangladesh

Table 1.6: Atlantic Basin tropical cyclone fatalities by region, from Rappaport (1995).

Location	Fatalities	Percent of basin-wide deaths
Greater Antilles	45,000	29
Offshore Losses	35,000	22
Lesser Antilles	35,000	21
United States mainland (Galveston storm: 8,000)	25,000	16
Mexico and Central America	20,000	12
Elsewhere (Azores, Bahamas, Bermuda, Canada, Cape Verde Islands, South America, Ireland)	1,000	< 1

Table 1.7: Population statistics for the U.S. coastal counties and parishes along the Gulf of Mexico in 1900, 1950, and 2000, from Keim and Muller (2009).

State	No. of Counties	1900	1950	2000
Florida	23	175,000	841,000	4,916,000
Alabama	2	76,000	272,000	540,000
Mississippi	3	50,000	127,000	364,000
Louisiana	11	474,000	930,000	1,611,000
Texas	14	178,000	1581,000	5,006,000
Total	53	953,000	3,751,000	12,437,000

fatalities (McTaggart-Cowan 2008). It is widely known that drowning caused the majority of deaths in these storms. Storm surge is also responsible for increased destruction and damage to infrastructure, as the Gulf coast continues to develop. Hurricane Katrina was the costliest natural disaster in U.S. history, carrying a price tag of around $81 billion (McTaggart-Cowan 2008). Future U.S. surge events threaten costly infrastructure damage, as more than 60,000 miles of roads are located in the 100-year coastal floodplain (Chen 2007).

1.4.3 Western North Pacific

The most catastrophic storm surge events along the coast of East Asia have inflicted more fatalities than along the Gulf of Mexico, but less than along the Bay of Bengal. Although the highest storm surge levels in East Asia are lower than in the Gulf of Mexico, higher fatality totals in the most extreme events have probably occurred because the coasts of East Asia have been historically more densely populated. The most deadly tropical cyclones to impact coastal East Asia during the twentieth century both struck China, killing 50,000 people in 1912 and 60,000 people in 1922 (NOAA 1999). Coronas (1922, pg. 435) reports that, "This [The 1922 Swatow Typhoon] will go down to history as one of the worst, if not the worst typhoon, that has ever visited the Far East." Although an estimate of the proportion of deaths caused by storm surge in these events is not available, several sources provide evidence that the 1922 typhoon generated a storm surge that devastated the region around the city of Swatow, China. A New York Times (Anonymous 1922) article reports that the typhoon generated a destructive tidal wave in this region, while the *Monthly Weather Review* (Anonymous 1922, pg. 435) indicates that a tidal wave accompanied the storm, and that, "houses that escaped being blown down

were washed away by the waters which spread over the whole country side, and the loss of life was enormous." The proportion of deaths caused by storm surge is usually very high in such widespread surge events, and reaches 40,000 casualties even if one conservatively estimates that storm surge induced only two-thirds of the casualties in this disaster.

Storm surges cause lower death tolls at other locations of East Asia, outside of mainland China, although the effects of such surges are still locally catastrophic, killing thousands of people. This hazard has produced more deaths than other hazards in Hong Kong, as typhoons in 1906 and 1937 killed 10,000 and 11,000, respectively (Wyss and Yim 1996). The Isewan Typhoon, which produced Japan's worst modern-day surge in 1959, killed 4,687 (Kawai 1999).

Although Frank and Husain (1971) and Dube (1997) indicate that a typhoon killed 300,000 in China in the 1880s, and a 1923 cyclone killed 250,000 in Japan in 1923 (see Tables 1.3 and 1.4), a review of other scholarly sources questions the credibility of these events. Frank and Husain (1971) state that the Chinese typhoon occurred in 1881, Dube (1997) provides the year as 1886, and Gunn (2008) reports that an intense typhoon struck Vietnam in 1881. While it is possible that a catastrophic typhoon struck Southeast Asia sometime in the 1880s, these conflicting accounts cast doubt upon the details, specifically, the extraordinary number of deaths- five times that of the next highest fatality total in this region. Details are clearer about the 1923 Japanese disaster. An intense earthquake near Tokyo, which produced catastrophic fires, was the driving force behind this tragedy, which killed more than 100,000 (Himoto 2007; Schencking 2008). The unfortunate timing of a passing typhoon during this event helped to fan the flames

into a raging inferno that was responsible for more than 90% of the deaths (Himoto 2007). While this nearby typhoon may have exacerbated the tragedy, it was not the initial cause of this disaster, and no sources indicate that storm surge contributed to this catastrophe.

1.4.4 Australia and Oceania

Storm surge inundations kill fewer people in Australia and Oceania than in the other ocean basins (Zerger 2002). Lower coastal populations may partially explain this observation. Vast areas of Oceania may only contain several thousand people, as islands are generally spread out around a large area. De Scally (2008) reports that 1,000-2,000 deaths is the greatest toll from a single cyclone in the Cook Islands, and this occurred more than 400 years ago. The Australian coastal zones most susceptible to tropical cyclones have historically contained few people, especially compared to South and East Asia. This explains how Tropical Cyclone Mahina (1899), the most intense landfalling cyclone in modern Australian history, only killed several hundred people, mostly from drowning in sunken ships off the coast (Nott 2000).

Although death tolls in this region are small compared to other regions, surge inundations sometimes trigger devastating long-term effects in Oceania, such as starvation and disease (Spennemann 1996; De Scally 2008), which can traumatize high proportions of the population. Therefore, storm surges may produce many more casualties from indirect effects than by actual drowning. Inundations that wash over entire islands can destroy agriculture, disrupt food and water supply, and be a long-term agent for death by famine or epidemic.

1.5 Conclusion

While the physical processes that influence the genesis and movement of tropical cyclones impact global storm surge levels, additional variables such as cyclonic size and forward speed, as well as the shape and bathymetry of coastlines, create distinctive storm surge climatology. Geographically, the Bay of Bengal observes the highest surge levels and by far the most casualties, sometimes totaling in the hundreds of thousands in a single event. The Gulf of Mexico experiences the second highest surge levels, although death rates are much lower than along the Bay of Bengal. Population density along the Gulf of Mexico is lower, and technological infrastructure is more thoroughly developed, enabling storm warnings to reach a higher proportion of the population. The western North Pacific experiences more intense cyclones and higher fatalities than the Gulf of Mexico, but fewer fatalities than the Bay of Bengal. Although Australia and Oceania experience the fewest fatalities, surges can sweep over entire islands, inducing long-term starvation and disease.

CHAPTER 2. CONSTRUCTING A STORM SURGE DATABASE FOR THE U.S. GULF COAST

2.1 Introduction

Coastal flooding from storm surge creates natural disasters that are among the most deadly and costly to impact the United States. The most extreme of these events within the United States have occurred along the Gulf of Mexico. Examples of such disasters include the 1900 Galveston Hurricane, which claimed more than 6,000 lives (Rappaport and Fernandez-Partagas 1995), and Hurricane Katrina, the damage from which totaled more than 80 billion U.S. dollars (McTaggart-Cowan et al. 2008).

Storm surge, however, remains poorly understood by both coastal populations and the scientific research community. Lives and property are endangered as coastal populations underestimate the threat of surge inundations, which are both localized and complex. Meanwhile, storm surge modeling remains a frontier in meteorology and oceanography, as surge forecasts are commonly inaccurate. The National Hurricane Center's prediction of an 18-25 foot surge in Hurricane Gustav (National Hurricane Center 2008) is a recent example of surge forecast overestimation, as the actual maximum surge was only 13 feet (Beven and Kimberlain 2009). Likewise, in 2004, the National Hurricane Center predicted a 10-13 foot surge in Hurricane Charley (National Hurricane Center 2004); in reality the maximum surge was only 7 feet (Pasch et al. 2004).

Scientific developments, such as improved forecast models and statistical analysis, as well as public education resources, suffer from the absence of credible storm surge research that accurately depicts the maximum height and location of historic surge events. Such research is desperately needed to accurately inform coastal populations of

localized and regional surge potential, while providing the scientific community with historical storm surge climatology for statistical analysis and forecast model verification.

In this chapter, a storm surge database for the U.S. Gulf coast is constructed to meet this dire need. The database identifies the maximum surge height and peak surge location for storm surge events. Although this information does not depict the regional extent of specific surges, or a list of all historic surge levels at a particular location, these data are useful for understanding surge height potentials for the entire basin and regions within the basin, identifying locations that observe enhanced or reduced numbers of peak surges, and potentially for understanding the relationship between specific tropical cyclone characteristics and resultant surge heights.

2.2 Defining Surge Thresholds, Geographic and Temporal Ranges

The database utilizes a minimum surge threshold of 1.22 meters (4 feet), meaning that it includes all surges that equal or exceed this level. This height was chosen because the National Hurricane Center associated this surge level with the landfall of a category one hurricane on the Saffir-Simpson Scale (National Hurricane Center 2002) at the time that this research commenced. After Hurricanes Katrina (2005) and Ike (2008) generated surge heights well beyond generalizations suggested by the Saffir-Simpson scale, the National Weather Service decided to stop associating this wind scale with suggested surge heights (National Oceanic and Atmospheric Administration 2010).

The temporal range for the database is the 130-year period from 1880-2009. This time frame is chosen because Elsner and Jagger (2007) note that the most reliable historical hurricane data are available beginning approximately 1880. Landsea et al. (2004) provide estimated dates of accurate tropical cyclone records for segments of the

U.S. Gulf of Mexico and Atlantic coastline (Table 2.1). They estimate that every segment of the Gulf of Mexico coast provided reliable tropical cyclone data by 1880 (some sooner than this date), with the exception of southwest Florida, which did not provide accurate data until around 1900. Despite this later date for southwest Florida, 1880 was chosen as the starting date for this database as a compromise to produce a reasonably accurate record, thereby maximizing spatial and temporal coverage for the entire Gulf Coast.

Table 2.1: Estimated dates of accurate tropical cyclone reports for segments of the U.S. Gulf of Mexico based on U.S. Census and other historical data. This data was provided by Landsea et al. (2004), as part of Table 7.10 on page 209.

Location	Estimated start date of reliable tropical cyclone records
TX- S	1880
TX- C	1850
TX- N	1860
LA	1880
MS	1850
AL	< 1851 (1830)
FL- NW	1880
FL- SW	1900

The United States Gulf of Mexico (GOM) coastline is chosen as the geographic area of this analysis based on several reasons. Storm surge inundations from tropical cyclones embody the most severe disasters along this coastline, in terms of both human and financial losses, and will likely cause the most catastrophic losses associated with potential climate change in this region (*Global Climate Change Impacts in the United States* report, pg. 114). Also, as this stretch of coastline is a portion of the larger United

States Atlantic Basin coastline, all of which is susceptible to tropical cyclone-generated storm surges, this research establishes a climatological methodology on a smaller-scale project that can be applied to more extensive future research. Also, extreme GOM storm surges are generally considered larger than those recorded along the East coast of the United States. Finally, funding for this research, provided through NOAA's Regional Integrated Sciences and Assessments (RISA) program, has been allocated to the Southern Climate Impacts Planning Program (SCIPP) region, which includes the states of Arkansas, Louisiana, Mississippi, Oklahoma, Tennessee and Texas, three of which border the GOM and experience hazards from storm surge.

The boundaries for this region extend from South Padre Island, Texas, eastward along the entire Gulf coast to the southern tip of the Florida Everglades. The Florida Keys are included as the extreme southeast border of the GOM, following the example set by Keim and Muller (2009). A very precise eastern boundary in the Florida Keys is required, as the chain of islands extends northeastward to points off the southeastern coast of Florida. North Key Largo is chosen as this easternmost point, specifically along the boundary of County Road 905A, from Dagny Johnson Key Largo Hammock Botanical State Park to the Florida Peninsula.

2.3 Creation of a Storm Surge Database

The creation of a storm surge database required a two-step process. The first step entailed creating a list of every tropical cyclone that potentially generated a 1.22-meter storm surge. The second step required examining historical records for the maximum storm surge level and location for each event on the list.

A hybrid approach, utilizing historical hurricane data from two sources, provided the most accurate information for creating a list of potential surge events. The sources were a database contributed by Landsea (2005), made available through the Atlantic Oceanographic and Meteorological Laboratory (AOML), and data provided by the Unisys Weather Hurricane Data Website. Each of these sources contributed unique information and complimented each other well for the creation of a storm surge database skeleton.

The AOML dataset provided information on tropical cyclones that affected the continental U.S. between 1851-2005. The vast majority of these events, with only a few exceptions, generated at least sustained hurricane force winds (sustained winds greater than 33 m/s), henceforth called "hurricanes." The categories of data contained in this list also provided useful structure for the storm surge database. Data on tropical cyclone name, month and year of landfall, the maximum Saffir-Simpson Category observed in affected states, the highest Saffir-Simpson wind speed category observed in the U.S., the lowest U.S. central pressure (mb), and maximum U.S. winds (kts), were directly copied from the AOML Website into the storm surge database. In addition to providing helpful database structure, this source provided a plethora of storm data already available in tabular form that could be directly imported into the storm surge database. Cyclones that impacted the Atlantic coast, but not the GOM, were deleted from the list.

The Unisys data provided tropical cyclone best-track maps for the North Atlantic Basin from 1851-present, from data made available by The National Oceanic and Atmospheric Administration's (NOAA) National Hurricane Center. One of the benefits of the Unisys data was that it provided the most up-to-date tropical cyclone tracking

information, as the Website utilized the latest HURDAT re-analysis data (Landsea et. al 2008; Landsea et al. 2009). Another benefit was that Unisys provided easy-to-interpret tropical cyclone tracking maps, which plotted the cyclone position in 3-hour or 6-hour intervals, depending on the year of the cyclone, as well as color-coded intensity levels. This useful graphic display provided an effective resource for quick analysis of tropical cyclones that may have produced storm surges in the United States.

In addition to providing data for landfalling hurricanes, the Unisys maps also provided data for landfalling tropical cyclones with at least sustained tropical storm force winds (sustained winds greater than 17 m/s), henceforth called "tropical storms," as well as tropical cyclones that did not make landfall in the United States, but potentially generated storm surges. Tropical storms that are geographically large or move slowly when approaching landfall have potential to generate 1.22-meter surges, and, therefore must be included in the storm surge database. Tropical cyclones that pass near U.S. coasts but do not make landfall in the U.S. may still generate U.S. storm surges, and, therefore, must be included in the database as well. The most common examples include tropical cyclones that make landfall in northeastern Mexico, yet still generate storm surges in southeastern Texas, such as Hurricane Gilbert in 1988, and tropical cyclones that generate storm surges in the Florida Keys, while bypassing the islands without officially making landfall, such as Hurricane Lili in 1996. Less likely, but still possible, are tropical cyclones which stall offshore and generate a 1.22-meter storm surge before dissipating without making landfall, such as Hurricane Jeanne in 1980. Unisys' graphical display of tropical cyclone tracks provides an excellent resource to identify other events that have such potential.

A 300-kilometer buffer from the U.S. coastline was utilized to incorporate tropical cyclones that did not make U.S. landfall, but potentially generated a 1.22-meter surge. Every tropical cyclone that passed within this buffer was included in the database. This buffer size was chosen because it likely includes all cyclones that generated tropical storm force winds in the United States. Keim et al. (2007) generalize that winds of at least tropical storm force extend outward 240 km on the strong side of averaged-sized Category 3-5 cyclones, however, because larger-than-average cyclones produce larger wind fields, a 300-kilometer buffer was adopted. Cyclones that did not pass within 300 km of the U.S. Gulf coast are unlikely to generate tropical storm force winds in the U.S. and were therefore not included in the database.

Hurricanes Anita (1977) and Lili (1996) are examples of storms that generated U.S. storm surges from considerable distances. Anita generated a 1.68-meter surge at South Padre Island, Texas, even though the cyclone made landfall in Mexico, about 270 km south of Brownsville, Texas (Lawrence 1978). Although Lili's closest approach to the U.S. was approximately 250 km, as the storm tracked over Cuba, south of Key West, Florida, the cyclone produced a 1.83-meter surge in the Florida Keys.

Cyclones provided by the AOML database (landfalling hurricanes) were thus combined with landfalling tropical storms and tropical cyclones that passed within 300 km of the GOM coast, both provided by Unisys, to create a master list of every cyclone that potentially generated a storm surge. For cases in which the AOML and Unisys data differed, such as maximum U.S. wind speed or minimum pressure, Unisys data was usually used because it contained the latest HURDAT re-analysis data (Landsea et. al 2008; Landsea et al. 2009).

A unique ID number identifies each potential surge event in the database. Some cyclones produced double records. These are storms that generated two distinctive surges, usually separated by at least 12 hours. The most common double surge pattern is an initial surge in southwest Florida or the Florida Keys, followed by an event elsewhere in the GOM. The database uses decimal IDs to identify double surges. For example, the identification numbers for Hurricane Ike are 418.1 and 418.2, corresponding to potential surge events in southwest Florida and the upper Texas coast, respectively. Very rarely, updated data provide a new surge event that was not included in the original database. In this case, the new event fits between the preceding and following events, with a decimal number of "point 5," such as 317.5.

The estimated date, time, and location of Greatest Surge Potential (GSP) were added to the database to aid the search for maximum storm surge level. Usually the date and time of GSP corresponded with landfall. However, for cases in which the cyclone did not make landfall, or for cases in which cyclones remained stationary offshore for extended periods of time, traveled in loops, or exhibited other unusual behavior, the date and time of GSP may differ from landfall. Location of the GSP was classified according to the most likely of eleven regional zones in which the highest surge occurred. If the GSP likely occurred near the border of a zone, or the most likely location for maximum surge was unclear, a secondary zone was also defined. Therefore, the database indicates a Primary Impacted Surge Zone (PISZ) and Secondary Impacted Surge Zone (SISZ). The zones were arbitrarily defined as segments of coast bounded by cities or distinctive geographic features. These zones, which are listed in Table 2.2, played a central role in the methodology for obtaining historical newspapers.

Table 2.2: Surge zones along the Gulf of Mexico Coast.

Zone Number	Western Boundary	Eastern Boundary
1	Texas/Mexico Border	Corpus Christi, TX
2	Corpus Christi, TX	Galveston, TX
3	Galveston, TX	Texas/ Louisiana Border
4	Texas/ Louisiana Border	Grand Isle, LA
5	Grand Isle, LA	Louisiana/ Mississippi Border
6	Louisiana/ Mississippi Border	Mississippi/ Alabama Border
7	Mississippi/ Alabama Border	Alabama/ Florida Border
8	Alabama/ Florida Border	Apalachicola, FL
9	Apalachicola, FL	Tampa Bay, FL
10	Tampa Bay, FL	Everglades, FL
11	Key West, FL	North Key Largo, FL

After a cyclone was included in the database, and assigned a date, time and location of GSP, the storm was classified as having high, moderate or low potential for generating a 1.22-meter surge. Generally, cyclones that generated hurricane force winds on the GOM coast were classified as high potential, cyclones that generated tropical storm force winds were classified as moderate potential, and cyclones that produced winds less than tropical storm force were classified as low potential. However, this rule was not steadfast as some subjective climatological decisions were made. For example, a stationary tropical storm centered 100 km offshore may be classified as high surge potential, whereas a tropical storm that tracked westward across the Florida peninsula may be classified as low potential, because the strongest winds along the Gulf coast were blowing offshore, north of the circulation center. These classifications became important

for historical surge research, as they directed research towards the highest potential surges.

The high, moderate, and low classifications utilized maximum U.S. wind speed from the AOML data. If AOML data did not exist, and no other data were available to indicate maximum U.S. wind speed, the maximum U.S. wind speed was estimated from Unisys' tropical cyclone tracking data at 6-hour intervals.

The average spatial extent of wind speeds provided by Keim et al. (2007) again prove useful for estimating maximum U.S. wind speeds produced by cyclones that did not make landfall. They estimate that on average, the strong side of a tropical cyclone, tropical storms will produce tropical storm force winds to an extent of 80 km; Category1-2 hurricanes will produce hurricane force winds to a distance of 80 km, followed by tropical storm force winds for an additional 80 km; and Category 3-5 hurricanes will produce major hurricane force winds (greater than or equal to 49 m/s) for 80 km from the center of circulation, followed by hurricane force winds for the next 80 km, and tropical storm force winds for the remaining 80 km away from the center. These generalizations were very useful for estimating maximum winds observed on the GOM coast, which corresponded to the potential for the storm to generate a 1.22-meter surge.

These procedures produced a database skeleton of 463 potential storm surge events from 1880-2009. The events were produced by 421 unique tropical cyclones, 42 of which generated double surges. Of these 463 events, 161 were classified as high potential, 126 as moderate potential, and 176 as low potential for generating a 1.22-meter or higher storm surge.

2.4 Identifying Storm Surge Levels

After the list of 463 potential storm surge events was created, historical research attempted to find the maximum surge levels for as many events as possible. Research utilized 53 sources from several types of literature, including 21 Federal government sources, 16 books and online resources, and 16 newspaper sources. Appendix A lists sources by category and the corresponding date(s) of publication.

2.5 Source Information

Government documents include all relevant information published by agencies in the U.S. Federal Government, with the exception of the U.S. Army Corps of Engineers (USACE). USACE data were not incorporated into this research for several reasons. The primary reason was that USACE post-storm documentation primarily focuses on river discharge rates, stage levels, and water levels at flood control devices, such as artificial levees, dams and canals. Maximum water level heights at these structures are often influenced to such an extent by the constructed device that they no longer accurately represent maximum storm surge heights. Although USACE data are very detailed and useful for engineering applications, these data do not necessarily depict maximum surge heights. However, some of the sources utilized by this study reference USACE data in a summarized version, which often includes maximum storm surge levels.

The document titled, *History of Hurricane Occurrences along Coastal Louisiana*, published in 1972, is one exception to the absence of USACE data. This summarized report was referenced for surge information associated with the August, 1926, hurricane in Louisiana, and the August, 1940, hurricane that impacted Louisiana and Texas. See Appendix A.1 for a complete list of government sources.

Books utilized by this study are generally classified into one of three categories: publications that focus on particular storm events, recount tropical cyclone history for a specific region or state, or paint a broader picture of global or basin-wide tropical cyclone history. Books such as Roberts' (1969) *Extreme Hurricane Camille, August 14th through 22nd, 1969*, provide in-depth history of a particular event in a specific location. His narrative very clearly relives the story of Hurricane Camille, including detailed descriptions of the storm surge, during a horrific night along the Mississippi coast in August, 1969. Works such as Barnes' (2007) *Florida's Hurricane History,* provided regional tropical cyclone history, focused on Florida. Publications such as Elsner's (1999) *Hurricanes of the North Atlantic: climate and society,* provided a broader perspective of tropical cyclone history in the North Atlantic basin, contributing information for the entire Gulf coast over an extended time period. See Appendix A.2 for a complete list of books and online publications.

Newspapers utilized in this research were daily periodicals published in cities or towns located near the Gulf of Mexico, with the exception of Online newspapers that published storm accounts from syndicated national stories. Dates of newspaper availability depended on the specific publication in question, as well as the archive length at libraries that participated with the Interlibrary Loan Department at Louisiana State University. The Houston Chronicle and Miami Herald were not utilized. Both of these publications may be useful to future, more localized storm surge studies. The Miami Herald may particularly provide insight for surges that impacted the eastern Florida Keys. See Appendix A.3 for a complete list of newspapers.

2.6 Obtaining Data from Sources

Obtaining data from government sources required little time and effort, thanks to the easy accessibility of National Hurricane Center tropical cyclone reports and *Monthly Weather Review* publications. The National Hurricane Center provides online archives of every tropical cyclone since 1958. Books also provided easy access to storm surge data, as no special orders were required for this research. Obtaining newspapers, however, was a much more time-consuming task.

The first step for acquiring historical newspapers was to look for digitized papers online. Internet searches for hurricane-related newspaper articles sometimes yielded results. The Florida Digital Newspaper Library (http://www.uflib.ufl.edu/digital/collections/fdnl/cuban.htm), available through the University of Florida, was a helpful resource for Florida cyclones. Another useful online resource was a historical newspaper archive found at www.newspaperarchive.com. The most relevant newspapers archived on this site were *The Panama City News-Herald* and *The Galveston Daily News*.

If government documents, books, and online newspapers yielded no information about a particular cyclone, newspapers were ordered through the Interlibrary Loan (ILL) Department at Louisiana State University. This department cooperates with participating university and municipal libraries to obtain research materials. In this case ILL obtained historical newspapers from other libraries through microforms.

The procedure utilized for ordering materials through ILL was very systematic. For a given surge event, all newspapers published in the PISZ and SISZ were requested for the date of GSP as well as the two following dates. For example, newspapers from

August 30- September 1, 1932, were ordered for *The Key West Citizen* (Zone 11), *Collier County News* (Zone 10), *The Naples Daily News* (Zone 10), *The Fort Myers News-Press* (Zone 10), *The Tampa Tribune* (Zone 10), and *The Saint Petersburg Times* (Zone 10), for a cyclone that made landfall in the eastern Florida Keys, then moved northwest across the Everglades, and departed the west coast of the Florida Peninsula, near Fort Myers, in late August, 1932. The database defines the date of GSP as August 30, the PISZ as Zone 11, and the SISZ as Zone 10. This order of six separate newspapers for three different dates yielded a total order of 18 newspaper-dates for this one event.

Approximately 1300 newspaper-dates were requested through ILL. ILL obtained about 60 percent of these requests, meaning they acquired approximately 780 requests. Online newspapers yielded approximately one-third as many newspaper-dates as the ILL procedure, or about 260. This means that a total of approximately 1040 separate newspaper-dates were utilized by both Online newspapers and orders through ILL. Given the assumption that an average of three newspaper pages are read for each newspaper-date, this portion of the storm surge database research analyzed over 3,000 pages of newspaper from 16 different sources.

2.7 Canceled Orders

All events were canceled from the newspaper research if the probability of a tropical cyclone generating a 1.22-meter surge was classified as low in the database. This procedure enabled high and moderately probable surge events to receive more attention, and kept the volume of newspapers ordered more manageable. As these events were canceled in the database, they are not considered missing data.

The period in which most of these events were canceled was the time period that depended most upon newspaper archives, 1880-1955. In this period, 113 events were originally canceled. Non-newspaper sources classified two of these events, a September, 1920 surge in Tampa, Florida, and a September, 1955 event in south Texas, as having surges greater than 1.22 meters. Non-newspaper sources also confidently classified two other events as not having generated a 1.22-meter surge. These events were an October 1895 event that impacted the upper Texas coast, and a June 1922 storm that affected the lower Texas coast. The other 109 events remained canceled throughout the duration of this study, meaning that although it was unlikely that these events generated at least a 1.22-meter surge, this was not proven. In contrast, only two events with low probabilities of generating 1.22-meter surges, Hurricane Frederic's potential surge in the Florida Keys (1979), and Hurricane Dennis' (1981) potential surge in southwest Florida and the Florida Keys, were canceled from the period 1956-2009, because research from this period did not rely heavily on newspaper archives. National Hurricane Center tropical cyclone reports were utilized for most events from this period, even if the probability of the cyclone generating at least a 1.22-meter surge was low.

Storm surge heights of at least 1.22 meters were identified for some of the events classified as having a low probability for generating such surge levels in the 1956-2009 period. From the 63 low-probability surge events in this period, 9 yielded surges $\geq$ 1.22 meters, or about 14 percent of the possible surges. If this ratio holds true for the period from 1880-1955, 14 percent of the 109 canceled storm surges would yield 15 additional 1.22-meter or greater surge events, the heights of which would mostly reach two meters or less.

2.8 Determining Surge Height from Anecdotal Descriptions

Some anecdotal sources of storm surge data do not provide a quantitative value to describe the maximum storm surge level. Rather, the maximum surge depth must be estimated based on damage descriptions. Unfortunately, no scientific literature provides a system for converting damage descriptions to surge depth. Therefore, it was necessary to create such a system, especially to classify older surge events that lacked the scientific infrastructure to measure, record and disseminate the storm surge depth.

Fortunately, some anecdotal accounts that provided a quantitative maximum surge height also included detailed descriptions of the damage inflicted upon commercial and residential buildings, transportation infrastructure, industrial equipment, marine infrastructure, beach erosion, and, in general, the water depth in settled areas. These surge heights and storm descriptions were utilized to create a categorical system in which increasingly destructive anecdotal descriptions were associated with specific, incremental increases of surge depth. This system then enabled the assignment of surge heights to some older (1880-1955) anecdotal surge accounts, the majority of which were small or moderate surges, usually less than 3.05 meters (10 feet).

These categories are listed below, beginning with Surge Level 1 and ending with Surge Level 4. Each category provides the associated maximum storm surge height range, damage description and anecdotal references that make this association. The lowest category, Surge Level 1, describes storm surges that do not equal or exceed 1.22 meters. Although this may appear confusing, as 1.22 meters defines the minimum threshold for inclusion into the database, this category was warranted so these magnitude surge levels could be identified in the literature, and not included in the database. The

highest category, Surge Level 4, describes storm damage for 2.44-meter or greater surges. Although surges on the Gulf of Mexico sometimes substantially exceed this level, the obvious visible thresholds, such as flooding of roads and coastal structures, is surpassed, making anecdotal distinctions between surges of various magnitudes in this category more difficult. Also, these events are so severe that the maximum surge depth was likely measured and preserved in the historical record. Figure 2.1 displays a summarized version of these surge categories in the form of a schematic that associates surge levels with damage descriptions.

2.8.1 Anecdotal Storm Surge Categories

2.8.1.1 Surge Level 1: Surge Height: < 1.22 Meters

Damage Description: The water level increased, perhaps accompanied by waves, but relatively minor damage was reported. Marine infrastructure, such as docks, wharves, piers, marinas, or bath houses may have sustained some damage. Non-elevated industrial equipment located outside the protection of seawalls or levees may have been damaged as well. Minor beach erosion may have occurred. If accompanied by wave action, water may have washed up against, or even over, smaller seawalls, and may have reached coastal roads.

Snapshot: Water is high, but mostly remained in marine areas; water did not generally reach buildings and barely crossed coastal roads if it reached them at all.

References:

Storm info: Ella, 1958, Florida Keys

Source: Kurtsweil, J.P., 1958

Quote(s): “Tides were two feet above normal. There was no flooding, but great quantities of seaweed, sand and small rocks were washed onto the boulevard at the southeast portion of the island.”

Storm info: Beulah, 1959, Texas

Source: National Weather Bureau, 1959

Quote(s): “Tides 2 to 3 feet above normal and rough seas were reported along the lower Texas coast. No reports of damage or loss of life have been received.”

Storm info: Judith, 1959, Florida

Source: Tampa Tribune, October 19, 1959, Pg. 4

Quote(s): “A 75-foot long section of boardwalk next to Naples’ city fishing pier was washed away in the pounding surf – three feet above normal.”

“The Fort Myers-to-Naples stretch, south of the storm’s center, felt the main force of the blow but there was comparatively little damage.”

Storm info: Tropical Storm #1, 1960, Texas

Source: Mozeney, R.P., 1960

Quote(s): “One shrimp boat beached. One shrimp boat and two crewmen missing. Three private fishing piers wrecked at Bayside on Copano Bay.”

Storm info: Danielle, 1980, Louisiana

Source: National Hurricane Center, 1980

Quote(s): “Tides were no more than 2 to 3 feet above normal on the southwest Louisiana and upper Texas coasts. Beach erosion was minor.”

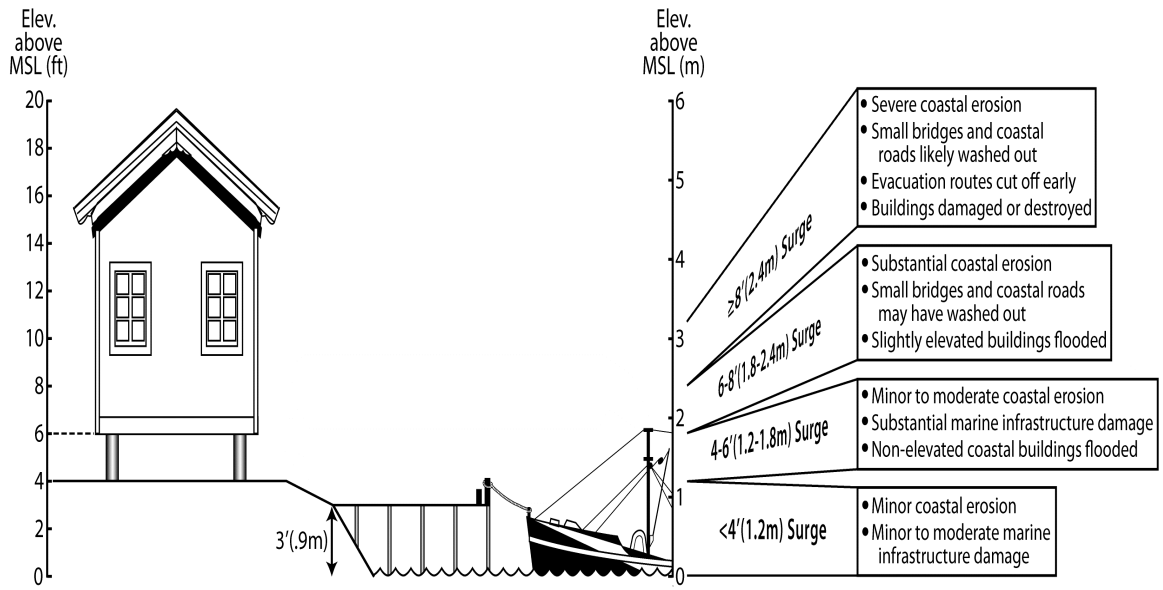

Figure 2.1: Generalized impact of surge heights on Gulf Coast communities. Marine infrastructure is estimated at .9 meters (3 feet), ground level of communities is estimated at 1.22 meters (4 feet), and slightly elevated buildings in these communities is estimated at 1.83 meters (6 feet) above MSL. Generalized damage descriptions associated with surge heights are listed in the right portion of diagram.

2.8.1.2 Surge Level 2: Surge Height: ≥ 1.22 Meters and < 1.83 Meters

Damage Description: Water washed over, and may have damaged, coastal roads and smaller sea walls. Beach erosion occurred and was substantial if accompanied by large waves. Non-elevated structures in the coastal zone that were not protected by levees or seawalls likely flooded. Marine infrastructure, such as docks, wharves, marinas, bath houses, as well as other structures located adjacent to the water, may have sustained substantial damage or have been washed away, especially if accompanied by wave action.

Snapshot: Water damaged marine areas, crossed coastal roads and flooded non-elevated coastal buildings.

References:

Storm info: "Great Miami Hurricane", 1926, Florida Panhandle

Source: Mitchell, C.L., 1926, Pg. 413

Quote(s): "On the 21st the tide was estimated at 4.2 feet at 6:30 a. m.; it was then overflowing low ground along the water front with highest waves running possibly 5.0 feet, portions of Water Street being then from 6 to 8 inches under water."

Note: The previous quote refers to Apalachicola, Florida.

Storm info: Unnamed storm, 1936, Florida

Source: Barnes, 2007, Pgs. 160-161

Quote(s): "Just after the storm center passed, an "abnormally high tide" occurred, which measured 5.5 feet above normal and left water 18 inches deep in the streets of Everglades City."

Storm info: Unnamed storm, 1941, Florida

Source: Sumner, H.C., 1941, Pg. 303

Quote(s): “The lowest pressure, at Everglades City, 995.6 millibars (29.40 inches), was accompanied by winds exceeding 65 miles per hour and a tide of 4.1 feet which flooded the town and surrounded low country to a depth of about 1 foot.”

Storm info: Baker, 1950, Florida Panhandle

Source: *Dothan Eagle*, September 1, 1950, Pg. 1

Quote(s): “Some beach property and wharves were damaged when water rose five and half feet above normal.”

Storm info: Esther, 1957, Mississippi

Source: *Times-Picayune*, September 19, 1957, Pg. 5

Quote(s): “US Highway 90 along the beach was pronounced unsafe for travel by the state police which sent extra troopers to detour motorists as five-foot tides smashed over the seawall.”

Storm info: Ella, 1958, Texas and Louisiana

Source: Lichtblau, S., 1958

Quote(s): “Highest tides were between 2 and 4 feet along the Texas and Louisiana coasts. Some coastal roads were closed due to tide and waves.”

Storm info: Candy, 1968, Texas

Source: Sugg and Hebert, 1969, Pg. 233

Quote(s): “Tides ranged up to 4 ft in San Antonio Bay and Corpus Christi Bay and were 2 to 3 ft elsewhere on the central and upper Texas coasts. Damage was confined mainly to the formation of cuts along Padre Island and coastal oil industry equipment.”

Storm info: Bob, 1979, Louisiana, Mississippi, Alabama

Source: National Hurricane Center, 1979, Pg. 1

Quote(s): “Tides were generally 3 to 5 feet above normal and rainfall totals between 3 and 6 inches…No serious flooding was reported in Louisiana, Mississippi, or Alabama.” “A number of boats were sunk or damaged and there was considerable pier damage due to high tides and rough seas.”

Storm info: Jeanne, 1980, Texas

Source: National Hurricane Center, 1980, Pg. 2

Quote(s): “Tides of 2 to 4 feet above normal occurred along the Texas coast accompanied by a prolonged period of rough seas and heavy swells. However, only minor beach erosion was reported.”

Storm info: Gilbert, 1988, Texas

Source: National Hurricane Center, 1988, Pg. 2

Quote(s): “Tides of 3 to 5 feet above normal were reported along the Texas coast with a number of low-lying roads under water. There was considerable beach erosion on Padre Island.”

Storm info: Alberto, 1994, Florida Panhandle

Source: *Intelligencer*, July 4, 1994, Pg. 41

Quote(s): “A 5-mile stretch of U.S. Highway 98 from Destin west to Fort Walton Beach was closed for two hours because a sea wall protecting the highway had eroded.”

Source: Rappaport (1994), Pg.3

Quote(s): “A storm tide of 5 feet was estimated near Destin. A 3 foot storm surge (NGVD) occurred at Panama City, Panama City Beach, Turkey Point and Apalachicola.”

Storm info: Josephine, 1996, Louisiana

Source: National Weather Service, Lake Charles, LA, 2009

Quote(s): “The highest tide noted was 5.5 feet at Bayou Bienvenue, near Lake Borgne. Highway 1 was under a foot of water. A few homes and roads were also flooded in Orleans and St. Bernard Parishes, outside the flood control levees.”

2.8.1.3 Surge Level 3: Surge Height: ≥ 1.83 Meters and < 2.44 Meters

Damage Description: Widespread damage or even destruction of marine infrastructure, as well as industrial infrastructure located outside flood protection levees. Coastal communities were flooded, as water entered non-elevated and slightly elevated (one meter or less) structures in the coastal zone. Coastal roads were flooded. Small bridges as well as portions of roadway may have been washed out. Substantial coastal erosion was observed. Storm surge impacted the coast and areas slightly inland.

Snapshot: Water damaged coastal structures, such as residences and businesses, as well as infrastructure, such as roads, bridges and causeways.

References:

Storm info: Florence, 1953, Florida

Source: *The Panama City News-Herald*, September 27, 1953, Pg. 1

Quote(s): “For a short time Port St. Joe was isolated from the east and west but roads to the north remained open. A washed- out bridge east of the city interrupted travel between Port St. Joe and Apalachicola while high tides on the west at Hiland View, a Port St. Joe suburb, cut the route between this city and Panama City.”

Source: Barnes, 2007, Pg. 194

Quote(s): “Tides were five feet above normal at Apalachicola and Carrabelle and “six or seven feet” at Panacea.”

Note: These quotes associate a surge height of 6 to 7 feet with washed out bridges. However, Barnes reports the surge at Apalachicola was only 5 feet. As Apalachicola was located closer than Panacea to the washed out bridges, it is possible that the surge height was around 5 feet where the bridges washed out.

Storm info: Flossy, 1956, Florida

Source: Barnes, 2007, Pg. 195

Quote(s): "Flossy's highest tides in Florida ranged from five to six feet and caused minor damages to piers and small craft. Beachfront erosion was severe, and several homes were destroyed."

Storm info: Gladys, 1968, Florida

Source: Sugg and Hebert, 1969, Pg. 236

Quote(s): "Highest tides were estimated at 6.5 feet, causing considerable beach erosion and flooding of coastal areas."

Storm info: Delia, 1973, Texas

Source: Hebert and Frank, 1974, Pg. 286

Quote(s): "Tides of 4 to 6 ft MSL in Galveston Bay caused flooding of the Baytown area and an estimated $3 million in losses for homeowners."

Source: *Baytown Sun*, September 5, 1973, Pg. 1

Quote(s): "At least 500 people fled their Brownwood homes Tuesday during a threat of tides five to seven feet above normal."

Source: *Baytown Sun*, September 6, 1973, Pg. 1

Quote(s): "More than 1,000 Brownwood residents were evacuated early Thursday as tidal waters gushed over the elevated perimeter roadway in the worst flood since Hurricane Carla. At least 140 homes were flooded…"

"A maximum 6.4 foot-tide at 4:24 a.m. Thursday was 1.5 feet above the Valentine's Day flood of 1969 and five feet below the devastating Carla flood in September, 1961."

Storm info: Chantal, 1989, Texas

Source: Gerrish, H.P., 1989, Pg. 3

Quote(s): "Tides at High Island were 7.0 feet MSL…There was extensive beach erosion from High Island to Sea Rim State Park."

2.8.1.4 Surge Level 4: Surge Height: ≥ 2.44 Meters

Damage Description: Severe coastal erosion was observed. Severe damage was inflicted on marine infrastructure, as well as any industrial equipment, residential or commercial structures located outside flood protection levees. Structures in coastal zone, even if elevated or protected by levees, may have been damaged or completely destroyed. Small bridges and coastal roads were likely washed out. Evacuation routes were cut off hours before the peak surge level arrived. Levees may have overtopped. Surge likely penetrated inland.

Snapshot: Water greatly damaged coastal structures, washing some away, or creating complete loss. Water also penetrates inland.

References:

Storm info: Danny, 1985, Louisiana

Source: National Weather Service, Lake Charles, Louisiana, 2009

Quote(s): “Storm surges of 8 feet were seen along the coast of South Central Louisiana. Highway 46 near Hopedale in St. Bernard Parish was impassable due to the high waters. The pier at Grand Isle State Park was damaged, while a pier near Slidell was demolished. Coastal erosion was greatest in Terrebonne and Lower Jefferson Parishes.”

Storm info: Juan, 1985, Louisiana

Source: National Weather Service, Lake Charles, Louisiana, 2009

Quote(s): “Storm surges were 8 feet at Cocodrie…LA 1 south of Leeville and LA 3090 near Fourchon were destroyed. Three bridges were washed out near Lacombe on LA 434. Levees were overtopped in Lockport, Marrero, Oswego, and Myrtle Grove; this added to the already serious flooding. Two hundred cattle were drowned in Terrebonne Parish. Grand Isle was under 4 feet of sea water; 1200 residents were trapped on the island as the storm surge cut off any evacuation attempts early on.”

Storm info: Allison, 1995, Florida

Source: Pasch, R.J., 1996

Quote(s): “Maximum storm surge heights were estimated at 6 to 8 ft from Wakulla through Dixie counties…”

“Damage was greatest in the coastal sections of Dixie, Levy, Taylor and Wakulla counties, mainly from storm surge effects, with 60 houses and businesses damaged. A house collapsed at Bald Point in Franklin County. About 5000 people evacuated from the coast. Other costal effects included mostly minor beach erosion, damage to sea walls and coastal roadways, and the sinking of several small boats.”

Source: *New Mexican*, June 6, 1995, Pg. 4

"More than 65 coastal homes, three hotels and at least one restaurant were flooded as the morning storm caused the ocean to surge 8 feet along a 150-mile stretch of Florida's Big Bend, where the Panhandle meets the Peninsula."

Storm info: Josephine, 1996, Florida

Source: Pasch, R.J., 1997

Quote(s): "County officials estimated storm tides (storm surge plus astronomical tide) ranged from up to 9 feet in Levy County...These tides produced widespread flooding of roads, dwellings, and businesses."

2.9 Estimating Elevations of Coastal Communities

In addition to providing insight on storm damage, anecdotal accounts also enable the elevation of coastal communities to be estimated. Mitchell's (1926, pg. 413) observation from Apalachicola, Florida, that, "On the 21st the tide was estimated at 4.2 feet…portions of Water Street being then from 6 to 8 inches under water," reveals that the elevation of Apalachicola was approximately 1.13 meters (3.7 feet). Sumner (1941) and Barnes (2007) provide elevation estimates for Everglades City, Florida, of .94 meters (3.1 feet), and 1.22 meters (4 feet), respectively. Sumner (1941, pg. 303) states, "The lowest pressure, at Everglades City, 995.6 millibars (29.40 inches), was accompanied by winds exceeding 65 miles per hour and a tide of 4.1 feet which flooded the town and surrounded low country to a depth of about 1 foot," while Barnes (2007, pgs. 160-161) recounts that, "Just after the storm center passed, an 'abnormally high tide' occurred, which measured 5.5 feet above normal and left water 18 inches deep in the streets of Everglades City." Larson (1999, pg. 12), meanwhile, estimates that the average elevation of Galveston, Texas, at the time of the 1900 Galveston Hurricane, was around 1.33

meters (4.35 feet), as he states, “Its highest point, on Broadway, was 8.7 feet above sea level; its average altitude was half that…”

The preceding quotes reveal that elevations of coastal communities differ slightly along the Gulf of Mexico. Generally the highest elevations are located along barrier islands of Texas and the Florida Panhandle. Elevations of communities in these areas generally average from 1.22 to 1.68 meters (4 to 5.5 feet). Communities surrounded by wetlands usually have lower altitudes, generally between .91 and 1.22 meters (3 to 4 feet). Many of these communities are located in southern Louisiana and southwestern Florida. Everglades City, Florida, is an excellent example of this type of community, estimated, as previously stated, to have an elevation somewhere between .94 meters and 1.22 meters (3.1 feet and 4.0 feet).

For the sake of constructing the storm surge database, coastal communities were estimated to have an elevation of 1.22 meters (4 feet), unless otherwise noted in the text. This level appears to provide consensus between elevations of lower and higher communities. The elevation of coastal roads was estimated at .91 meters (3 feet), as road elevations are often slightly lower than the elevations of the communities they connect. These generalizations enabled the assignment of quantitative surge heights to anecdotal damage and water level descriptions. The practice of slightly elevating structures in coastal communities explains the reason that the most common threshold for flooding of buildings in coastal communities is around 1.83 meters (6 feet). Although many of these communities have elevations around 1.22 meters (4 feet), a 1.22-meter surge may cause minimal damage, washing under many of the structures. Figure 1 depicts the estimated

elevations of communities, buildings, and marine infrastructure in a schematic that also associates surge heights with generalized damage descriptions.

2.10 Conflicting Accounts

Although most anecdotal storm accounts for a given surge event complimented each other well, sometimes accounts differed substantially. In these cases the highest surge level reported was not always adopted into the database. Rather, all information from every source was considered, and a most likely surge estimate was selected based upon the majority of information, with the database erring on the side of conservative estimates. Scientific sources were usually given more weight than non-scientific journalism or anecdotal accounts. Credibility of source was also considered; information from less credible sources was given less weight.

Consider the example of Hurricane Inez, which crossed the Florida Keys from east to west in 1966. Sugg (1967) lists a maximum surge of 1.52 meters at Big Pine Key, Florida. Williams and Duedall (2002), however, report a substantially higher surge level of 4.72 meters, generally located in the Florida Keys. How is such a discrepancy resolved in the database?

Several factors contributed to the final surge level selected for the database. Fortunately, Sugg (1967) reported seven regional surge observations in a table of meteorological data, and these levels, which ranged from .61-1.52 meters, supported the notion of a smaller maximum surge level. Barnes (2007) supported Sugg's (1967) position that the largest surge occurred at Big Pine Key, as he referenced a U.S. Weather Bureau report that the most violent winds occurred at this location. Although it does not provide surge data, this wind report indicates that Big Pine Key likely experienced the

hurricane's eyewall, an observation that supports Sugg's (1967) location of maximum surge. Without this supporting evidence, one might assume that the maximum surge level reported by Williams and Duedall (2002) was taken from a location closer to the hurricane eyewall, therefore supporting the theory of a higher surge. Barnes (2007) eliminates this possibility. The final pieces of evidence confirming the selection of a lower surge level are inaccuracies of Williams and Duedall's (2002) maximum surge data for other events. These inaccuracies include overestimations of surge levels on freshwater Lake Okeechobee. For example, they listed maximum surge heights of 6.58 meters at Clewiston, Florida, in September 1947, 5.79 meters at Canal Point, Florida, in September 1948, 7.32 meters at Belle Glade, Florida, in August 1949, and 5.88 meters at Clewiston, in October 1950. These surge heights are greatly overestimated, and likely pertain to the lake water level above mean sea level, not storm surge heights. Such observations would rank among the greatest all-time events in the Gulf of Mexico (Appendix B.1), a basin that is much more suitable for large surges than an inland freshwater lake. In a fact sheet pertaining to Lake Okeechobee's Herbert Hoover Dike, which was completed in 1937, and would have existed from the 1947 through 1950 hurricane seasons, The United States Army Corps of Engineers (2006) states, "*The Corps tries to manage Lake Okeechobee water levels between 12.5 – 15.5 feet," and, "The water level in Lake Okeechobee has never been higher than 19 feet,"* indicating that maximum surges on the lake should be no higher than approximately 1.98 meters (6.5 feet). This smaller surge level is much more appropriate for inland Lake Okeechobee, and reveals large overestimations in the surge data provided by Williams and Duedall (2002).

The factors involved in this example depict the complexities of historical storm surge research, as well as the painstaking details by which this study depicts Gulf coast storm surge history as accurately as possible. The overestimations of Williams and Duedall's (2002) surge data, coupled with Sugg's (1967) seven surge observations ranging from .61-1.52 meters, and supporting evidence from both the Sugg (1967) and Barnes (2007), indicating that Big Pine Key observed the most severe storm conditions, paint the picture that the lower-level surge observation was likely closer to reality. A maximum surge level of 1.52 meters at Big Pine Key, Florida was entered into the database for Hurricane Inez.

2.11 Database Results

This study utilized the sources previously mentioned to identify 241 surge events, or 52.1 percent of the possible 463 surges listed in the database skeleton. Of these classified events, 193 surges, or 41.7 percent, observed heights of at least 1.22 meters high. Of the remaining possible events, 43 surges, or 9.3 percent, were classified as surges lower than 1.22 meters (without identifying a maximum surge height); 114 surges, or 24.6 percent, were canceled; and 65 potential surge events, or 14 percent, were classified as missing (see Table 2.3).

Surge levels ranged in height from Hurricane Katrina's 8.47-meter surge along the Mississippi coast, to 1.22-meter surges generated by twenty separate events. The top 10 events generated maximum surge heights of at least 4.88 meters, and the top two surge events, Hurricanes Katrina and Camille, generated peak surges in the same location, Pass Christian, Mississippi. Appendix B.1 provides the maximum surge height, peak surge

location, surge height rank, as well as the name and year of the tropical cyclone, for each event that generated a surge at least 1.22 meters high.

Table 2.3: Storm surge database statistics for number of classified, non-classified, canceled and missing surges, from 1880 to 2009.

Data Type	Number	Percentage
Total possible events	463	100
Total classified events	241	52.1
≥ 1.22m classified events	193	41.7
< 1.22m classified events	48	10.4
< 1.22m non-classified events	43	9.3
Canceled events	114	24.6
Missing events	65	14

2.12 Summary and Conclusion

This study utilized a tropical cyclone database from the Atlantic Oceanographic and Meteorological Laboratory (AOML), as well as the Unisys Corporation's tropical cyclone best track data, to generate a database skeleton of 463 possible surge events between 1880-2009 along the U.S. Gulf coast. Each potential surge event was given a unique ID number, as well as a date, time and location of Greatest Surge Potential (GSP), to facilitate the identification of the maximum surge height and location of peak surge. The research utilized 53 sources, including 21 Federal government sources, 16 books and online publications, as well as more than 3,000 pages of newspaper from 16 periodical titles, to classify surge events. Because some of the anecdotal narratives found in this research provided damage descriptions without listing maximum surge heights, this study

utilized 30 quotes from regional tropical cyclone literature to create a system that estimates maximum surge height from damage descriptions. This research classified the maximum surge height and peak surge location for 241 surge events, of which 193 were at least 1.22 meters high.

This database provides crucial storm surge observations that will improve public education for this deadly hazard, while providing empirical data that may ameliorate the accuracy of surge forecasting models. Additional contributions from this study include providing data for localized and regional statistical analysis, as well as contributing data to improve the understanding of the relationship between tropical cyclone characteristics and resultant peak surge heights.

CHAPTER 3. PERSPECTIVES ON STORM SURGE ACTIVITY THROUGH SPATIAL ANALYSIS, TIME SERIES ANALYSIS AND CORRELATION TESTS

3.1 Introduction

Tropical cyclone-generated storm surges create natural disasters that are among the most catastrophic to impact the United States. The most extreme impacts of this hazard, in terms of both loss of life and property damage, have occurred along the Gulf of Mexico. Examples of such disasters include the 1900 Galveston Hurricane, which claimed more than 6,000 lives (Rappaport and Fernandez-Partagas 1995), and Hurricane Katrina, the damage from which totaled more than 80 billion U.S. dollars (McTaggart-Cowan et al. 2008).

As storm surge is a complex hazard that is poorly understood, increased understanding and awareness of surge risks would benefit broad segments of society with interests along the U.S. Gulf coast. Coastal populations would benefit from increased awareness, as more people would likely heed evacuation warnings if they were better informed about the characteristics and risks of storm surge. Emergency management workers, military response units, law enforcement personnel, and health care workers would benefit from information that could help them improve emergency preparations. Planners, developers, and insurance providers would benefit from data that could help them make improved development and financial decisions, which could help mitigate economic losses. Finally, the scientific research community would benefit from the availability of surge data and statistical surge analyses, which would likely improve surge forecasting.

Recent studies have discovered spatial and temporal trends related to the frequency of hurricane strikes along the U.S. coastline. Elsner et al. (2006) estimated

return periods of a hurricane at least as intense as Hurricane Katrina between Texas and Maine, and between Texas and Alabama. Parisi and Lund (2008) estimated return periods of category 1-5 hurricane strikes along the entire U.S. coast, from Texas to Maine. Keim et al. (2007) calculated the return periods of major hurricane strikes (winds > 50 m/s), hurricane strikes (winds > 33 m/s), and tropical storm strikes (winds > 17 m/s), at 45 specific locations from Texas to Maine.

Several studies characterized hurricane frequency trends for the entire North Atlantic basin. Landsea et al. (1999) found that multidecadal variability predominantly influenced hurricane frequencies over time. Holland and Webster (2007) concluded that multi-decadal North Atlantic hurricane activity is best described as three periods of relatively consistent frequencies separated by sharp transitions. Finally, Goldenberg et al. (2001) predicted that enhanced levels of hurricane activity observed from 1995 to 2005 were likely to persist for an additional 10 to 40 years.

Additional studies investigated correlations between climatic teleconnections and hurricane activity in the North Atlantic basin. These teleconnections are anomalous atmospheric or oceanic conditions that affect circulation patterns, sometimes over distances of thousands of kilometers. Variability in these patterns impact North Atlantic hurricane activity, as anomalous phases of these climate variables influence the development of hurricanes, as well as their tracking patterns.

Significant correlations between the El Niño-Southern Oscillation (ENSO) teleconnection and hurricane activity in the North Atlantic are well-established (Gray 1984); (Bove et al. 1998); (Landsea et al. 1999); (Murnane et al. 2000); (Saunders et al. 2000); (Elsner et al. 2001); (Jagger et al. 2001); and (Mestre and Hallegatte 2008). The

equatorial eastern Pacific Ocean warms during El Niño events, enhancing atmospheric convection in this region, which, in turn, increases wind shear and hinders formation of tropical cyclones over the western North Atlantic basin. North Atlantic Sea Surface Tempertures (SSTs) are also positively correlated with hurricane variability in that same basin, as hurricane activity increases during periods of higher SSTs (Saunders and Harris 1997); (Kimberlain and Elsner 1998); (Landsea et al. 1999); (Goldenberg et al. 2001); and (Elsner et al. 2008). Saunders and Harris (1997) concluded that variations in North Atlantic SSTs are the predominant cause of variability in North Atlantic hurricane activity. Elsner et al. (2001); and Jagger et al. (2007) correlated negative phases of the North Atlantic Oscillation (NAO) with increased probabilities of U.S. hurricanes, as the mid-oceanic high weakens and moves southwest during negative NAO phases, encouraging hurricanes that develop off the coast of Africa or in the Caribbean Sea to track further west and threaten the U.S. coastline. Elsner and Jagger (2008) confirmed a significant negative correlation between U.S. hurricane landfalls and solar activity. They found that hurricane activity decreases when solar intensity increases, because increased levels of radiation heat the upper layers of a hurricane, reducing the maximum potential cyclonic intensity. Additional environmental variables that influence hurricane activity include the stratospheric Quasi-Biennial Oscillation, Caribbean sea-level pressures and 200mb zonal winds, and African West Sahel rainfall activity (Landsea et al. 1999).

While the aforementioned analyses correlate environmental conditions with hurricane activity, and offer utility for predicting risk of hurricane strikes, such studies offer limited insight into the correlation between environmental conditions and storm surge activity, as relationships between tropical cyclone characteristics and resultant

maximum surge heights are not well understood. Although enhanced levels of hurricane activity in the North Atlantic likely increase frequencies and magnitudes of surge events along the U.S. coastline, statistical analyses of potential correlations between surge activity and environmental conditions are required to understand these relationships more clearly.

3.2 Objectives

While previous studies analyzed relationships between teleconnections and hurricanes, there is an absence of similar studies that examine storm surge. As such, the unique storm surge database developed in Chapter 2 provides unprecedented opportunities to analyze storm surge activity along the U.S. Gulf coast. This chapter analyzes this hazard through three primary objectives.

- Map the location and height of the peak storm surge levels for all 193 surge events provided in the 130-year surge database and to examine spatial patterns of surge;
- Analyze time series of surge frequencies and magnitudes over time to examine trends in the data;
- Analyze potential relationships between environmental conditions and storm surge activity. Predominantly, this chapter will investigate relationships between storm surge activity and ENSO activity (Southern Oscillation Index), the NAO index, North Atlantic SSTs (Atlantic Multidecadal Oscillation) index, and solar activity (Sun Spot Numbers).

3.3 Spatial Analysis

Locations of peak surge level for all 193 events in the storm surge database were plotted in a Geographic Information System (GIS) (See Figure 3.1). The unique point plotted for each event represents the location of peak surge level, even though the surge associated with many of these events inundated extensive portions of the coast. The associated database was then populated with the surge height for each event. Multiple peak surges in one location are depicted by a linear progression of points proceeding inland perpendicular to the coastline. In these cases events plotted closer to the coast receive higher surge values. Cartographically, circles depict all surge events; larger, darker circles represent larger magnitude events. Therefore, surge history at locations that observed multiple peak surges is plotted in a linear fashion, with larger, darker circles, representing larger magnitude events, closer to the coast.

Plotting peak surge locations and heights in a GIS environment forms the foundation for a wide variety of surge analyses, as the database can be populated with descriptive and quantitative information associated with each surge event. Information such as storm name, storm dates, the name of peak surge location, and the date and time of peak surge, provide broader descriptions of each surge event. The foundational mapping work conducted in a GIS environment also enables spatial analysis of surge patterns in relation to atmospheric teleconnections in subsequent discussion.

3.3.1 Discussion of Spatial Surge Patterns

Surge activity is greatest along much of the central and western Gulf, from approximately Dune Allen Beach, Florida, westward along the extreme western Florida Panhandle, and the Alabama, Mississippi, Louisiana and Texas coasts. The Florida Keys

also experience heightened surge activity. Locations in the Florida Panhandle east of Dune Allen Beach, however, as well as the entire west coast of Florida, depicted noticeably lower storm surge frequencies and magnitudes.

The pattern of observations for surge events with peak magnitudes ≥ 4m characterizes the distinction between enhanced activity in the central and western Gulf and reduced activity along the eastern Gulf coast, especially along the west coast of

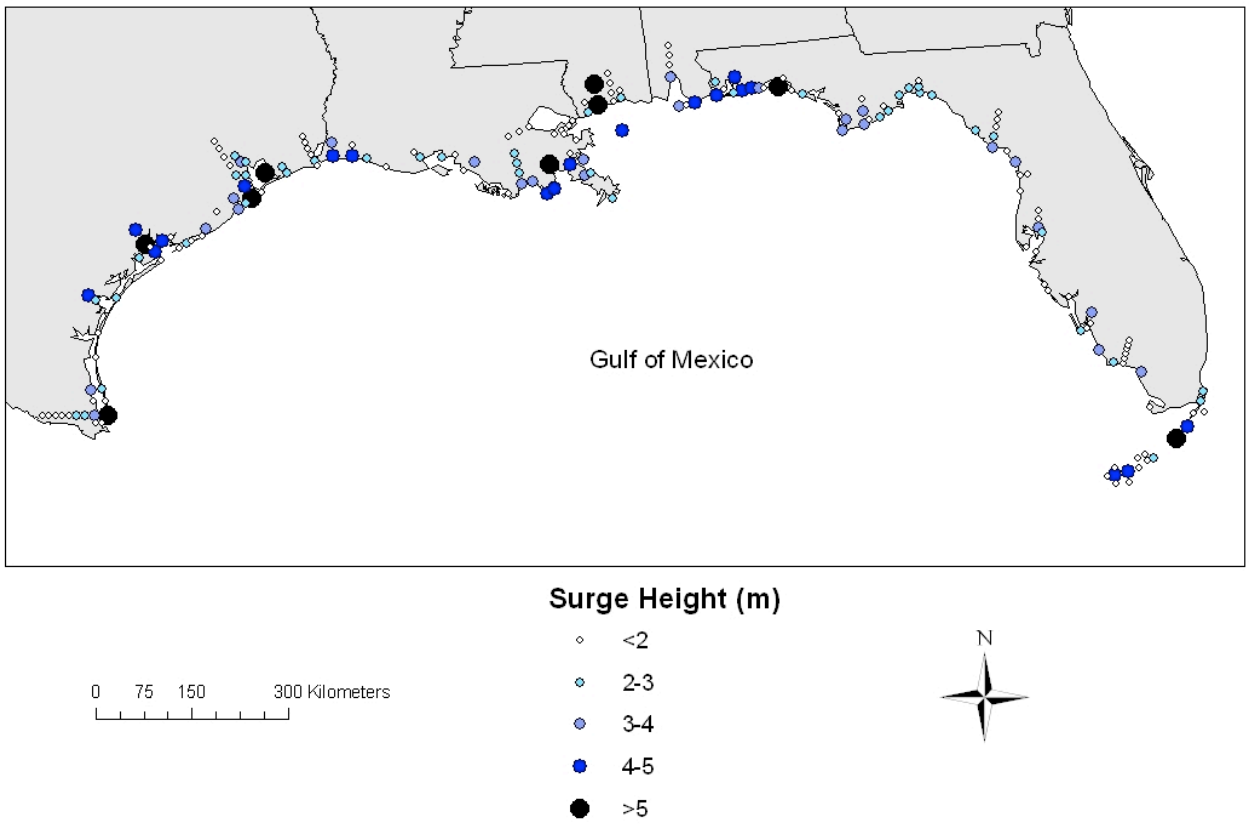

Figure 3.1: Location and height of peak storm surge levels along the U.S. Gulf coast from 1880 to 2009.

Florida. Of these 28 surges, 24 are located in the western and central Gulf, while the remaining four events occurred in the Florida Keys. None of these surges occurred along the west coast of Florida, east of Dune Allen Beach.

Figure 1 also reveals that the largest magnitude events, those ≥ 5 meters, typically occured along the Texas, Louisiana and Mississippi coasts, where seven of the nine events occurred. These observations reinforce the urgency of surge research in the western Gulf.Pass Christian, Mississippi observed the two highest surges, Hurricane Katrina's (2005) 8.47-meter surge, and Hurricane Camille's (1969) 7.5-meter surge. These extraordinary events are not likely coincidental. The shallow waters south of the Mississippi coast, associated with deltaic lobes from the Mississippi River, likely contributed to enhanced surge levels in this area. Chen et al. (2008) hypothesize that Hurricane Katrina may have produced a maximum surge height four meters lower had Katrina tracked over the wide, sloping continental shelf located off the coast of Alabama.

South Padre Island, Texas observed nine peak surges- the most of any location. The high frequency of peak surges at this location can be explained, at least in part, by its position as the southernmost barrier island along the Texas coast. Landfalling hurricanes in Mexico produced several of these events, enabling South Padre Island to record the highest U.S. surge, as surge levels generally decreased as distance from the hurricane increased. Galveston, Texas, observed eight surges, the second highest of any location along the Gulf Coast.

3.4 Analysis of Trends in Surge Frequencies and Magnitudes

3.4.1 Annual Frequency Series

Time series plots are useful for understanding changes in frequencies and magnitudes over time. The annual frequency series depicts the number of "major" surges

(maximum surge height ≥ 3m), and the number of "minor" surges (maximum surge height ≤ 3m) (Figure 3.2). Red line segments depict major surges, while blue line segments depict minor surges. As these line segments are stacked, the total height of both segments combined depicts the number of observed surges in a given year along the U.S. Gulf Coast.

The frequency of total annual surges generally increased from the start of the time series until approximately 1965. The period from 1966 until 1994 experienced reduced surge frequencies, especially between the years 1966 through 1984. Surge frequencies dramatically increased during the period 1995 to 2009.

Missing data in the early portion of the study period likely contributed to low annual frequencies, particularly before 1929. Especially missing from the dataset are minor surges, as records from many of these smaller events probably did not endure through time. This likely explains the much higher proportion of major surges compared to minor surges in the early part of the record. Major surges generally inflicted substantial damage, increasing the likelihood that anecdotal accounts of these events were recorded. Between 1880 and 1928, the database records 24 minor surges and 22 major surges, a ratio of 1.1 minor surges to every major surge. This ratio increases to 3.7 minor surges to every major surge between 1929 and 2009. Between 1929 and 2009, only 1.4 percent of potential surge events are missing from the database (see Chapter 2), meaning that the vast majority of events, including minor surges, are likely recorded. The proportion of missing data increases to 14 percent for the entire 130-year dataset.

SST variability likely also impacts variations in surge activity. Table 3.1 depicts warm and cold phases of the Multidecadal mode, a two-phase mode derived by SST

anomaly data, now commonly called the Atlantic Multidecadal Oscillation (AMO), as defined by Landsea et al. (1999).

Warm and cold phases of this mode oscillate, with each phase lasting between approximately two and four decades. The cold AMO phase experienced between 1894 and 1925, in conjunction with higher proportions of missing data from this period, likely contributed to suppressed surge frequencies in the database. Better data quality combined with a shift to the warm AMO phase likely explains increased surge frequencies from the 1930s until the mid-1960s. Reduced surge frequencies correlate well with the cold AMO phase from the 1970s through the early 1990s, while increased activity between 1995 and 2009 coincides with the most recent shift to the warm phase. The two most active surge seasons, in terms of total observed surges, both occurred within this most recent warm phase. Nine surges, including three major surges, were observed in 2005, and five surges occurred in 1998.

Two interesting observations should be noted in regard to surge frequencies over time. The first observation is that the same number of total surges and major surges are observed during the first half and second half of the period with the most accurate data, 1929 to 2009. The first half of this period, 1929 to 1969.5 (1969 is split between the first and second halves), observes 73.5 surges and 15.5 major surges, the exact number as the 1969.5 to 2009 period (Table 3.2). The second observation is that the early portion of this study identified more major surges than the latter portion, even though the latter portion contains more comprehensive data. The early half of the storm surge database, the 65-year period from 1880 to 1944, observes 27 major surges, whereas only 26 major surges are observed between 1945 and 2009 (Table 3.2). Also, the first 49 years (1880 to 1928)

identify 22 major surges, or an average of .45 surges annually, whereas the last 81 years of this study (1929 to 2009), the period with the most accurate data, observes only 31 surges, or an average of only .38 surges annually. Surprisingly, the majority of those first 49 active years belonged to the AMO cold phase, which lasted from 1894 to 1925.

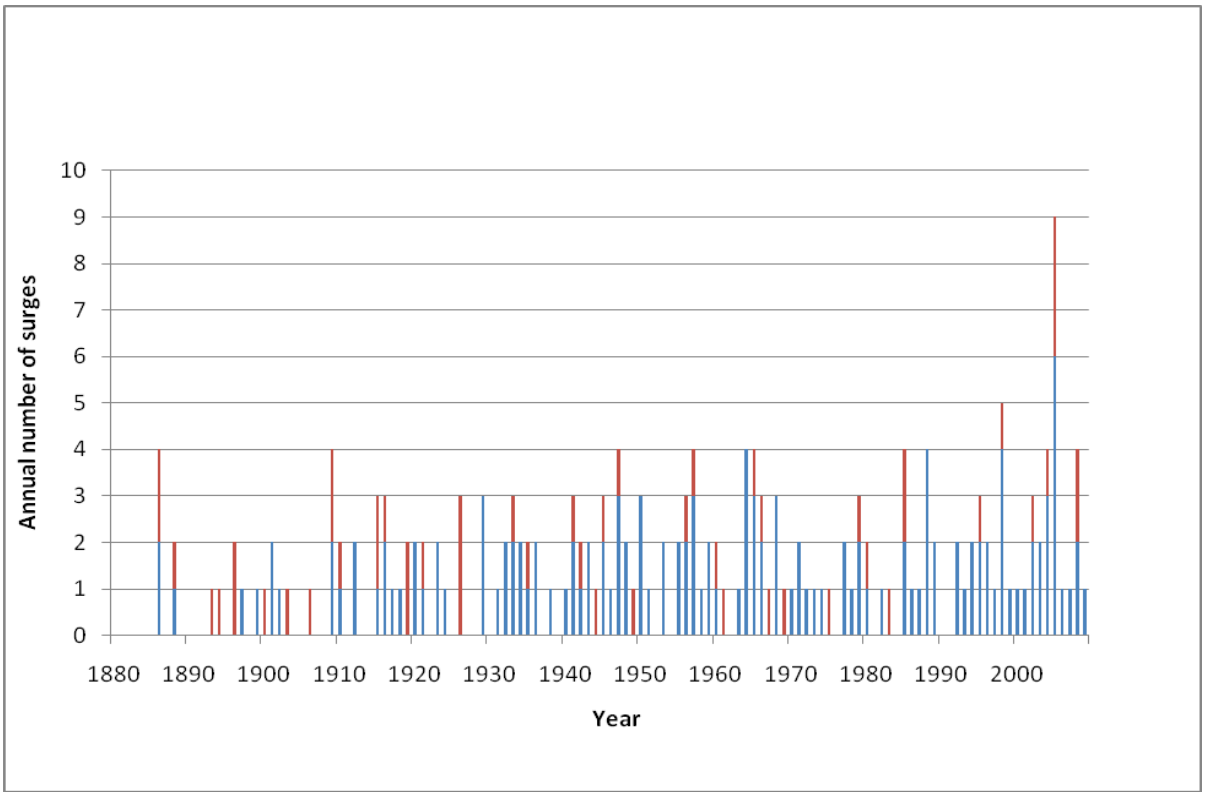

Figure 3.2: Annual surge frequencies along the U.S. Gulf Coast from 1880 to 2009. Blue line segments depict minor surges (≤ 3m). Red line segments depict major surges (≥ 3m).

Table 3.1: Atlantic Multidecadal Oscillation (AMO) phases, as defined by Landsea et al. (1999).

Time Period	AMO Phase
1857 to 1868	Indeterminate
1869 to 1893	Warm North Atlantic
1894 to 1925	Cold North Atlantic
1926 to 1970	Warm North Atlantic
1971 to 1994	Cold North Atlantic
1995 to 2009	Warm North Atlantic*

* Originally classified as indeterminate

Table 3.2: Comparison of surge frequencies and major surge frequencies in the first and second halves of the time periods 1880 to 2009, and 1929 to 2009.

Time Period		All surges (≥ 1.22m)	Major surges (≥ 3m)
130 years	1880-1944 (65 years)	71	27
	1945-2009 (65 years)	122	26
81 years	1929-1969.5 (40.5 years)	73.5	15.5
	1929-1969.5 (40.5 years)	73.5	15.5

3.4.2 Annual Series of Maximum Surge Magnitudes

An annual series is a list of maximum annual magnitudes. In this case, an annual series of surge data lists the highest annual maximum surge level observed along the entire U.S. Gulf Coast (Figure 3.3). Although missing data are evident before approximately 1930 in the annual series, numerous surges ≥ 4m are observed in the record. A period of relatively high magnitude surges occurred from the 1930s to 1940s. Although the Carolinas observed high magnitude events in the early 1950s (Keim et al. 2007), the Gulf of Mexico observed slightly decreased levels. Surge magnitudes increased once again from the late 1950s to 1960s, culminating with Hurricane Camille's (1969) 7.5-meter surge. A sudden decrease in magnitudes is apparent from 1970 until 1994, especially during the early 1990s. Magnitude levels dramatically increased from the mid-1990s until the end of the record.

These patterns generally parallel the variability of the annual frequency series. In both datasets, missing data are apparent in the early part of the record, followed by increasing activity from approximately the 1930s until the 1960s, reduced activity in the 1970s until early 1990s, and, finally, dramatic increases in the last fifteen years of the record. A slight, but interesting, difference is visible in these records during the late

1960s. Reduced activity, associated with the transition into the AMO cold phase, appears to commence for the annual frequency series in 1966, after the 1964 and 1965 seasons both observed four surges, a level that was not again repeated for 20 years. Decreased activity in the annual series of maximum magnitudes, however, is delayed approximately four years, as the late 1960s observed unusually high magnitudes. Hurricane Beulah's (1967) 5.5-meter surge, and Hurricane Camille's (1969) 7.5-meter surges, which ranked 7th and 2nd, respectively, on the all-time surge list, both occurred during this span. Ironically, they were both the only observed surges in their respective years. During this brief period, it appears as though annual surge frequencies were already declining, but the few surges that did occur were catastrophic. Reduced levels of maximum annual surge magnitudes eventually coincided with annual frequencies, beginning in approximately 1970.

3.5 Testing for Relationships between Climatic Variables and Surge Activity

Potential relationships between environmental conditions and surge activity were investigated. The climatic variables tested included the Southern Oscillation Index (SOI), the North Atlantic Oscillation (NAO) index, and Sun Spot Numbers (SSN), which indicate solar activity. The SOI, AMO index, and NAO index are chosen because they correlate the strongest with North Atlantic hurricane activity. For example, exceedence probabilities of hurricane winds vary substantially with phases of ENSO, the NAO index, and North Atlantic SSTs (Jagger et al. 2001); (Jagger and Elsner 2006); (Jagger et al. 2007). This chapter also investigates potential relationships between surge activity and solar activity because recent research (Elsner and Jagger 2008) has proven that high sunspot numbers correlate with fewer intense tropical cyclones in the Gulf of Mexico.

Testing these four variables for correlations with surge activity relates well to research conducted by Elsner et al. (2009), which tests these same four variables to construct a visibility network that identifies unusual years from a time series of U.S. hurricane counts.

Indices associated with each of these variables are tested for correlation with six annual frequency series- the annual frequency series for all surges and major surges during the periods 1880-2009 (130 years), 1900-2009 (110 years), and 1929-2009 (81 years). These dates are chosen because data quality improves for each successive period. Indices are also tested for correlation with an annual series of maximum surge magnitudes corresponding with each of these three time periods. Therefore, nine tests are

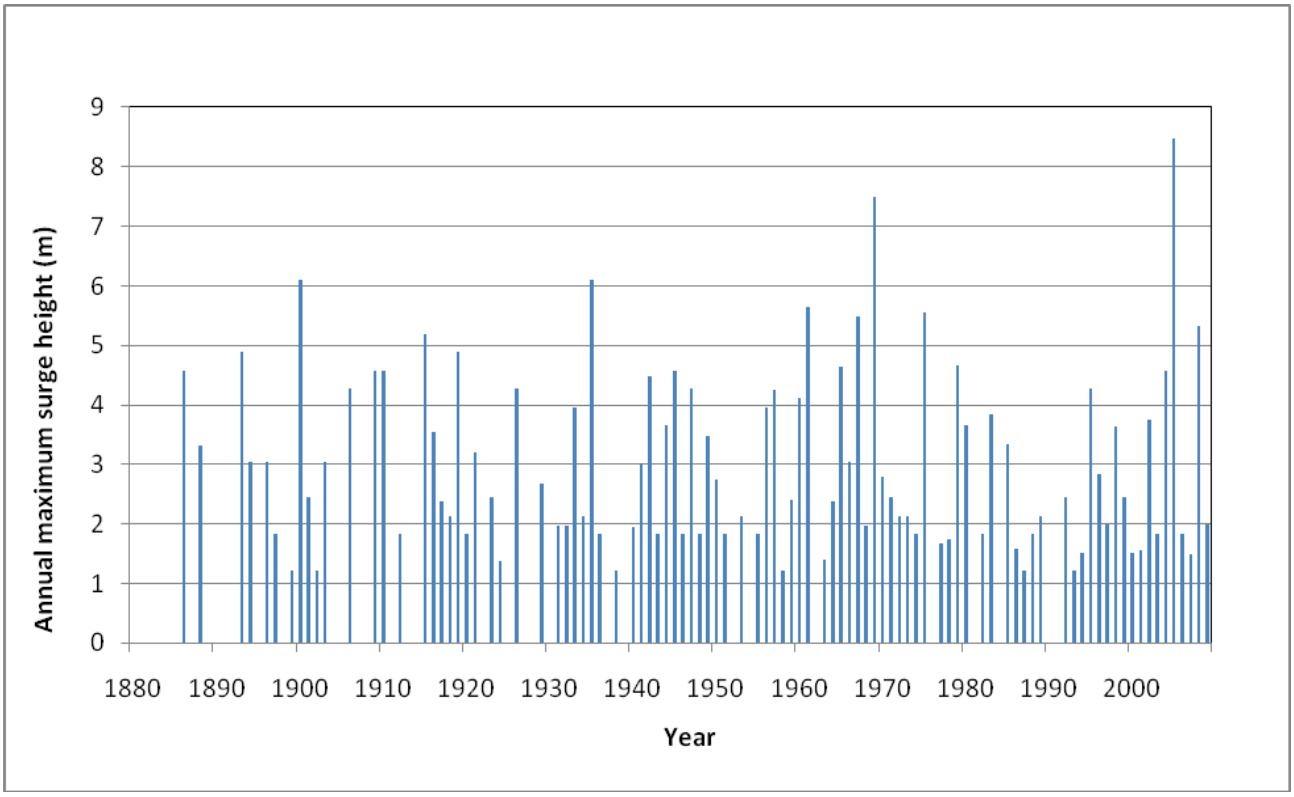

Figure 3.3: Annual series depicting maximum annual surge magnitudes along the U.S. Gulf coast from 1880 to 2009.

run for each index, six related to annual frequency series and three related to annual series of maximum surge magnitudes. Tables 3.3a-f reveal results of these tests. Spearman rs values indicate direction and strength of the correlation, with higher values indicating stronger correlation. Confidence levels for these correlations are determined as percentages, and are calculated by the equation "confidence level = (1- probability values) x (100)," indicating that smaller probability values (p-values) represent higher confidence levels.

3.5.1 Southern Oscillation Index (SOI)

The SOI measures normalized sea level pressure differences between Tahiti and Darwin, Australia. Ropelewski and Jones (1987) developed a method to calculate monthly index values, which are made available through the Climatic Research Unit (CRU) of the University of East Anglia. El Niño events are associated with negative index values, as the SOI is anti-correlated with equatorial Pacific SSTs (Jagger and Elsner 2008). During El Niño events, enhanced convection over the eastern Pacific increases wind shear over the western North Atlantic, suppressing development of Atlantic tropical cyclones. As the ENSO phase during the North Atlantic hurricane season correlates the closest with tropical cyclone development in that basin, August to October monthly SOI values were averaged, creating one index value per hurricane season, in accordance with methods utilized by Jagger and Elsner (2008).

The SOI is essentially the atmospheric component of the El Niño Southern Oscillation (ENSO) teleconnection. It is chosen for statistical testing over other possible ENSO indices, such as Niño 3.4- a popular index often utilized in climate studies, based on equatorial Pacific SSTs. Although the SOI is noisier than the Niño 3.4 index (Jagger et al.

2007), as atmospheric pressure varies more frequently than SSTs, this chapter employs the SOI for several reasons. The SOI utilizes observed climate data for a longer period than Niño 3.4, as the SOI uses historical atmospheric pressure readings to construct the index back to 1866 (Elsner and Jagger 2005). Niño 3.4, however, relies on Pacific SST data, which had not been consistently observed until the satellite era. Also, the precedent of utilizing the SOI for North Atlantic hurricane research is well established. Elsner and Jagger (2005), Jagger et al. (2007), Jagger and Elsner (2008), and Mestre and Hallegatte (2008) all utilize this index as an indicator of the ENSO phase.

3.5.1.1 Discussion of SOI Correlations

The SOI correlated positively with surge frequencies and magnitudes. The tests between the SOI index and every surge time series produced higher Spearman r-values than tests utilizing any other climatic variable in this study. Spearman r-values for the surge frequency tests ranged from .1683 to .2236.

Confidence levels of these tests were higher than all other climatic variables, with the exception of the 110-year major surge frequency test, in which the confidence level of the NAO index was even higher than the SOI index. Confidence levels for these results exceed 95% for the 130-year major surge test, and both the 110-year total surge test and 110-year major surge test

Spearman r-values for the three magnitude tests were even higher, and very consistent with each other. Values ranged from .2466 to .2475. Confidence levels for all three of these tests exceeded the 95% level.

Basically, this means that we can expect higher surge frequencies and magnitudes when SOI values are elevated, and La Niña conditions prevail. This may be useful information for predicting surge activity along the Gulf Coast.

Tables 3.3a-f Results of correlation tests comparing climatic indices and annual surge frequencies or maximum annual surge magnitudes. Spearman r-values indicate direction and strength of the correlation. Percentage confidence levels for these correlations are calculated by the equation (1- probability values) x (100).

a. Annual surge frequency test for the period 1880-2009 (130 years)

Variable	All surges (surge level ≥ 1.22m)		Major surges (surge level ≥ 3m)	
	Spearman r	P-value	Spearman r	P-value
NAO	-.1630	.0622	-.2145	.0144
SOI	.1702	.0530	.1823	.0380
SSN	-.0231	.7937	.0068	.9389
SST	.1463	.0967	.1371	.1197

b. Annual surge frequency test for the period 1900-2009 (110 years)

Variable	All surges (surge level ≥ 1.22m)		Major surges (surge level ≥ 3m)	
	Spearman rs	P-value	Spearman rs	P-value
NAO	-.1559	.1037	-.2415	.0112
SOI	.2020	.0345	.2236	.0190
SSN	-.0204	.8320	-.0003	.9973
SST	.1750	.0675	.1477	.1234

c. Annual surge frequency test for the period 1929-2009 (81 years)

Variable	All surges (surge level ≥ 1.22m)		Major surges (surge level ≥ 3m)	
	Spearman rs	P-value	Spearman rs	P-value
NAO	-.1137	.3116	-.1422	.2049
SOI	.1989	.0752	.1683	.1330
SSN	-.0456	.6858	-.0023	.9834
SST	.0673	.5497	.1265	.2597

d. Maximum annual surge magnitude test for the period 1880-2009 (130 years)

Variable	Spearman rs	P-value
NAO	-.0810	.4346
SOI	.2475	.0158
SSN	.0079	.9390
SST	.0348	.7376

e. Maximum annual surge magnitude test for the period 1900-2009 (110 years)

Variable	Spearman rs	P-value
NAO	-.0933	.3865
SOI	.2469	.0206
SSN	-.0126	.9068
SST	.0394	.7151

f. Maximum annual surge magnitudes for the period 1929-2009 (81 years)

Variable	Spearman rs	P-value
NAO	-.0327	.7877
SOI	.2466	.0398
SSN	-.0228	.8507
SST	.0218	.8577

3.5.2 Sea Surface Temperatures (Atlantic Multidecadal Oscillation)

The Atlantic Multidecadal Oscillation Index is utilized as an indicator of SST anomalies in the North Atlantic. This index, which is derived through SST data, is utilized to classify the AMO into warm and cold phases, a topic that is discussed in greater length in the surge frequency analysis portion of this chapter. Data are obtained from the National Oceanic and Atmospheric Administration's (NOAA) Earth System Research Laboratory- Physical Sciences Division. These data, which covers the period 1856 to present, computes area-weighted averages, covering the North Atlantic Ocean from latitudes 0 to 70 degrees north. Jagger and Elsner (2008) also utilized area-weighted SST coverage for the North Atlantic, covering the same latitudes. Although Jagger and Elsner (2008); and Elsner et al. (2008) averaged monthly SST anomalies from August to October, this chapter averages monthly SST anomalies from July to October. July is included because SST anomalies in this month correlate well with hurricane activity, yet the North Atlantic basin is not as tropically active as it is from August to October. High levels of hurricane activity from August to October generally have a cooling influence on SSTs, therefore, reducing positive SST anomalies that may have enhanced hurricane development in the first place.

3.5.2.1 Discussion of Sea Surface Temperature Correlations

SSTs correlated positively with surge frequencies in all six tests. Spearman r-values ranged from .0673 to .1750 (Tables 3.3 to 3.5), and were highest for the two 110-year tests. Although none of these correlations exceeded the 95% confidence level, the 110-year test of all surge frequencies produced a Spearman r-value of .1750, at a confidence level that exceeded 93%.

SSTs also correlated positively with surge activity in all three surge-magnitude tests. However, the correlations were weak, as Spearman r-values ranged from only .0218 to .0348. As might be expected, confidence levels of these correlations were low, as probability values ranged from .7151 to .8577 (Tables 3.6 to 3.8).

3.5.3 North Atlantic Oscillation (NAO)

The NAO index is comprised of the difference in sea level pressure between Gibraltar and a station in southwest Iceland (Jones et al. 1997). This index is utilized as an indicator of atmospheric pressure patterns in the North Atlantic, which impacts North Atlantic hurricane tracks (Elsner et al. 2001); (Jagger and Elsner 2008). High NAO values indicate that the mid-oceanic high pressure system, commonly referred to as the Bermuda or Azores High, is stronger than normal and shifted eastward, enabling Atlantic hurricanes to curve northward, reducing the threat of landfalls in the southeast U.S. and the Gulf of Mexico (Elsner et al. 2001). Low NAO values correspond with weaker mid-oceanic high pressure, shifted to the southwest, which encourages hurricanes to track westward parallel to latitude lines, and, therefore, increases the probability of hurricane impacts to the southeast U.S. and Gulf of Mexico (Elsner et al. 2001).

Surge activity is tested against the May-June NAO index average, as the index values for these two months correlate best with hurricane tracking variability (Elsner et al. 2001); (Jagger and Elsner 2008). In accordance with Elsner et al. (2001) and Jagger and Elsner (2008), NAO index data are obtained from The Climatic Research Unit (CRU). CRU's NAO data Webpage (http://www.cru.uea.ac.uk/cru/data/nao/) provided the NAO index values for the period 1880 to 2000, and Tim Osborn's climate data Webpage, also made available through CRU

(http://www.cru.uea.ac.uk/~timo/datapages/naoi.htm), provided index values from 2001 to 2009.

3.5.3.1 Discussion of NAO Correlations

The NAO index correlated negatively with surge frequencies in all six tests. Spearman r-values ranged from -.1137 to -.2415 (Tables 3.3 to 3.5). Probability values indicate that the correlation between major surge frequencies in the 130-year and 110-year dataset and the NAO index exceeds the 95% confidence level.

The NAO index also correlated negatively with surge activity in all three surge-magnitude tests. However, the correlation was not as strong, and confidence levels were lower. Spearman r-values ranged from -.0327 to -.0933 (Tables 3.5 to 3.7), and probability values ranged from .3865 to .7877.

3.5.4 Sun Spot Numbers (SSN)

Monthly total sunspot numbers (SSN) are utilized as an indicator of solar intensity. In accordance with Elsner and Jagger (2008), September sunspot numbers are used for testing, because September corresponds with the peak of hurricane season in the North Atlantic. Solar data are obtained from the Solar Influences Data Analysis Center (SIDC) in Brussels, Belgium, which provides these data beginning in the mid-18th century. In congruence with the other climatic variables, sunspot data are tested against annual surge frequency and magnitude data.

3.5.4.1 Discussion of SSN Correlations

No significant relationships were discovered between solar activity and annual surge frequencies. In fact, the probability values of the sunspot vs. surge frequency correlation tests indicate that the relationship between solar activity and surge frequency

was less significant than any other climatic variable. Probability values ranged from .6858 to .9973 (Tables 3.3 to 3.5).

Similar results were found in the correlation test between solar activity and annual maximum surge magnitudes. No significant relationships were discovered for all three time periods, and the probability values were the highest of any climatic variable for the 130-year and 110-year test. Probability values ranged from .8507 to .9390 (Tables 3.6 to 3.8).

3.6 SOI Tercile Analysis

The SOI index is derived by the difference in sea level air pressure at Tahiti and Darwin, Australia. As air pressure at Tahiti is usually higher, the index is normalized to account for typical air pressure values. Positive index values indicate that air pressure differences between these sites is greater than normal, negative values indicate that the difference is less than normal, or that the air pressure at Darwin is actually lower than Tahiti. High index values are classified as La Niña phases, and low index values are classified as El Niño phases.. Average annual August to October SOI values were divided into terciles, or groups that contained the highest one-third, the middle one-third, and the lowest one-third values. The upper, middle and lower terciles are associated with SOI values ranging from .24 to 2.61, -.63 to .21, and -2.33 to -.66, respectively. Because the entire dataset contains 130 years of data, each group contained either 43 or 44 values. The lower tercile is the most descriptive of El Niño conditions, however, this does not mean that every year in this tercile was scientifically classified as an El Niño year. Likewise, the upper tercile generally describes La Niña conditions. The middle tercile is best described as neutral.

Table 3.4 depicts the total number of all surges (≥ 1.22m), major surges (≥ 3m), and extreme surges (≥ 5m) that occurred during each period. As expected, the highest number of surges in all three categories occurred during "La Niña" years. The lowest number of surges in all three categories occurred in "El Niño" years, with the exception of extreme surges, as "Neutral" and "El Niño" years both observed two extreme events.

Table 3.4: The number of surges ≥ 1.22m, 3m, and 5m, corresponding with SOI indices in the upper one-third, middle one-third, and lower one-third terciles between 1880-2009.

Tercile	Surges ≥ 1.22m	Surges ≥ 3m	Surges ≥ 5m
Upper one-third (La Niña)	73	23	5
Middle one-third (Neutral)	67	19	2
Lower one-third (El Niño)	53	11	2

Figures 3.4 through 3.6 depict storm surge maps associated with each SOI tercile. As in the map previously discussed (Figure 3.1), the location and height of peak storm surge levels is mapped, with larger, darker, circles representing higher peak surge levels. The enhanced surge frequencies and magnitudes of the "La Niña" tercile, compared to the "Neutral" and "El Niño" terciles, are perhaps the most striking feature of these maps. Heightened surge activity is apparent along most of the U.S. Gulf coast, especially the central and western Gulf, as well as the Florida Keys, in association with the upper tercile. Especially noticeable are the five extreme surge events in this group, identified as the 1915 New Orleans Hurricane, the 1935 Labor Day Hurricane, Hurricane Beulah (1967), Hurricane Eloise (1975), and Hurricane Ike (2008). The most distinct feature on the "Neutral" map is increased surge activity in the Florida Panhandle and the west coast of Florida. In fact, if one considers the Mississippi/ Alabama border as a division between

the eastern and western Gulf coast, more major surges (≥ 3m) occured in the eastern Gulf (12 events) than the western Gulf (7 events) in association with this tercile, an observation that contradicts general surge patterns. Not only are surge magnitudes in the eastern Gulf higher than the western Gulf during this period, but they are also higher than the eastern Gulf during the upper tercile. Although the "El Niño" period observed the least surge activity, Apalachee Bay, Florida, observes slightly more activity during these years than other periods, and the five surges observed at Galveston, Texas, during "El Niño" years constitute the greatest number at that location. One of these events is the great Galveston Hurricane of 1900, which brings up an important point. Both Hurricane Camille (1969) and the great Galveston Hurricane, which rank all-time as the number two and three surge heights, respectively, struck during "El Niño" years. This sobering fact should caution us that although statistical analysis of predictive climatological relationships is credible and useful, it only takes one extreme event to unleash a devastating surge catastrophe.

3.7 Analysis of the AMO Data Table

Table 3.5 contains the total number and average annual number of all surges (≥ 1.22m), major surges (≥ 3m), and extreme surges (≥ 5m), observed during all years of the surge record, all warm-phase AMO years, all cold-phase AMO years, and during the five alternating warm and cold phases, classified by Landsea et al. (1999). As might be expected, the combination of all warm-phase AMO years produced higher annual averages of total surges, major surges, and extreme surges, than averages produced over the entire 130-year study. On the contrary, the combination of all cold-phase AMO years produced lower annual surge averages than the 130-year averages. Analysis of the annual

averages of all surges produced during the five alternating phases reveals that the smallest annual average occurred during the 1880-1893 warm phase, most likely because data are missing from this period. This average more than doubles during the 1894-1925 cold phase, then oscillates, as expected, with higher averages observed during AMO warm phases. The 1995-2009 warm phase experienced the highest annual average, at 2.6 surges per year. The pattern for major surges is somewhat different. Because anecdotal accounts of major surges from the late 1800s were likely recorded, problems with missing data are less evident for these events. Therefore, the 1880-1893 warm phase observes more major surges than the succeeding 1894-1925 cold phase. Surprisingly, the annual average continues declining during the 1926-1970 warm phase. The 1995-2009 warm phase experienced the highest value of any period, at .6 events annually. This period also observed the highest average number of extreme surges, .13, followed by the 1926-1970 warm phase. The cold phases observed lower values, and the 1880-1893 warm phase did not observe any of these events.

3.7.1 Analysis of AMO Maps

Figures 3.7 and 3.8 depict maps of surge activity during all AMO warm and cold phases. Enhanced surge frequencies and magnitudes are evident around the basin as a whole during AMO warm phases. An interesting observation, however, is that higher frequencies of major surges (≥ 3m) actually occurred in the eastern Gulf than in the western Gulf, during AMO cold phases, a trend that counters general patterns of surge activity. If the Mississippi/ Alabama border is chosen as a boundary between the eastern and western Gulf, 13 of these surges occurred in the east and only eight in the west. Additionally, the eastern Gulf of Mexico experienced higher frequencies of major surges

during all AMO cold-phase years than it did during all warm-phase years, a trend that contradicts variability trends in the western Gulf.

Figures 3.9 through 3.13 depict surge activity during alternating warm and cold AMO phases. The limited activity observed during the 1880 to 1893 warm phase mostly occurred in the western Gulf of Mexico. A busier map during the 1894 to 1925 cold phase suggests improved data quality over time. Similar to the map of all cold-phase AMO surges, frequencies of major surges (≥ 3 meters) in the eastern Gulf are higher than the western Gulf during this period, even though the frequencies of all surges (≥ 1.22 meters) in the western Gulf are slightly higher. Basin-wide surge activity continued to increase during the 1926-1970 warm phase. The western Gulf especially observed high surge activity, including three of the four extreme events (≥ 5 meters) experienced during this period. Surge activity decreased again during the 1971-1994 cold phase, and similar to the previous cold phase, more major surges occurred in the east than in the west during this period, although surge frequency was greater in the west. Finally, activity increased again during the 1995-2009 warm phase, especially along the central Gulf coast, where eight major surges occurred between Chambers County, Texas, and Fort Walton Beach, Florida.

Perhaps the most interesting observation from these maps is the difference between the patterns of increased surge activity in the western Gulf during AMO warm phases, compared with cold phases, in which the magnitudes of major surges in the eastern Gulf actually surpass the western Gulf. The association of landfall locations with points of tropical cyclone origin may reveal some clues regarding this variability. It is likely that surge activity in the western Gulf is affected to a higher degree by AMO phase

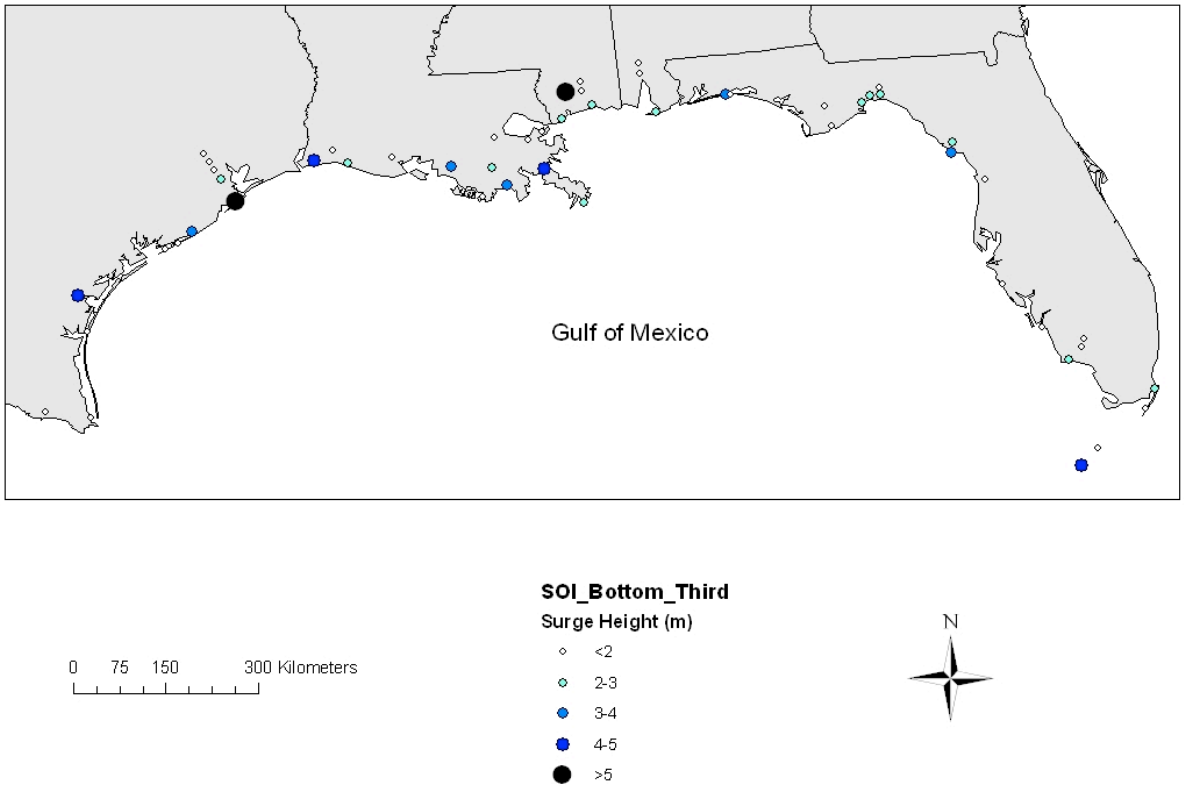

Figure 3.4: Location and height of peak storm surge levels during the lower 1/3 SOI tercile, generally associated with El Niño conditions (1880-2009).

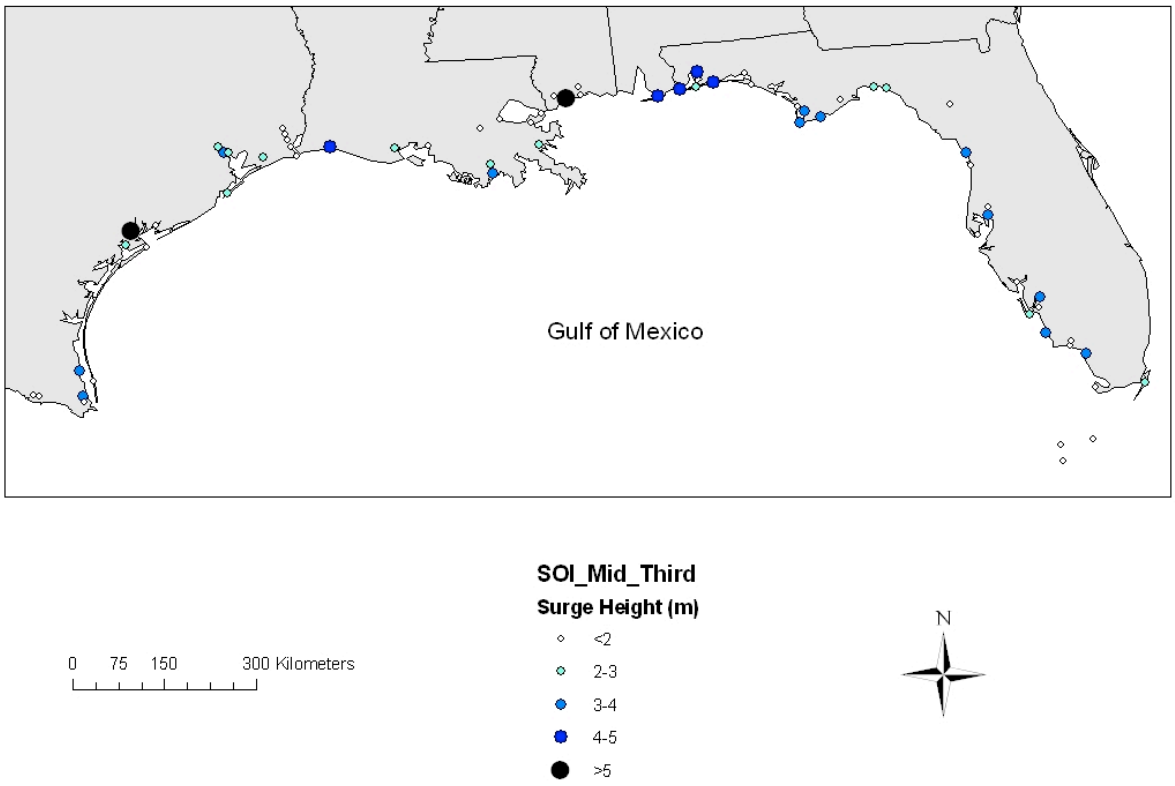

Figure 3.5: Location and height of peak storm surge levels during the middle 1/3 SOI tercile, generally associated with neutral ENSO conditions (1880-2009).

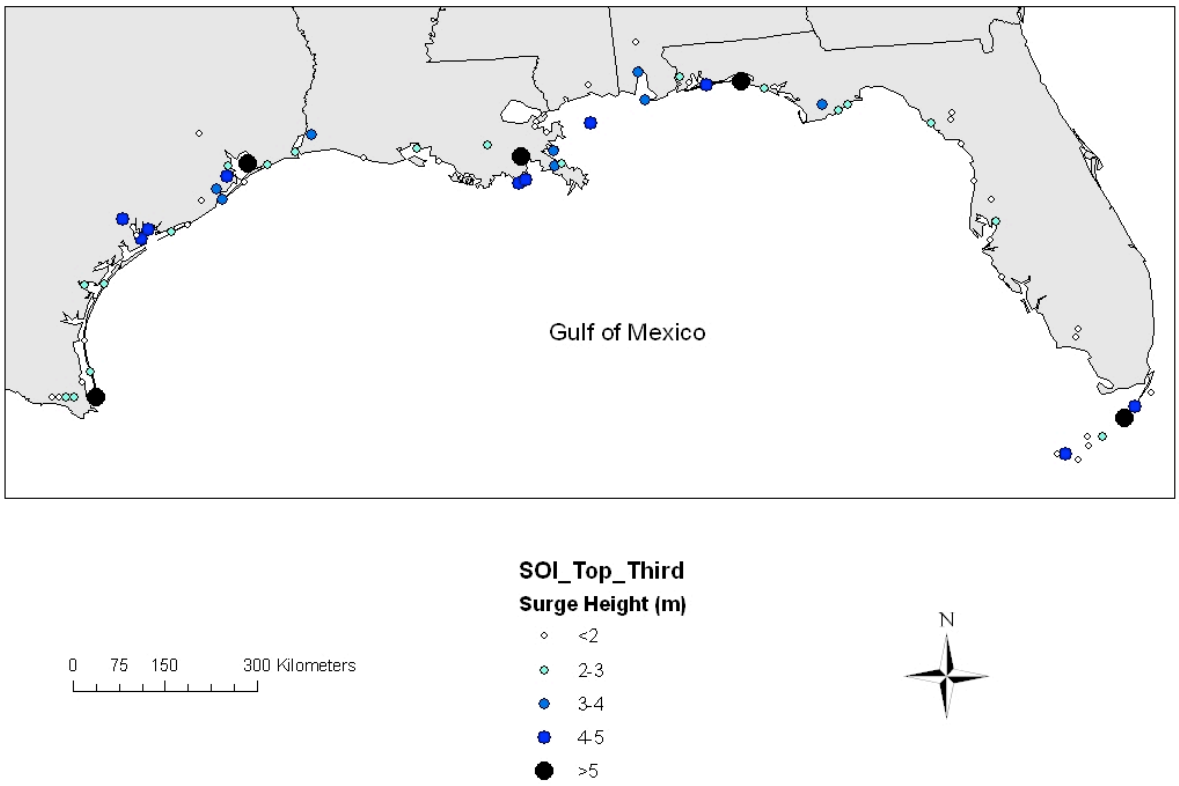

Figure 3.6: Location and height of peak storm surge levels during the upper 1/3 SOI tercile, generally associated with La Niña conditions (1880-2009).

Table 3.5: The number and annual average number of surges associated with AMO phases as defined by Landsea et al. (1999).

AMO Phase	Years	Surges ≥ 1.22m	Annual Avg ≥ 1.22m	Surges ≥ 3m	Annual Avg ≥ 3m	Surges ≥ 5m	Annual Avg ≥ 5m
All Phases for All Years	130	193	1.48	53	.41	9	.07
All Warm Phase Years	74	124	1.68	32	.43	6	.08
All Cold Phase Years	56	69	1.23	21	.38	3	.05
1880-1893 Warm Phase	14	7	.5	4	.57	0	0
1894-1925 Cold Phase	32	36	1.13	15	.47	2	.06
1926-1970 Warm Phase	45	78	1.73	19	.42	4	.09
1971-1994 Cold Phase	24	33	1.38	6	.25	1	.04
1995-2009 Warm Phase	15	39	2.6	9	.6	2	.13

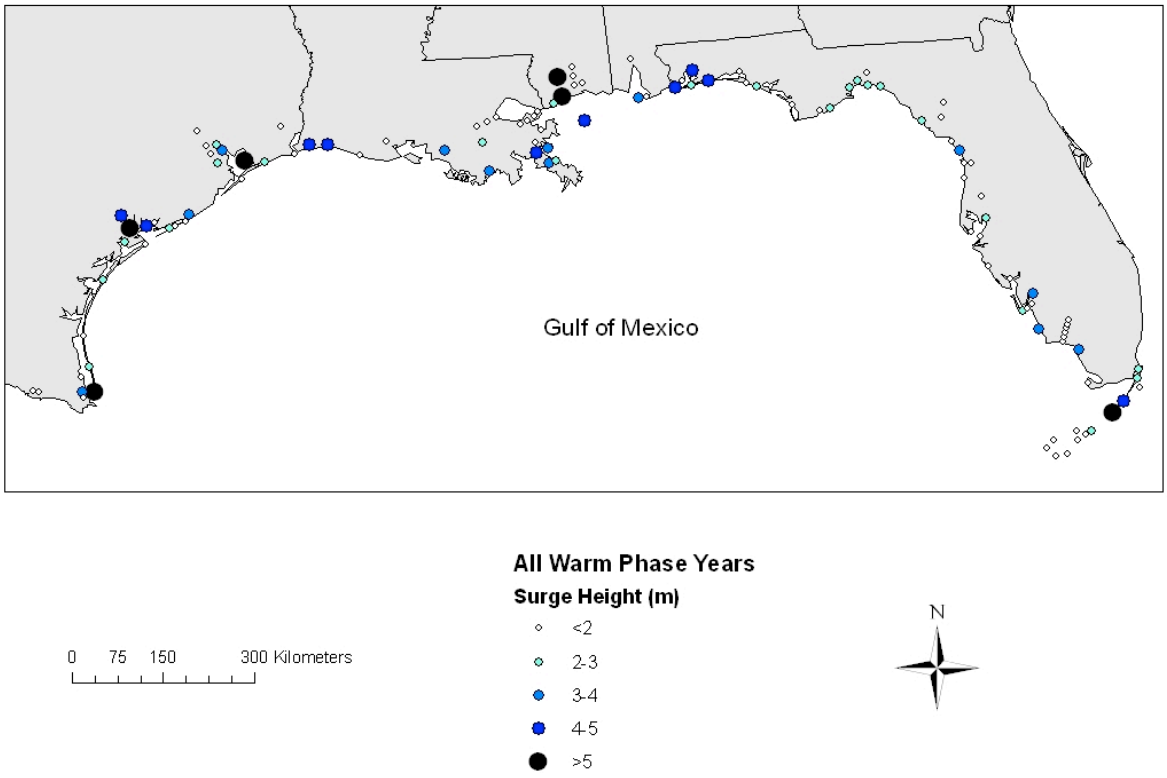

Figure 3.7: Location and height of peak storm surge levels during all AMO warm phases (1880-2009).

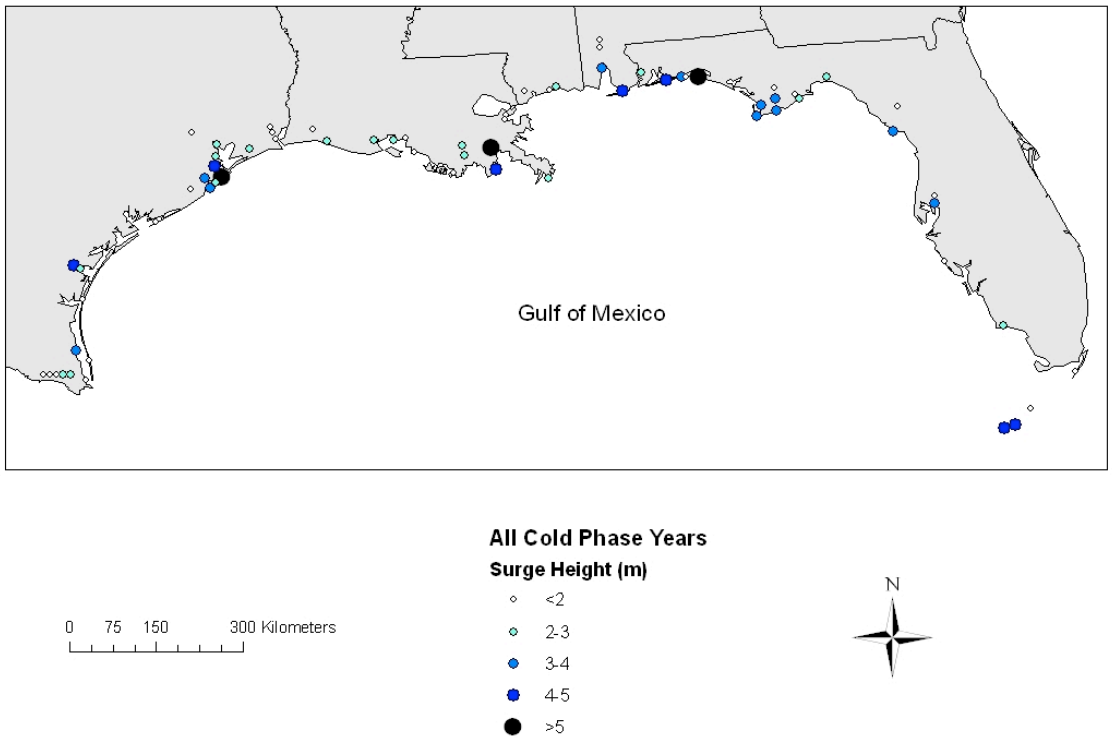

Figure 3.8: Location and height of peak storm surge levels during all AMO cold phases (1880-2009).

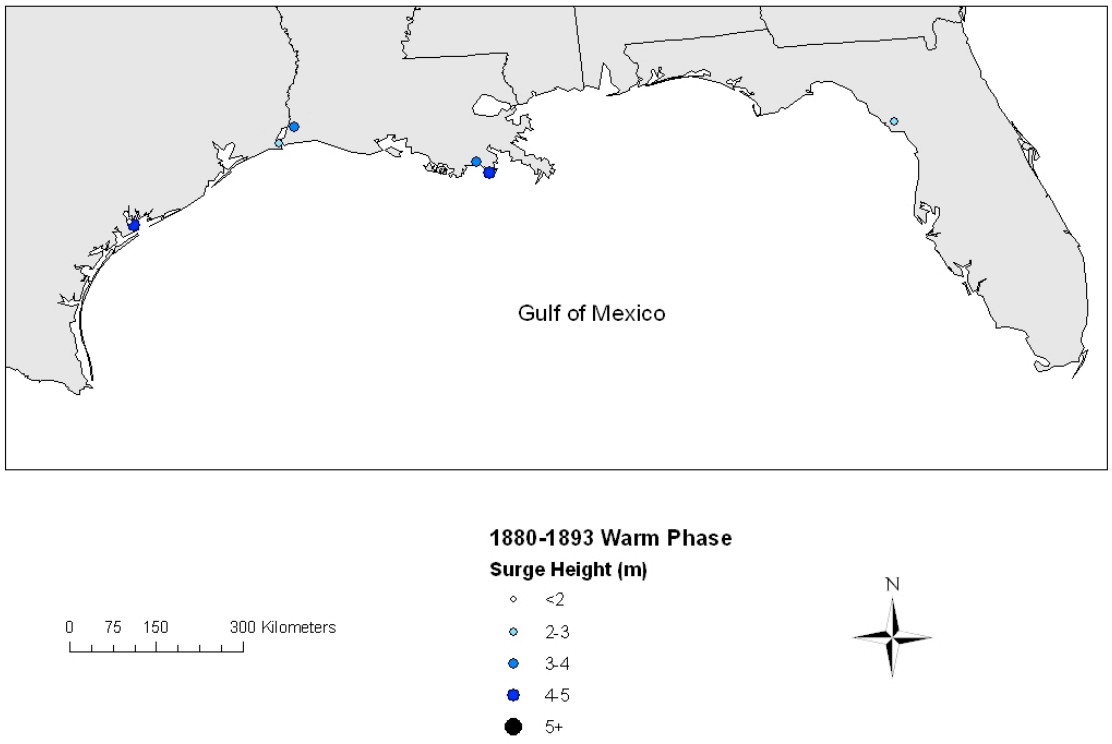

Figure 3.9: Location and height of peak storm surge levels during AMO warm phase (1880-1893).

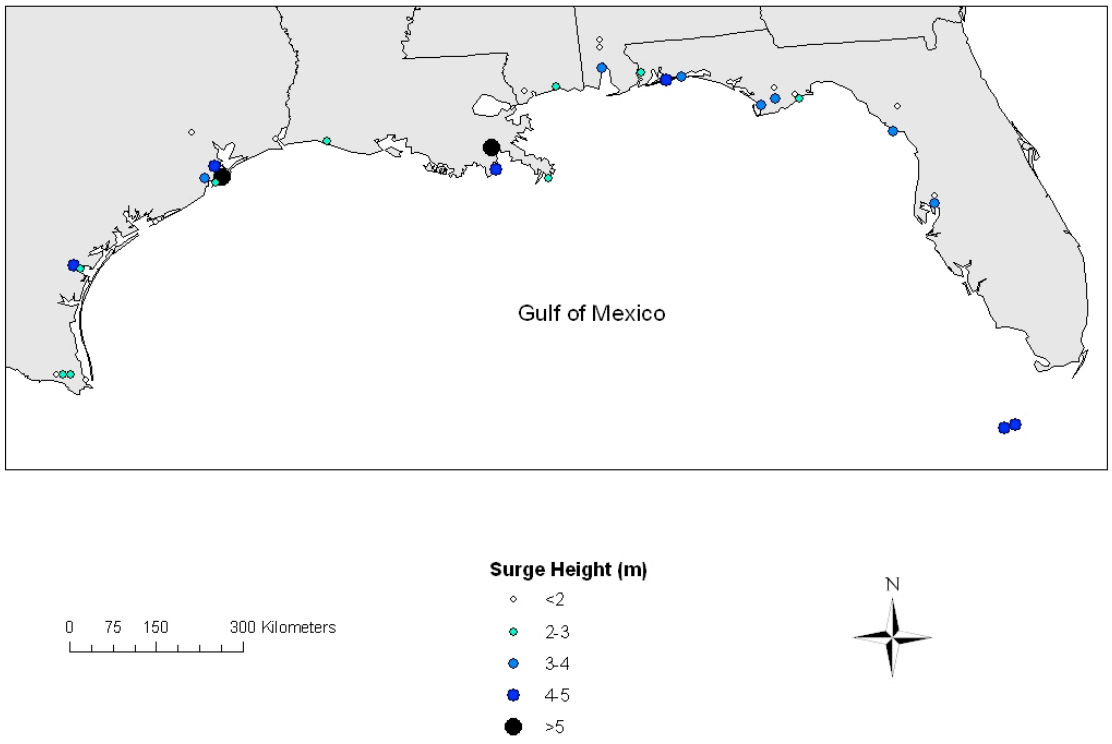

Figure 3.10: Location and height of peak storm surge levels during the AMO cold phase (1894-1925).

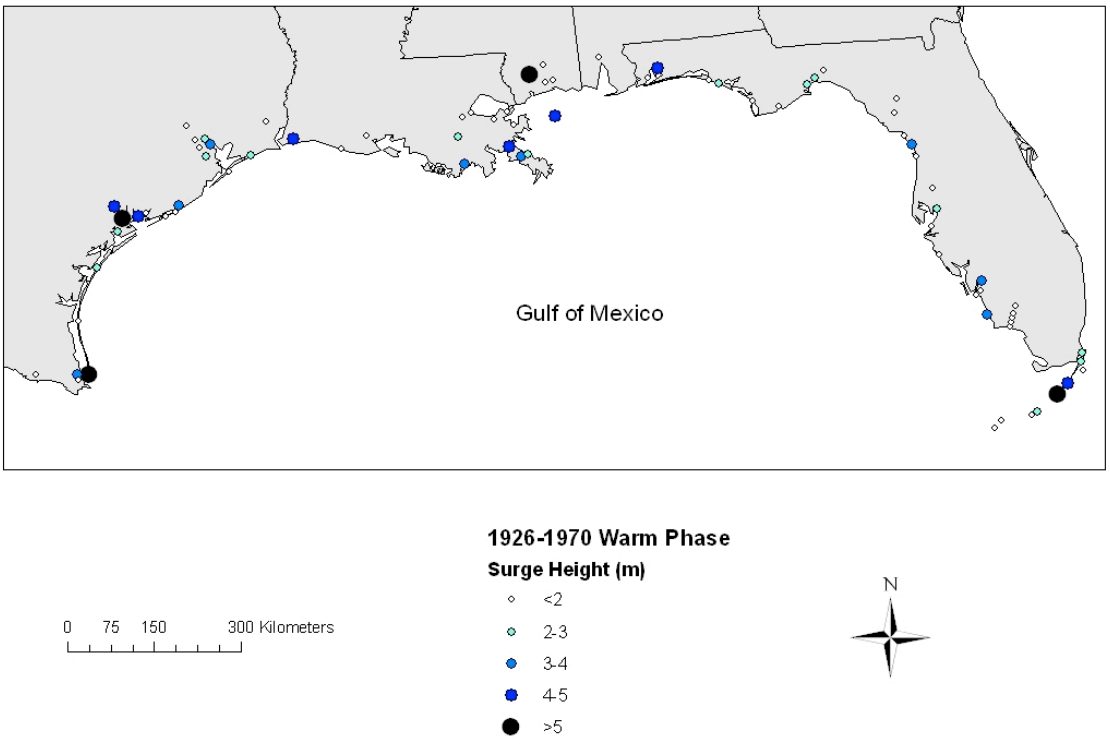

Figure 3.11: Location and height of peak storm surge levels during the AMO warm phase (1926-1970).

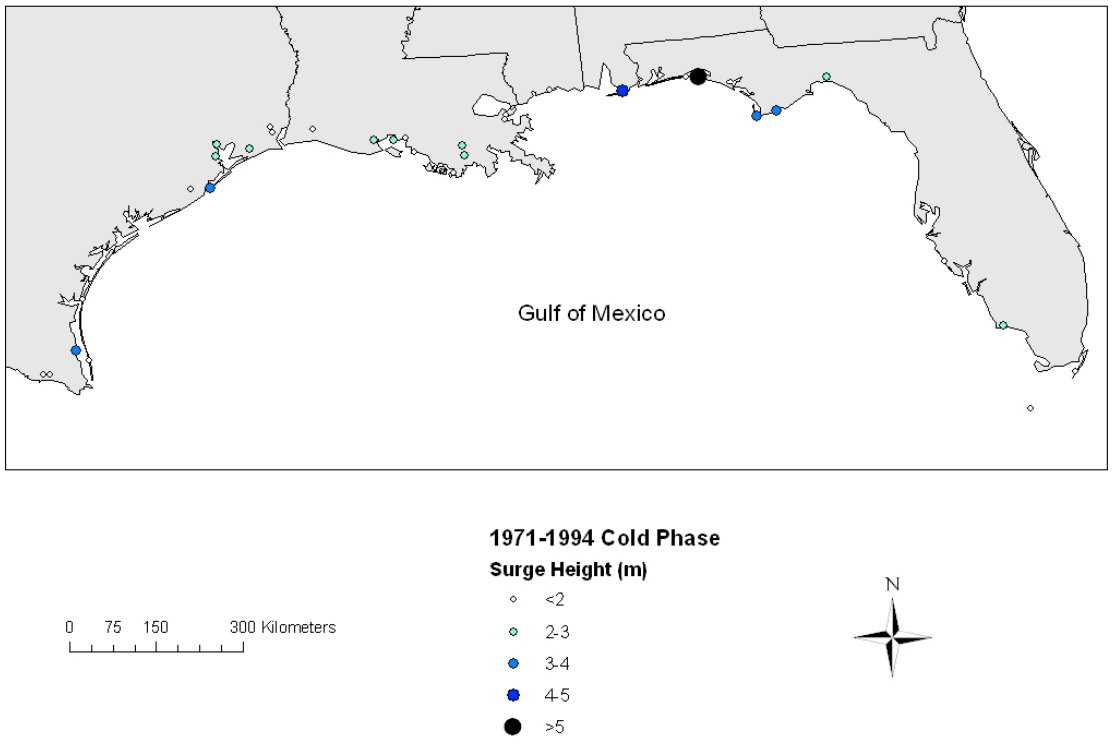

Figure 3.12: Location and height of peak storm surge levels during the AMO cold phase (1971-1994).

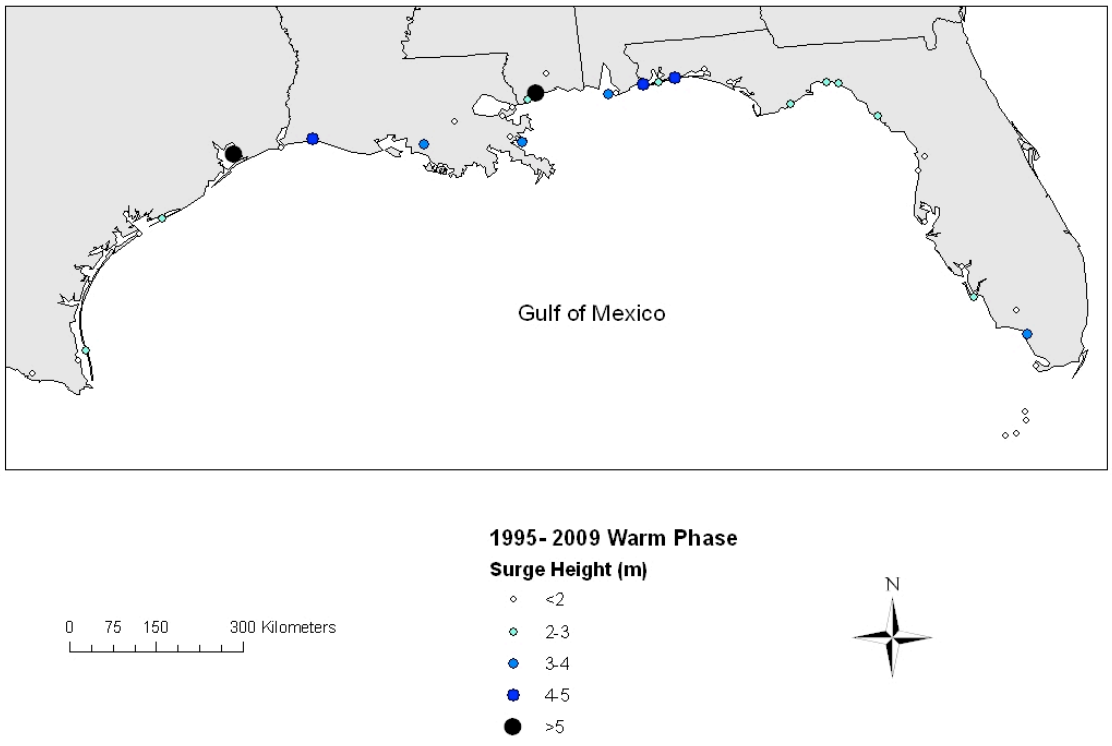

Figure 3.13: Location and height of peak storm surge levels during the AMO warm phase (1995-2009).

changes, as higher proportions of hurricanes originating in the tropical Atlantic Ocean (outside of the Gulf of Mexico) make landfall in the western Gulf. The Florida Peninsula blocks many of these storms from making direct landfall in western Florida, likely shielding western Florida from enhanced surge activity associated with AMO warm phases. Landfalling hurricanes in the eastern Gulf of Mexico must approach the coast from the south or southwest, meaning many of these storms originate over the Gulf of Mexico or Caribbean Sea. As water temperatures and atmospheric conditions conducive for tropical cyclone development in these regions may differ from the larger North Atlantic as a whole, perhaps the variability of hurricanes that develop in these regions is affected to a lesser degree by AMO cold phases. Investigation into the mechanisms responsible for these patterns is an interesting topic for future research.

3.8 The Wilcoxon Rank Sum Test

The Wilcoxon Rank Sum Test was utilized to compare differences between annual surge frequencies and magnitudes observed during cold and warm AMO phases. This test is the non-parametric equivalent of the T-Test, which can be utilized to determine the likelihood that two samples derive from the same parent population. In this case we are interested to test the likelihood that annual surge frequencies or magnitudes observed during warm and cold AMO phases derive from the same parent population. Probability values of $\leq .05$ indicate that the null hypothesis, which states that the two samples are from the same parent population, is rejected with at least 95% confidence.

Frequency tests of all AMO cold-phase vs. all AMO warm-phase surges ($\geq$ 1.22m) were conducted, as well as tests of all AMO cold-phase vs. AMO warm-phase major surges ($\geq$ 3m). Results for the three major time periods utilized in this paper, the

130-year period, 110-year period, and 81-year period, are provided in Table 3.6. In a similar fashion, the test compared magnitudes observed during all cold and warm AMO years. Results of this test are provided in Table 3.7. Results of all frequency and magnitude tests reveal that only the 110-year test of all surge frequencies rejected the null hypothesis at a confidence level of at least 95%. The probability value for this test, .0172, reveals that the null hypothesis is rejected with more than 98% confidence, indicating that it is very likely that the 110-year list of all AMO cold-year frequencies derives from a different parent population than the 110-year list of all AMO warm-year frequencies.

3.9 Summary and Conclusion

Tropical cyclone-generated storm surges create catastrophic natural disasters on the U.S. Gulf coast. Although recent studies have discovered useful information regarding spatial and temporal trends of U.S. hurricane strikes, trends in hurricane variability over time, and correlations between environmental conditions and hurricane activity, such studies offer limited insight into trends and potential relationships associated with surge activity, as the relationships between tropical cyclone characteristics and resultant maximum surge heights are not well understood. This chapter investigated storm surge activity along the U.S. Gulf coast through three primary objectives: mapping the location and height of peak storm surge levels for all 193 surge events provided in the 130-year database, analyzing time series of surge frequencies and magnitudes, and investigating potential relationships between surge activity and the Southern Oscillation Index (SOI), North Atlantic Oscillation (NAO) index, North Atlantic Sea Surface Temperatures (SSTs), and solar activity.

Table 3.6: The Wilcoxon Rank Sum Test was utilized to compare differences between annual surge frequencies observed during cold and warm AMO phases for all surges (≥ 1.22 meters) and major surges (≥ 3m). Results are provided in the form of the two-tailed P-value for normal approximation. Values ≤ .05 indicate the populations are significantly different at 95% confidence level.

Years	P-value of all AMO cold-phase surges vs. all AMO warm-phase surges (surge level ≥ 1.22m)	P-value of major AMO cold-phase surges vs. major AMO warm-phase surges (surge level ≥ 3m)
1880-2009 (130 years)	.1627	.5379
1900-2009 (110 years)	.0172	.3337
1929-2009 (81 years)	.0760	.1468

Table 3.7: The Wilcoxon Rank Sum Test was utilized to compare differences between maximum annual surge magnitudes observed during cold and warm AMO phases. Results are provided in the form of the two-tailed P-value for normal approximation. Values ≤ .05 indicate the populations are significantly different at 95% confidence level.

Years	P-value of maximum annual surge magnitudes observed during AMO cold phases vs. AMO warm phases
1880-2009 (130 years)	.2071
1900-2009 (110 years)	.4118
1929-2009 (81 years)	.0953

Spatial analysis revealed enhanced surge activity along much of the central and western Gulf, from the western Florida Panhandle to the south Texas coast, as well as the Florida Keys. Seven of the nine most extreme surge events (≥ 5 meters) occurred in this region, specifically along the Mississippi, Louisiana, and Texas coasts. The eastern Florida Panhandle and west coast of Florida observed noticeably less surge activity. The time series of annual surge frequencies and maximum annual surge magnitudes reveal similar patterns. Reduced activity levels in the early portion of the record, likely attributed to missing data, is followed by enhanced activity, especially from the 1930s through 1960s. The frequency series experiences a sharp decline in activity commencing in 1966, a pattern that is delayed by four years in the magnitude series, as the maximum annual magnitudes of the few surges that occurred during the late 1960s were unusually large. Both datasets reveal suppressed activity from the 1970s through early 1990s, followed by dramatic increases in surge frequencies and magnitudes from 1995 to 2009. These patterns coincide closely with oscillating warm and cold AMO phase changes, as classified by Landsea et al. (1999).

Potential relationships between surge activity and the Southern Oscillation Index (SOI), Atlantic Multidecadal Oscillation (AMO) index, North Atlantic Oscillation (NAO) index, and Sun Spot Numbers (SSN) were investigated. Indices associated with these climatic variables were tested against annual surge frequency indices of total surge (≥ 1.22 meters) and major surges (≥ 3 meters), as well as an index of maximum annual surge magnitudes. The SOI index correlated highest with surge activity, followed by the NAO index, which anti-correlated with surge activity. Tests between the SOI and every surge time series produced higher Spearman r-values (absolute values) than tests utilizing any

other climatic variable. Confidence levels of the 130-year major surge frequency test, and both 110-year surge frequency tests exceeded 95%. The spearman values for all three magnitude tests were slightly higher, and very consistent with each other. Confidence levels for all three tests exceeded the 95%. Confidence levels associated with the NAO index exceeded 95% for the 130-year and 110-year major surge frequencies.

SOI tercile analysis depicts highest surge activity during the upper tercile, when relatively high index values indicate the El Niño Southern Oscillation (ENSO) teleconnection has shifted towards La Niña characteristics. Lowest surge activity is evident during the lowest tercile, when El Niño conditions prevail. This pattern coincides with findings that North Atlantic hurricane activity is generally suppressed when El Niño conditions prevail in the equatorial Pacific. Surge maps associated with the three terciles indicate enhanced activity, especially along the central and western Gulf Coast and in the Florida Keys, during the upper tercile. Basin-wide surge activity is reduced in association with the middle tercile, with the notable exception of the Florida Panhandle and Florida west coast, which actually experienced increased surge activity. The lowest levels of surge activity are associated with SOI values in the lower tercile.

Analysis of surge activity associated with AMO phase changes reveals that all warm-phase AMO years observed higher annual averages of total surges (≥ 1.22 m), major surges (≥ 3 m), and extreme surges (≥ 5 m), than all combined years, which also observed higher annual averages than all cold-phase years. Surge maps associated with AMO phases revealed heightened basin-wide surge activity during AMO warm phases, especially in the western Gulf. Interestingly, the eastern Gulf observed higher frequencies of major surges (≥ 3 m) during cold phases than the western Gulf. The correlation

between tropical cyclone point-of-origin and landfall location may reveal clues about this pattern, as it is possible that hurricanes originating in the tropical Atlantic Ocean, which are influenced to a greater degree by AMO phase changes, more commonly generate surges along the western Gulf coast.

Finally, the Wilcoxon Rank Sum Test was utilized to determine the likelihood that annual surge frequencies and maximum annual surge magnitudes observed during warm and cold AMO phases derived from the same parent population. Only the 110-year test of all surge frequencies ($\geq$ 1.22 meters) rejects the null hypothesis at a confidence level of at least 95%, revealing that it is very likely that the 110-year list of all AMO cold-year frequencies derives from a different parent population than the 110-year list of all AMO warm-year frequencies.

CHAPTER 4. CALCULATING BASIN-WIDE STORM SURGE RETURN PERIODS ALONG THE U.S. GULF COAST

4.1 Introduction

Tropical cyclone-generated storm surge is a deadly and costly natural hazard along the U.S. Gulf coast. Extreme examples of such disasters include the Galveston Hurricane of 1900, which inflicted more than 6,000 fatalities (Rappaport and Fernandez-Partagas 1995), and Hurricane Katrina, the costliest U.S. natural disaster, which exceeded $80 billion in economic losses (McTaggart-Cowan et al. 2008).

The adverse impacts of such disasters will likely escalate in the future as increasing population and infrastructure crowd the coast. The population of coastal counties and parishes along the U.S. Gulf coast had more than quadrupled from 1950 to 2000, increasing from less than four million to more than 12 million inhabitants (Keim and Muller 2009, see Table 4.1). The dense network of infrastructure that accompanies such population growth increases the likelihood that future economic losses from surge hazards will increase. An extensive network of coastal roads and highways, for example, are vulnerable to damage from surge inundations, as more than 60,000 miles of roads in the U.S. are located in the 100-year coastal floodplain (Chen et al. 2007).

Unfortunately, there is an absence of scientific research that has analyzed regional surge statistics, such as the probability of specific surge levels occurring along the U.S. Gulf coast. Such analyses would be valuable for both coastal populations and the scientific research community. Improved understanding of surge risks would ameliorate public education of this hazard, while improving planning and emergency management operations. Businesses that rely on hazard risk-assessment, such as the insurance sector, would stand to benefit from this type of analysis as well. Finally, the scientific research

Table 4.1: Population of U.S. coastal counties and parishes along the Gulf of Mexico in 1900, 1950, and 2000, from Keim and Muller (2009).

State	No. of Counties	1900	1950	2000
Florida	23	175,000	841,000	4,916,000
Alabama	2	76,000	272,000	540,000
Mississippi	3	50,000	127,000	364,000
Louisiana	11	474,000	930,000	1,611,000
Texas	14	178,000	1581,000	5,006,000
Total	53	953,000	3,751,000	12,437,000

community would likely benefit, as improved knowledge of this hazard would enhance grant-funded research related to natural hazards along the Gulf coast. Although such research has not been conducted for the U.S. Gulf Coast, Walton (2005) researched surge probabilities and return periods in the New York- Long Island area.

Several papers in recent years, however, have conducted regional analyses of hurricane strikes. Elsner et al. (2006) calculated the estimated return periods of tropical cyclone strikes at least as intense as Hurricane Katrina, concluding that, on average, a hurricane of at least this magnitude can be expected to occur once every 14 years from Texas to Maine, and once every 21 years between Texas and Alabama. Keim et al. (2007) estimated the return periods of major hurricanes (winds > 50 m/s), hurricanes (winds > 33 m/s) and tropical storms (winds > 17 m/s), at 45 locations along the U.S. Atlantic-basin coast, from Texas to Maine, demonstrating that portions of coastal North Carolina observe the shortest return periods for tropical storm force winds, while Key Largo, Florida, experiences the shortest return periods for hurricane and major hurricane force

winds. Parisi and Lund (2008) calculated return periods of category 1-5 hurricane strikes along the entire Texas to Maine coastline, as well as the Gulf States region (Texas to Alabama), East Coast region (Georgia to Maine), and Florida. They also calculated the return period of some notable U.S. landfalling hurricanes striking the continental U.S.

While these papers are useful for estimating the return periods of winds associated with landfalling hurricanes, they do not convey the recurrence intervals of maximum storm surge heights, as the relationship between maximum wind speeds of landfalling tropical cyclones and resultant storm surge heights is not well understood. Although it may seem reasonable that stronger winds at landfall should generate higher surges, some notable hurricanes in recent years cast doubt upon this assumption. Hurricane Ike (2008), which made landfall on the upper Texas coast as a Category 2 hurricane, generating maximum winds of 95 kts/hr at landfall (Berg 2009), produced a massive 5.33-meter storm surge (Berg 2009), while Hurricane Charley (2004) made landfall as a Category 4 hurricane, packing maximum winds of 130 kts/hr at landfall (Pasch et al. 2005), but only produced a 2.13-meter surge (Pasch et al. 2005). Likewise, Hurricane Katrina (2005) generated a larger surge than Hurricane Camille (1969), even though they followed a similar track and Camille's maximum sustained winds were more intense at landfall (Knabb, R.D. et al. 2005).

Therefore, considering both the potential threat of surge impacts along the U.S. Gulf coast, and the lack of statistical surge analyses in this region, this research endeavors to examine this hazard through three primary objectives. The first objective is to determine the best method to derive quantile estimates for surge events along the U.S. Gulf coast. These estimates pertain to the frequency of specific surge magnitudes in this

region. The second objective is to calculate surge heights associated with 100-year, 50-year, 25-year, 20-year, 10-year, 5-year and 2-year return periods. The final objective is to determine appropriate applications of this study to real-world stakeholders in the Gulf coast region.

4.2 Methods

4.2.1 Data

This study utilizes a unique storm surge database developed in Chapter 2 for statistical analysis. This database identified the peak height and location of surge events along the U.S. Gulf coast, utilizing a minimum height threshold of 1.22 meters. As this database identified 193 surges between 1880-2009, it represents the most comprehensive list of observed storm surges available for this region.

Unfortunately, this surge record is missing data for 14 percent of potential surge events in the 130-year record. This high proportion of missing data would likely introduce errors into return period calculations, as surge heights for a particular return period would be underestimated if the database is missing many actual surge events. Therefore, this study investigated the data quality of shorter time periods with later starting dates, anticipating a reduction in missing data, while maintaining a high quantity of observed surges.

The three time periods that are investigated, all of which conclude in the year 2009, are the 130-year period beginning in 1880, the 110-year period beginning in 1900 and the 81-year period beginning in 1929. In addition to the 130-year period that makes up the complete dataset, the 110-year and 81-year periods were investigated because the

earliest years of these time periods are missing relatively little data, therefore extending the data record without greatly increasing the amount of missing data.

The quantities of various data types for each of these three periods are depicted in Table 4.2. These data types are the total number of possible events, the number of classified events ≥ 1.22 meters, the number of classified events < 1.22 meters, the number of non-classified events < 1.22 meters, the number of canceled events, and the number of missing events in this database. The number of total possible events is the number of potential surge events generated by tropical cyclones that tracked within 300 km of the U.S. Gulf coast, while producing maximum sustained winds of at least tropical storm force strength. These cyclones have the potential to generate tropical storm force winds along the Gulf coast, as Keim et al. (2007) generalize that winds of at least tropical storm force strength extend outward up to 240 km on the strong side of averaged-sized major cyclones. Classified surges ≥ 1.22 meters are surges at least 1.22 meters high, in which the peak surge height and location were identified. Classified surges < 1.22 meters are surges < 1.22 meters high, in which the peak surge height and location were also identified. Non-classified surges < 1.22 meters are surges in which the peak surge height and location were not identified, but reliable historical sources indicate that the maximum surge height did not reach 1.22 meters. Canceled surges were potential surge events, generally between 1880 and 1957, in which there was a low probability that a surge of least 1.22 meters was observed, because the associated tropical cyclone did not generate tropical storm force winds along the Gulf coast. The vast majority of these events occurred between 1880-1957, because this time period relied heavily on microfiche records of historical newspapers. The process required ordering such media from libraries

and archives along the Gulf coast, and was therefore tedious and time consuming. As media requests were not placed for these low-probability surge events during this time period, most of these potential events were canceled. Finally, missing data pertains to potential events in which no reliable data could be found to classify the peak location and height of the storm surge, although there was a moderate or high potential that a surge ≥ 1.22 meters occurred.

The data quality of the three time periods were compared to select the time period that maximizes the quantity of surge observations, while minimizing the amount of missing data. Although the 130-year period provides 193 surge observations, the most of any time period, this period also reports 14 percent missing data, the highest of any period. The 110-year period provides 181 surge observations, only 12 fewer than the 130-year period, while cutting the proportion of missing data in less than half, to only 5.7 percent. Finally, the 81-year period provides 147 surge observations, while decreasing the amount of missing data to only 1.4 percent.

This study chose the 110-year time period as the primary dataset for statistical analysis, as it provided an abundant number of surge observations, while minimizing the proportion of missing data. The 81-year dataset was chosen as a secondary source for analysis, to verify results found in the analysis of the 110-year record. Although the 130-year record provided the most abundant amount of surge data, the high proportion of missing data cast doubt upon the quality of statistics generated from this dataset.

4.2.2 Quantile-Estimation Methods

Multiple methods were chosen to generate quantiles, or storm surge magnitudes associated with specific return periods, because the performance of quantile-estimation

Table 4.2: Storm surge database statistics for the total number of possible surge events, the number of classified, non-classified, canceled and missing events by time period.

Time Period	1880-2009 (130 years)		1900-2009 (110 years)		1929-2009 (81 years)	
Data Type	Num	Pct	Num	Pct	Num	Pct
Total Possible Events	463	100	383	100	296	100
≥ 1.22m classified	193	41.7	181	47.3	147	49.7
< 1.22m classified	48	10.4	47	12.3	44	14.9
< 1.22m non-classified	43	9.3	42	11	40	13.5
Canceled	114	24.6	91	23.8	61	20.6
Missing	65	14	22	5.7	4	1.4

methods varies depending on the characteristics of the dataset, type of extreme event, and geographic region of the study. The four methods chosen were the Gumbel, Beta-P, Huff-Angel and Southern Regional Climate Center (SRCC) methods. The Gumbel method was chosen because it has been used widely since Hershfield (1961) employed this method in Technical Paper No. 40- a foundational study of heavy rainfall return periods for the United States. Previous analysis on heavy precipitation events revealed that the Beta-P method is the best fit for partial duration series of heavy rainfall events in the northeastern U.S. (Wilks 1993; Wilks and Cember 1993). The Huff-Angel (Huff and Angel 1992) and SRCC (Faiers et al. 1997) methods employ regression techniques to estimate quantile values in the United States midwest and south-central states, respectively. The Kolmogorov-Smirnov statistic revealed that the Huff-Angel method produced the best fit in a study that utilized seven methods to estimate return periods in

western Texas, while the SRCC method out-performed the Huff-Angel method for large magnitude events, and was subjectively considered best (Keim and Faiers 2000).

4.2.3 Calculating Return Periods for Storm Surge Heights

Quantile estimates of storm surge are determined for 100-year, 50-year, 25-year, 20-year, 10-year, 5-year, and 2-year return periods. These values represent the basin-wide surge level that is expected to be equaled or surpassed during the corresponding time frame. These intervals represent a wide range of potential surge events, and are typical intervals selected for statistical flood analysis.

The first step in this analysis involved ranking all 181 surge observations recorded within the 110-year period. After this sequential list of surge rankings was constructed, a Partial Duration Series (PDS) of maximum surge heights was created. As the number of extreme events in a PDS equals the number of years in the data record (n), the 110-year PDS contained the 110 largest surges (Dunne and Leopold 1978). The largest magnitude event was 8.47 meters, the surge level generated by Hurricane Katrina, while the smallest event was 1.83 meters, recorded in 16 different storms.

The PDS was then utilized to calculate the exceedence probability, using the formula, "Exceedence Probability = Rank / (n+1)," where "n" is the number of years in the data record. This formula produced exceedence probability values ranging from a low value of .0090 for Hurricane Katrina, which was a large-magnitude, less probable event, to a high value of .9910 for the low-magnitude, more likely 110^{th}-ranked event. Exceedence probabilities were then utilized to calculate return periods, utilizing the formula, "Return Period = 1 / Exceedence Probability." Hurricane Katrina obtained the longest return period, 111 years, while the shortest return period was only1.009 years.

4.3 Results

Surge levels for associated return periods were provided by fitting the PDS surge data to the Gumbel and Beta-P distributions. The Huff-Angel and SRCC methods were also examined, which utilize linear regression graphing methods to depict a model of best fit. The Huff-Angel procedure utilizes a log-log graphing method, whereas the SRCC procedure utilizes a log scale on the x-axis (return period), and a linear scale on the y-axis (surge height). The graphs of these analyses are depicted as Figures 4.1 and 4.2.

Surge levels associated with the 100-year return period, utilizing all four methods, ranged from 7.26 meters to 14.91 meters. The Beta-P method estimated the highest surge level, which is a considerable overestimation considering the highest actual surge level in the past 130 years was 8.47 meters. The Gumbel method underestimated the surge levels for the 100-year event, a result that is congruent with Wilks (1993); and Keim and Faiers (2000), who discovered that the Gumbel method commonly underestimates high-magnitude, rare events. The values of the Huff-Angel and SRCC methods fell between these two extremes. Surge levels for the 2-year return period ranged from 2.51 meters to 2.9 meters. The Gumbel method calculated the maximum value while the Beta-P method calculated the minimum value, a result that is completely opposite of 100-year estimates. The values of the Huff-Angel and SRCC methods, once again, fell between these two extremes. Surge levels associated with return periods for all four methods are listed in Table 4.3.

4.4 Evaluation: Testing for Best Fit

The four methods were compared using methods similar to Keim and Faiers (2000) to see which produced the best fit to the data. The first step in this procedure was to calculate the expected number of events for each return period. This calculation is conducted by simply dividing the record length by the return period length. For example, we should expect 55 events with a 2-year return period during the 110-year record length, because of the simple equation (110 / 2 = 55).

Likewise, we should expect 11 events with a 10-year return period during this same time frame. The expected number of events are then compared with the actual number of events that equaled or surpassed a given surge level that is associated with a specific return period. For example, although we expect to observe 11 events with a 10-year return period, given the 10-year surge levels calculated by each method, we actually observed 10 surges that equaled or surpassed the Huff-Angel and Gumbel levels, 9 surges that equaled or surpassed the SRCC level, and only 8 surges that equaled or surpassed the Beta-P level. Table 4.4 compares the expected number of surges with the actual number of observed surges.

The Kolmogorov-Smirnov Statistic (KS-Statistic) was then utilized to compare which graphing procedure agrees better with expected results. The SRCC method produced the best fit results, followed by the Huff-Angel method, the Gumbel distribution, and, finally, the Beta-P distribution. Table 4.5 depicts a comparison of the KS-Statistic for all four methods. Lower values indicate a better fit, as Keim and Faiers (2000) indicate that smaller KS-Statistic values are assigned to procedures that produce a better fit to expected results.

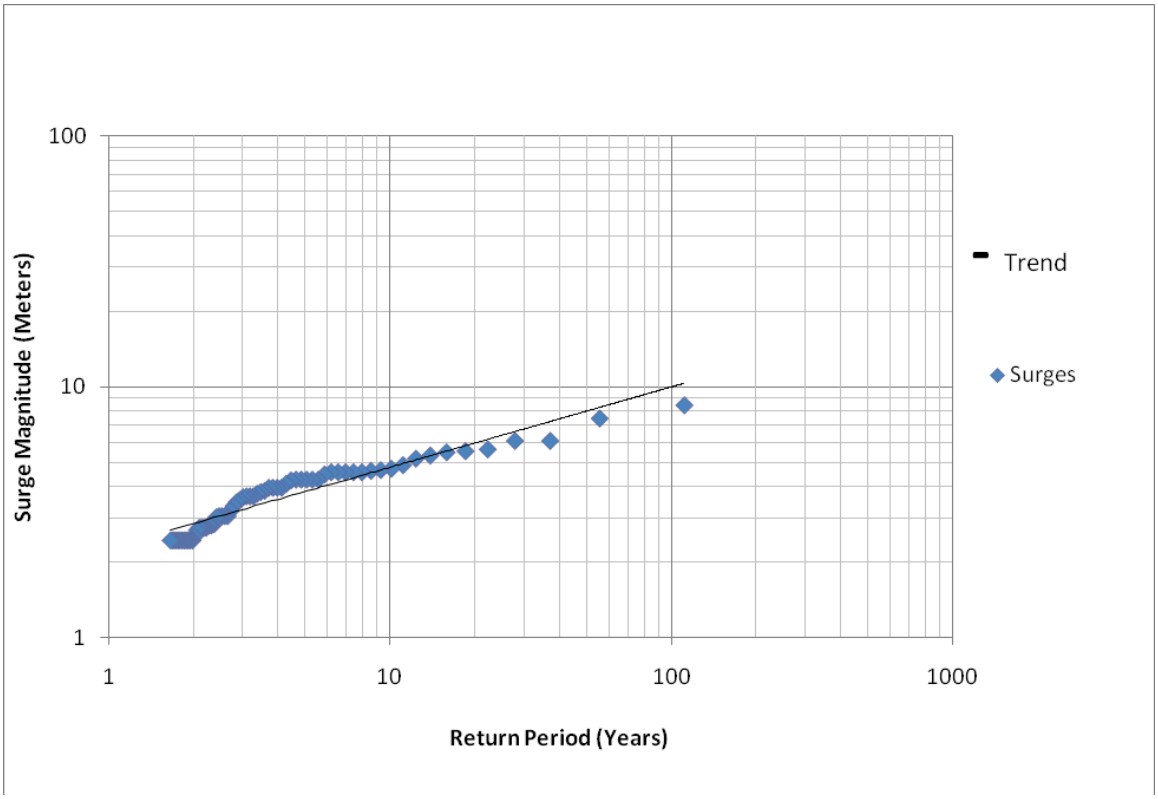

Figure 4.1: Return period estimates of maximum storm surge levels on the U.S. Gulf coast, utilizing the Huff-Angel graphing method to plot data from 1900-2009 (110 years).

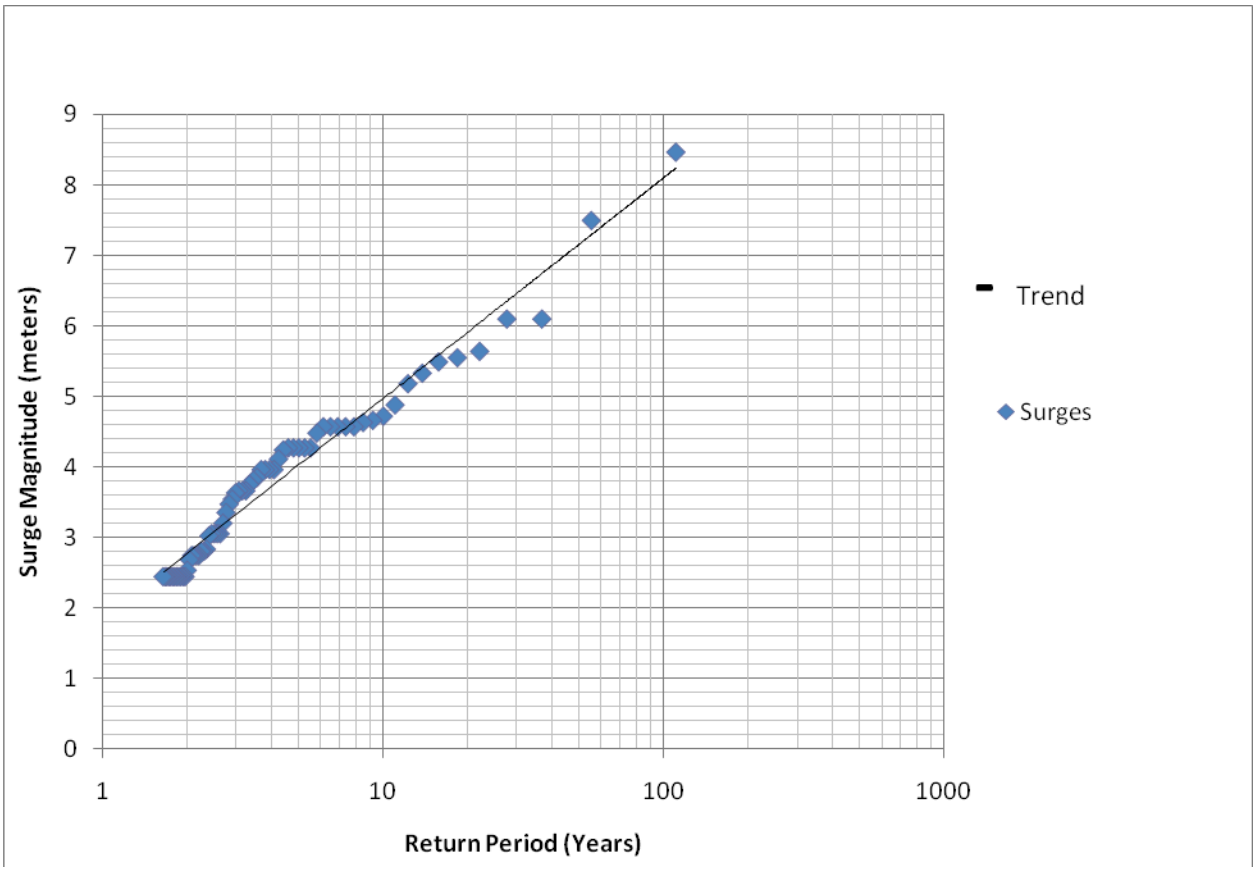

Figure 4.2: Return period estimates of maximum storm surge levels on the Gulf coast utilizing the SRCC graphing method to plot data from 1900-2009 (110 years).

Table 4.3: Surge levels (meters) associated with 100-year, 50-year, 25-year, 20-year, 10-year, 5-year, and 2-year return periods utilizing the Gumbel and Beta-P distribution methods, and the Huff-Angel and Southern Regional Climate Center (SRCC) linear regression methods.

Return Period (yrs)	Huff-Angel	SRCC	Gumbel	Beta-P
100	10	8.1	7.26	14.91
50	8	7.15	6.54	10.87
25	6.45	6.25	5.82	7.93
20	5.98	5.9	5.58	7.16
10	4.75	4.96	4.84	5.22
5	3.8	4.01	4.06	3.81
2	2.78	2.75	2.9	2.51

4.5 Application

As the KS-Statistic supports use of the SRCC graphing method as the most accurate fit compared to expected results, the SRCC surge levels associated with each return period should be given thorough consideration. Table 4.6 lists the estimated surge height associated with specific return periods calculated by the SRCC method for this 110-year dataset. Values range from a 100-year surge height of 8.1 meters to a 2-year surge height of 2.75 meters. The 81-year analysis, utilized for verification of the longer 110-year analysis, supports these values, as the surge heights in this period range from a 100-year height of 8.44 meters to a 2-year height of 2.63 meters. These results represent

return period levels for the entire U.S. Gulf coast, and are not necessarily indicative of values at a particular location.

While these surge heights are certainly impressive, perhaps the implications of these surge levels are best understood in light of expected impacts to Gulf coast communities. As anecdotal storm surge accounts from Chapter 2 revealed that the average elevation of Gulf coast communities is approximately 1.22 meters (4 feet), and the average elevation of slightly raised structures in these communities is approximately 1.83 meters (6 feet), simple subtraction yields 100-year surge levels of 6.88 meters above ground level, and 6.27 meters above floorboards of slightly elevated structures, in some Gulf coast community. Likewise, the estimated surge levels associated with 2-year return periods are approximately 1.53 meters above ground level, and .92 meters above the floorboards of slightly elevated structures. Table 4.7 lists estimated surge heights above ground level and slightly elevated structures for all return periods.

These results will be useful to a broad audience with interests along the U.S. Gulf coast. Estimates of water heights above ground level and the level of slightly elevated structures are particularly applicable to emergency management personnel, planners, and decision makers in both public and private sectors. Stakeholders in regional industries, ranging from oil and gas exploration to seafood production, will also benefit from this regional assessment of storm surge hazard. The objectives of this research also relate very well to the National Oceanic and Atmospheric Administration's (NOAA) Regional Integrated Sciences and Assessments (RISA) program, which funded this research through the Southern Climate Impacts Planning Program (SCIPP). This program employs

Table 4.4: Return periods, expected number of events and actual number of events calculated by each of the quantile-estimation methods.

Return Period (years)	Expected Events	Huff-Angel Actual Events	SRCC Actual Events	Gumbel Actual Events	Beta-P Actual Events
2	55	49	49	46	55
5	22	32	26	26	32
10	11	10	9	10	8
20	5.5	4	4	5	2
25	4.4	2	2	4	1
50	2.2	1	2	2	0
100	1.1	0	1	2	0

Table 4.5: Comparison of KS-Statistic values for each quantile-estimation method. Lower values indicate a better-fit line compared to expected results (Keim and Faiers 2000).

Method	Huff-Angel	SRCC	Gumbel	Beta-P
KS-Statistic	.06	.04	.07	.12

Table 4.6: Estimated surge heights associated with return periods by the Southern Regional Climate Center (SRCC) regression method.

Return Period	Surge Level (m)
100-year	8.1
50-year	7.15
25-year	6.25
20-year	5.9
10-year	4.96
5-year	4.01
2-year	2.75

Table 4.7: Estimated surge heights, water height above ground level, and water height above slightly elevated structures, for communities along the U.S. Gulf coast. The surge levels were estimated by the Southern Regional Climate Center (SRCC) regression method.

Return Period	Surge Level (m)	Water height above ground level (m)	Water height above level of slightly elevated structures (m)
100-year	8.1	6.88	6.27
50-year	7.15	5.93	5.32
25-year	6.25	5.03	4.42
20-year	5.9	4.68	4.07
10-year	4.96	3.74	3.13
5-year	4.01	2.79	2.18
2-year	2.75	1.53	.92

a regional approach to provide stakeholders with information that enables them to prepare for climate-related hazards (National Oceanic and Atmospheric Administration 2010). A detailed regional investigation of storm surge return periods also benefits emergency management planning on the Federal level. Federal planning and budgeting for hazard mitigation and disaster response depends heavily upon hazard risks that are realized at the national and regional level. In one sense, the Federal government is more concerned with the probability of a hurricane striking any point along on the U.S. coast, than it is with the exact location of landfall. Determining the magnitude of potential hazards, however, is an obvious challenge, as seen in the failures associated with Hurricane Katrina's recovery effort (Department of Homeland Security 2006). The Department of Homeland Security's *Nationwide Plan Review Phase 2 Report*, conducted in response to concerns associated with Hurricane Katrina's recovery, discusses the advantages of regional vulnerability assessment over investigations that are too localized and narrow in scope. It states…

"Catastrophic planning is hindered by parochial hazard analyses. The majority of jurisdictions use locally based hazard vulnerability and risk assessments to determine their planning requirements. The majority of the analyses do not take into consideration the magnitude of incidents that could occur in neighboring States and urban areas that could result in a serious impact to their community. Throughout the site visits, the results of narrowly focused local assessments were often presented as justification for not developing catastrophic incident plans or annexes." (Department of Homeland Security, 2006, pg. 76).

Statistical analysis of storm surge return periods along the Gulf of Mexico coast provides valuable information that depicts the scope of this hazard on a regional level, and therefore, helps the Federal government plan for surge-related disasters.
Finally, calculating regional storm surge return periods enables scientists to monitor changes in surge frequencies and magnitudes over time, potentially in association with climate change. Surge levels could also be evaluated against a backdrop of increased future impacts due to sea level rise (Smith et al. 2010). It stands to reason that these types of investigations display more credibility at a regional level than at a localized scale, because regional analyses average out localized surge extremes, providing a broader picture of surge trends over time. For this reason, climate reports commonly reference data at global, national or regional scales. The *Global Climate Change Impacts in the United States* report (2009), for example, concluded that storm surges associated with heightened sea levels and increasingly intense hurricanes embody the most costly potential consequences of climate change in the Southeastern United States. In light of such predictions, this regional storm surge analysis should likely benefit the scientific research community, as well as stakeholders, who are concerned with potential regional climate change impacts along the U.S. Gulf coast.

4.6 Summary and Conclusion

This study utilized the unique storm surge dataset developed in Chapter 2 to estimate storm surge heights associated with the 100-year, 50-year, 25-year, 20-year, 10-year, 5-year and 2-year return periods along the U.S. Gulf coast. The Kolmogorov-Smirnov Statistic indicates that the Southern Regional Climate Center (SRCC) linear regression method produced the best return period estimates, out-performing the Huff-

Angel regression method, and the Gumbel and Beta-P distribution methods. The SRCC method estimated surge levels ranging from 8.1 meters for the 100-year event, to 2.75 meters for the 2-year event.

As regional elevation estimates provided in Chapter 2 indicate that the ground level of typical Gulf coast communities is approximately 1.22 meters, and the elevations of slightly elevated structures in these communities is approximately 1.83 meters, we conclude that the 100-year water level above the ground is approximately 6.88 meters, and the 100-year water level above the floorboards of slightly elevated structures is approximately 6.27 meters, in some Gulf coast community. The water levels associated with 2-year surge levels range from approximately 1.53 meters above ground level, to .92 meters above the level of floorboards.

These results will be useful to a broad audience with interests along the U.S. Gulf coast. Estimates of water heights above ground level and the level of slightly elevated structures are particularly applicable to emergency management personnel, planners, and decision makers in both public and private sectors. Stakeholders in regional industries, ranging from oil and gas exploration to seafood production, will also benefit from this regional assessment of storm surge hazard. This research will also benefit Federal disaster planning specialists, who are particularly concerned with risk assessment on the national and regional levels. Finally, these results will likely benefit scientific research associated with the impacts of potential climate change, as such research often investigates the regional or global scale of climate impacts.

CHAPTER 5. CONCLUSION AND FUTURE RESEARCH

Abundant information is available on the ever-expanding field of hurricane science. Information about the physical processes involved in hurricane development, tracking, and landfall patterns, are readily accessible, as are detailed studies involving hurricane trends over time, and the impacts of hurricanes on populated coastlines. However, little information is available regarding the associated storm surges that are responsible for so much devastation. Those interested in this topic will find no published papers regarding a global overview of surge observations and impacts, no surge datasets based on observed data for any portion of the United States coastline, and no papers providing statistical analyses of this hazard along the shores of the United States. In light of these observations, this thesis conducted a global overview of storm surge observations and impacts, constructed a comprehensive database of historical surge observations for the U.S. Gulf Coast, and investigated this hazard through spatial analyses, time series analyses, testing correlations between climatic variables and surge activity, and calculating return period levels along the U.S. Gulf Coast.

5.1 A Global Overview of Tropical Cyclone-Generated Surge Hazards

Tropical cyclone-generated storm surges produce catastrophes that are among the most disastrous globally. The physical processes that create these disasters, however, are complex, and poorly understood by both coastal populations and the scientific research community. The predominant processes that influence the severity of surge inundations include maximum sustained winds, cyclonic size, forward cyclonic movement, coastal bathymetric characteristics, as well as coastline shape and the presence of natural and artificial obstructions to flowing water.

The Bay of Bengal, in the northern Indian Ocean, experiences the most severe surge events globally. The highest surges in this basin reach 12 to 14 meters (Jakobsen et al. 2006), and single surge events have killed up to 300,000 people (Frank and Husain (1971); Dube et al. (1997). The Gulf of Mexico, which borders eastern Mexico and the southeastern United States in the north Atlantic basin, experiences the second greatest surge heights globally. Maximum heights in this basin reach approximately 6 to 9 meters. Hurricane Katrina's (2005) 8.47-meter surge (Knabb et al. 2006) is a recent reminder of the potential severity of these events. Although East Asia experiences some of the world's most frequent and intense tropical cyclones, surge inundations are not as severe as in the previously mentioned basins, reaching maximum heights of approximately 3 to 6 meters (Li et al. 2004). Australia and Oceania observe similar maximum surge heights (Zerger 2001), although surge events in Oceania can wash over entire islands, inducing long term starvation and disease (Spennemann 1996; De Scally 2008).

5.2 Constructing a Historical Storm Surge Database for the U.S. Gulf Coast

The severity of this hazard along the U.S. Gulf coast warrants statistical analyses of this hazard, however, at the commencement of this research, no comprehensive surge database provided surge data for this region. As such, a substantial portion of this research involved the creation of surge database that depicted the location and height of peak surge events. This research endeavored to identify surge events that produced maximum surge heights $\geq$ 1.22 meters along the U.S. Gulf coast from 1880 to 2009.

The first step for database construction involved developing a skeleton of every possible surge event during this time period. A database of every hurricane that made landfall in the U.S. from 1851 to 2005, provided by Landsea (2005), produced a major

portion of this skeleton. The Unisys Corporation (2009) provided tropical cyclone tracking maps, which enabled hurricanes (maximum wind speeds > 33 m/s) that did not make landfall in the U.S., but still generated U.S. surges, to be included in the database. The database utilized a buffer of 300 km, meaning every tropical cyclone that passed within this buffer was included in the skeleton. Additionally, tropical storms (maximum winds > 17 m/s, but ≤ 33 m/s) that passed within the 300 km buffer, or made landfall in the U.S., were included in the skeleton as well, as these systems sometimes generate surges ≥ 1.22 meters, however, were not listed in Landsea's (2005) database. The data from both Landsea (2005) and the Unisys Corporation (2009) were compiled to generate a list of 463 potential surge events.

The second step for constructing the database involved identifying the location and height of the peak surge level associated with these events. This research utilized 53 sources, including 21 Federal government sources, 16 books and Online publications, as well as more than 3,000 pages of newspaper provided by 16 periodical titles. This effort identified 241 surge events, of which 193 were at least 1.22 meters high. The top 10 highest surge magnitudes classified during this 130-year period ranged from 4.88 to 8.47 meters.

5.3 Storm Surge Analysis

After the storm surge database was constructed, the 193 surges were then mapped, with circles indicating the location and maximum height of each peak surge level. The highest levels of activity were located along the central and western Gulf coasts, from the western Florida Panhandle to south Texas, as well as in the Florida Keys. Reduced surge activity is apparent along the west Florida coast and in the eastern Florida Panhandle.

Time series of annual surge frequencies and annual maximum surge magnitudes reveal similar patterns. The period from the 1930s until the 1960s displays enhanced surge activity, followed by suppressed activity during the 1970s until early 1990s. Activity dramatically increases again around 1995, and continues until the end of the record. These patterns of variability coincide well with alternate warm and cold phases of the Atlantic Multidecadal Oscillation classified by Landsea et al. (1999).

Surge activity was tested for potential correlations with the Southern Oscillation Index (SOI), North Atlantic Oscillation (NAO) index, North Atlantic SST anomalies, which are measured by the Atlantic Multidecadal Oscillation (AMO) index, and Sun Spot Numbers (SSN), which indicate solar activity. These climatic variables were tested against annual surge frequency for all surges (≥ 1.22 meters) and major surges (≥ 3 meters) for 130-year, 110-year, and 81-year surge records. The SOI index correlated the highest with surge activity, followed by the NAO index, which anti-correlated with surge activity. Spearman values for the SOI tests were higher (absolute values) than any other climatic variable, and confidence levels of the 130-year major surge frequency test, both 110-year surge frequency tests, and all of the surge magnitude tests exceeded the 95% level. The NAO index anti-correlated with surge activity, and correlations from the 130-year and 110-year major surge frequencies index exceeded the 95% confidence level.

SOI tercile analysis revealed elevated surge activity during the upper SOI tercile, when La Niña conditions generally prevail. Basin-wide activity is reduced in association with the middle tercile, although surge activity actually increases in western Florida and the Florida Panhandle during these periods. The lowest levels of surge activity occur during the lowest SOI tercile, when El Niño conditions are generally dominant.

Analysis of the Atlantic Multidecadal Oscillation (AMO) indicated that surge activity increased during warm AMO phases, especially in the western Gulf of Mexico. Surprisingly, surge activity increased in the eastern Gulf of Mexico during cold AMO phases, as the frequency of major (≥ 3m) surge events in the eastern Gulf to surpass those in the western Gulf during these periods. It is possible that the tropical cyclones that produce peak surges in the eastern Gulf originate in different locations from those that produce peak surges in the western Gulf, which may explain some of this variability.

5.4 Calculating Return Periods of Extreme Surge Levels

This research also calculated return periods associated with extreme surge levels along the U.S. Gulf coast. The Gumbel and Beta-P distributions, as well as the Huff-Angel, and Southern Regional Climate Center (SRCC) linear regression methods were utilized to estimate extreme surge levels associated with the 100-year, 50-year, 25-year, 20-year, 10-year, 5-year, and 2-year return periods. The Kolmogorov-Smirnov Statistic indicated that the SRCC method produced a line of best fit that matched the best with actual surge data. This method estimated the basin-wide 100-year event as an 8.1 meter-surge, and the 2-year event as a 2.75-meter surge. These results are useful for local and regional emergency management personnel, planners, decision makers, stakeholders in various industries, and Federal disaster management personnel.

5.5 Future Research

As storm surge research remains an important frontier in climate science, myriad opportunities in this field await the scientific research community. As the Gulf of Mexico and larger North Atlantic basin experiences a period of elevated tropical cyclone activity, future research into storm surge analysis should be prioritized.

Maintaining the surge database, predominantly through the completion of annual updates, will likely provide great benefits at low cost and effort. As the National Hurricane Center now provides detailed tropical cyclone reports on the Web, many of which list the location and height of maximum surge levels, this effort may only require several hours of work per year. Such effort may be especially important during the current tropically active period, because statistics calculated from this database could change substantially, especially after consecutively active years.

It also might be beneficial to investigate ways in which the database can be improved with the least effort possible. Although U.S. Army Corps of Engineers (USACE) data were not directly incorporated into the database, an investigation into the existence of possible USACE surge summary reports for locations on the U.S Gulf coast may yield beneficial results. Also, as the volume of scanned, historical newspaper articles available on the Web increases daily, it is possible that anecdotal accounts for some of the missing surge events will soon become accessible.

In addition to updates and improvements to the U.S. Gulf coast surge database, similar surge research should be conducted for the U.S. eastern seaboard, from South Florida to Maine. This entire region is susceptible to tropical cyclone strikes. The procedures utilized in this study to build the surge database, as well as many of the statistical methods could simply be duplicated for the East coast. If such an endeavor were completed, it would be possible to run statistical tests for the entire U.S. Atlantic basin.

Another area of potential future research involves the analysis of storm surge statistics, such as return periods, for specific portions of the Gulf coast. Unfortunately,

this effort would require much more work than simply extracting the peak surges along specific portions of coastline, because surges commonly inundate wide areas, impacting surge statistics for every location that observes elevated sea levels. For example, although Chambers County, Texas, just east of Galveston, observed the highest surge level in Hurricane Ike (2008), at 5.33 meters (Berg 2009), Ike inundated extensive portions of the central and western Gulf coast. Therefore, surge levels at many locations along the coast must be obtained to calculate surge statistics for specific points. Tidal gauge data is likely necessary for such work. Fortunately, such data are available through agencies such as the National Oceanic and Atmospheric Administration's (NOAA) Tides and Currents, which provides updated gauge data on the Web. Some of these gauges provide more than 30 years of data, enabling statistics, such as return periods, to be analyzed at the gauge location. Analyses of surge statistics at specific locations would likely provide crucial data for local planners and decision-makers, as such investigations may improve accuracy of surge-risk estimates at the local level.

Another potential topic for future research involves investigating the physical mechanisms responsible for generating enhanced surge activity in the eastern Gulf of Mexico during AMO cold phases, and during years associated with the middle SOI tercile, when El Niño Southern Oscillation (ENSO) "neutral" conditions prevail. Investigation into the points of tropical cyclone origin associated with specific landfall and peak surge locations may yield clues into these patterns. Peak surges along the west coast of Florida, for example, are likely produced by hurricanes that develop in the Gulf of Mexico or Caribbean Sea, regions that may differ substantially from the larger North

Atlantic basin, in terms of physical characteristics, such as SSTs, or prevailing circulation patterns.

Finally, and perhaps most importantly, future research must explore the relationships between tropical cyclone characteristics and resultant surge activity. The impacts of hurricane size, forward speed, maximum sustained winds at landfall and at increments of time preceding landfall, as well as the effects of bathymetry and local physical geography on the resultant peak surge levels are not well understood by the scientific research community. Future research on this topic would likely improve surge forecasts, which could save lives and reduce economic losses along the U.S. Gulf coast.

BIBLIOGRAPHY

Ali, A., 1980: Storm surges in the Bay of Bengal and their numerical modeling, SARC Report No. 125/80, Atomic Energy Commission, Dhaka, Bangladesh.

Ali, A., 1996: Vulnerability of Bangladesh to climate change and sea level rise through tropical cyclones and storm surges. *Water, Air, and Soil Pollution*, **92**, 171-179.

American Meteorological Society, 1973: Policy statement of the American Meteorological Society on hurricanes, as adopted by the Council on October 20, 1972. *Bulletin of the American Meteorological Society*, **54**, 45-47.

Anonymous, 1922: Typhoon death list now 50,000 at Swatow. *The New York Times*, Written by anonymous Associated Press author on August 11, 1922, published on the Web at: http://query.nytimes.com/mem/archive-free/pdf?res=9F01EEDB1339EF3ABC4952DFBE668389639EDE.

Anonymous, 1922: The Swatow Typhoon of August, 1922. *Monthly Weather Review,* **50**, Page 435.

Baker, E.J., J.C. Brigham, J. Anthony Paredes, and D.D. Smith, 1976: *The social impact of Hurricane Eloise on Panama City, Florida.* The Florida State University, Tallahassee, Florida. 64 pp. Report archived at National Sea Grant Depository and published on the Web at: http://nsgl.gso.uri.edu/flsgp/flsgpt76010.pdf

Barnes, J., 2007: *Florida's Hurricane History*. 2nd edition. University of North Carolina Press, 407 pp.

Berg, R., 2009: National Hurricane Center Tropical Cyclone Report on Hurricane Ike (AL092008), updated January 23, 2009. Published on the Web at http://www.nhc.noaa.gov/pdf/TCR-AL092008_Ike.pdf.

Baytown Sun, Baytown, Texas, Wednesday, September 5, 1973, Page 1. Author unknown.

Baytown Sun, Baytown, Texas, Thursday, September 6, 1973, Page 1. Author unknown.

Bevan, J., 2001: National Hurricane Center Tropical Cyclone Report on Hurricane Keith, updated January 29, 2001. Published on the Web at http://www.nhc.noaa.gov/2000keith.html.

Beven, J.L. II and T. B. Kimberlain, 2009: Tropical Cyclone Report, Hurricane Gustav, (AL072008), 25 August- 4 September 2008. Available on the Web at: http://www.nhc.noaa.gov/pdf/TCR-AL072008_Gustav.pdf

Bove, M.C., J.B. Elsner, C.W. Landsea, X. Niu, and J.J. O'Brien, 1998: Effect of El Niño on U.S. landfalling hurricanes, revisited. *Bulletin of the American Meteorological Society*, **79**, 2477-2482.

Chen, Q., L. Wang, R. Tawes, 2008: Hydrodynamic response of northeastern Gulf of Mexico to hurricanes. *Estuaries and Coasts*, **31**, 1098-1116.

Chen, Q., L. Wang, H. Zhao, S.L. Douglass, 2007: Prediction of storm surges and wind waves on coastal highways in hurricane-prone areas. *Journal of Coastal Research*, **23**, 1304-1317.

Cho, Y-S., L. Chokkalingam, B.-H. Choi, T-M. Ha, 2008: Observations of run-up and inundation levels from the teletsunami in the Andaman and Nicobar Islands: A field report. *Journal of Coastal Research*, **24**, 216-223.

Cline, I.M., 1915: The tropical hurricane of September 29, 1915, in Louisiana. *Monthly Weather Review*, Sept 1915, 456-473.

Cline, I, 1926: *Tropical Cyclones*. Macmillon Company, 301 pp.

Clyburn, J., M. Darst, M.T. Waddell, and F. Wetta, 1989: A Furious Form of Wind: Hurricanes and Their Impact on Two Texas Coastal Cities. Included as Chapter 3, pages 3-1 to 3-12, in *Living on the Edge: Collected Essays on Coastal Texas,* edited by Stephen Curley, Department of General Academics, Texas A&M University, Galveston, Texas.

Coronas, J., 1922: Ten depressions or typhoons in the far East during the month of August, 1922. *Monthly Weather Review*, **50**, 435.

De, U.S., R.K. Dube, G.S. Prakasa Rao, 2005: Extreme weather events over India in the last 100 years. *Journal of Indian Geophysical Union*, **9**, 173-187.

De Scally, F.A., 2008: Historical tropical cyclone activity and impacts in the Cook Islands. *Pacific Science*, **62**, 443-459.

Department of Homeland Security, 2006: *Nationwide Plan Review Phase 2 Report*. Report published June 16, 2006 in cooperation with the U.S. Department of Transportation, found on the Web at: http://www.dhs.gov/xlibrary/assets/Prep_NationwidePlanReview.pdf

Dothan Eagle, Dothan, Alabama, Friday afternoon, September 1, 1950. Author unknown.

Dube, S.K., A.D. Rao, P.C. Sinha, T.S. Murty, N. Bahulayan, 1997: Storm surge in the Bay of Bengal and Arabian Sea: The problem and its prediction. *Mausam*, **48**, 283-304.

Dunn, G.E., and B.I. Miller, 1960: *Atlantic hurricanes*. The Louisiana State University Press. 326 pp.

Dunn, G.E. and Staff at U.S. Weather Bureau, 1962: The hurricane season of 1961. *Monthly Weather Review,* March 1962, 107-119.

Dunne, T., and L.B. Leopold, 1978: *Water in Environmental Planning*. Published by W.H. Freeman and Company, New York, 818pp.

Dunnavan, G.M., and J.W. Diercks, 1980: An analysis of Super Typhoon Tip (October 1979). *Monthly Weather Review*, **108**, 1915-1923.

Elsner, J.B., 1999: *Hurricanes of the North Atlantic: climate and society*. Oxford University Press. 488 pp.

Eslner, J.B., B.H. Bossak, and X.-F. Niu, 2001: Secular changes to the ENSO-U.S. hurricane relationship. *Geophysical Research Letters*, **28,** 4123-4126.

Elsner, J.B., and T.H. Jagger, 2005: Prediction Models for Annual U.S. Hurricane Counts. *Journal of Climate*, **19**, 12, 2935-2952.

Elsner, J.B., T.H. Jagger, and A.A. Tsonis, 2006: Estimated Return Periods for Hurricane Katrina. *Geophysical Research Letters*, **33**, 8, Article Number: L08704.

Elsner, J.B. and T. H. Jagger, 2007: Comparison of Hurricane Return Levels Using Historical and Geological Records. *Journal of Applied Meteorology and Climatology*, 47, 368-374.

Elsner, J.B., and T.H. Jagger, 2008: United States and Caribbean tropical cyclone activity related to the solar cycle. *Geophysical Research Letters*, **35**, L18705, doi: 10.1029/2008GL034431.

Elsner, J.B., T.H. Jagger, M. Dickinson, and D. Rowe, 2008: Improving Multiseason Forecasts of North Atlantic Hurricane Activity. *American Meteorological Society*, **21**, 1209-1219.

Elsner, J.B., T.H. Jagger, and E.A. Fogarty, 2009: Visibility network of United States hurricanes. *Geophysical Research Letters*, **36**, L16702, doi: 10.1029/2009GL03929.

Faiers, G.E., B.D. Keim, and R.A. Muller, 1997: *Rainfall Frequency/ Magnitude Atlas for the South-Central United States*. SRCC Technical Report 97-1, published by the Southern Regional Climate Center, Department of Geography and Anthropology, Louisiana State University, Baton Rouge, Louisiana, 40 pp.

Frank, N.L., and S.A. Husain, 1971: Deadliest tropical cyclone in history. *Bulletin of the American Meteorological Society*, **52**, 438-&.

Garriott, E.B., 1900: West Indian hurricane of September 1-12, 1900. *Monthly Weather Review,* **28**, 371-378.

Gerrish, H.P., 1989: Preliminary Report, Hurricane Chantal, 30 July to 3 August 1989. Report published at the National Hurricane Center, Miami, Florida. Available on the Web at: http://www.nhc.noaa.gov/archive/storm_wallets/atlantic/atl1989-prelim/chantal/prelim03.gif

Global Climate Change Impacts in the United States report, 2009. The report was produced by an advisory committee chartered under the Federal Advisory Committee Act, for the Subcommittee on Global Change Research, and at the request of the U.S. Government. The report can be found on the Web at: http://downloads.globalchange.gov/usimpacts/pdfs/climate-impacts-report.pdf

Goldenberg, S.B., C.W. Landsea, A.M. Mestas-Nunez, and W.M. Gray, 2001: The recent increase in Atlantic hurricane activity: causes and implications. *Science*, **293**, 474-479.

Gray, W. M., 1998: The formation of tropical cyclones. *Meteorology and Atmospheric Physics*, **67**, 37-69.

Gray, W.M., 1975: Tropical cyclone genesis. Atmospheric science paper No. 234, Department of Atmospheric Science, Colorado State University, Fort Collins, CO.

Gray, W.M., 1975: Global view of tropical cyclone genesis. *Bulletin of the American Meteorological Society*, **56**, 322.

Gray, W.M., 1984: Atlantic seasonal hurricane frequency. Part I: El Niño and 30 mb quasi-biennial oscillation influences. *Monthly Weather Review*, **112**, 1649-1668.

Gunn, A.M., 2008: *Encyclopedia of disasters: environmental catastrophes and human tragedies*. Greenwood Press, 130-131.

Harris, L.D., 1963: Characteristics of the Hurricane Storm Surge. U.S. Weather Bureau, Technical Paper No. 48. Available on the Web at: http://www.csc.noaa.gov/hes/images/pdf/CHARACTERISTICS_STORM_SURGE.pdf

Hebert, P.J. and N.L. Frank, 1974: Atlantic Hurricane Season of 1973. *Monthly Weather Review*, **102**, 280-289.

Hebert, P.J., 1976: Atlantic Hurricane Season of 1975. *Monthly Weather Review*, **104**, 453-474.

Hershfield, D.M., 1961: *Rainfall frequency atlas of the United States for durations from 30 minutes to 24 hours and return periods from 1 to 100 years. Technical Paper No. 40,* Washington D.C.: National Weather Bureau, 115 pp.

Himoto, K., 2007: Risk of fire spread in densely built environments- a review emphasizing cities in Japan-. *Journal of Disaster Research*, **2**, 276-283.

Holland, G.J., 1997: The maximum potential intensity of tropical cyclones. *Journal of the Atmospheric Sciences*, **54**, 2519-2541.

Holland, G.J., and P.J. Webster, 2007: Heightened tropical cyclone activity in the North Atlantic: natural variability or climate trend? *Philisophical Transactions of the Royal Society,* **365**, 2695-2716.

Huff, F.A., and J.R. Angel, 1992:*Rainfall frequency atlas of the Midwest.* Bulletin 71, MCC Research Report 92-03. Published through the Midwestern Climate Center (NOAA), and Illinois State Water Survey, 141 pp.

Intelligencer, Doylestown, Pennsylvania, Monday, July 4, 1994, Page 41

Interagency Performance Evaluation Taskforce Report, 2006: Performance Evaluation of the New Orleans and Southeast Louisiana Hurricane Protection System, Draft Final Report of the Interagency Performance Evaluation Task Force. *U.S. Army Corps of Engineers*, Volume 1- Executive Summary and Overview, June 1, 2006.

Irish, J.L., D.T. Resio, J.J. Ratcliff, 2008: The influence of storm size on hurricane surge. *Journal of Physical Oceanography*, **38**, 2003-2013.

Islam, T., and R.E. Peterson, 2009: Climatology of landfalling tropical cyclones in Bangladesh, 1877-2003. *Natural Hazards*, **48**, 115-135.

Jagger, T.H., J.B. Elsner, and X. Niu, 2001: A dynamic probability model of hurricane winds in coastal counties of the United States. *Journal of Applied Meteorology*, **40**, 853-863.

Jagger, T.H., and J.B. Elsner, 2006: Climatology models for extreme hurricane winds near the United States. *Journal of Climate*, **19**, 3220-3236.

Jagger, T.H., J.B. Elsner, and M.A. Saunders, 2007: Forecasting US insured hurricane losses. Published in *Climate extremes and society,* by H.F. Diaz, and R.J. Murnane, Chapter 10, pgs. 189-208.

Jagger, T.H., and J.B. Elsner, 2008: Modeling tropical cyclone intensity with quantile regression, *International Journal of Climatology*, **29**, 1351-1361.

Jakobsen, F., M.H. Azam, M.M.Z. Ahmed, M. Mahboob-ul-Kabir, 2006: Cyclone storm surge levels along the Bangladeshi coastline in 1876 and 1960-2000. *Coastal Engineering Journal*, **48**, 295-307.

Jarvinen, B.J., and C.J. Neumann, 1985: An evaluation of the SLOSH storm surge model. *Bulletin of the American Meteorological Society*, **66**, 1408-1411.

Jones P.D., T. Jonsson, and D. Wheeler, 1997: Extension to the North Atlantic Oscillation using early instrumental pressure observations from Gibraltar and South-West Iceland. *International Journal of Climatology*, **17**, 1433-1450.

Jordan II, M.R., and C.A. Clayson, 2008: Evaluating the usefulness of a new set of hurricane classification indices. *Monthly Weather Review*, **136**, 5234-5238.

Kawai, H., 1999: Storm surge in Ise and Mikawa Bay caused by typhoon. *Proceedings of the Joint Meeting of the U.S.-Japan Cooperative Program in Natural Resources Panel on Wind and Seismic Effects*, *Journal Code: S0735A*, **31**, 320-332.

Keim, B.D. and G.E. Faiers, 2000: A comparison of techniques to produce quantile estimates of heavy rainfall in arid and mountainous environments: a test case in western Texas. *Journal of Arid Environments*, **44**, 267-275.

Keim, B., R. Muller, G. Stone, 2007: Spatiotemporal Patterns and Return Periods of Tropical Storm and Hurricane Strikes from Texas to Maine. *Journal of Climate*, **20**, 3498-3509.

Keim, B.D., and R.A. Muller, 2008: Overview of Atlantic Basin Hurricanes. Chapter 4, pp. 79-89, in: Walsh, P.J., S.L. Smith, L.E. Fleming, H.M. Solo-Gabrielle, W.H. Gerwick, *Oceans and Human Health*. Academic Press, Burlington, Massachusetts, 644 pp.

Keim, B.D., and R.A. Muller, 2009: *Hurricanes of the Gulf of Mexico*. Louisiana State University Press, 216 pp.

Kimberlain, T.B., and J.B. Elsner, 1998: The 1995 and 1996 North Atlantic hurricane seasons: A return of the tropical-only hurricane. *Journal of Climate*, **11**, 2062-2069.

Knabb, R.D. J.R. Rhome, and D.P. Brown, 2005: Tropical Cyclone Report, Hurricane Katrina, 23-30 August 2005. Report produced by the National Hurricane Center, Miami, Florida, and published on the Web at: http://www.nhc.noaa.gov/pdf/TCR-AL122005_Katrina.pdf

Knabb, R.D., J.R. Rhome, D.P. Brown, 2006: National Hurricane Center Tropical Cyclone Report on Hurricane Katrina. Published on the Web at: http://www.nhc.noaa.gov/pdf/TCR-AL122005_Katrina.pdf.

Kurian, N.P., N. Nirupama, M. Baba, K.V. Thomas, 2009: Coastal flooding due to synoptic scale, meso-scale and remote forcings. *Natural Hazards*, **48**, 259-273.

Kurtsweil, J.P., 1958: Narrative Report of Hurricane Ella. Report published as U.S. Weather Bureau Office Memorandum, Key West, Florida. Available on the Web at: http://www.nhc.noaa.gov/archive/storm_wallets/atlantic/atl1958/ella/preloc/psheyw.gif

Landsea, C.W., R.A. Pielke, Jr., A.M. Mestas-Nunez, and J.A. Knaff, 1999: Atlantic basin hurricanes: indices of climate changes. *Climatic Change*, **42**, 89-129.

Landsea, C.W., C. Anderson, N. Charles, G. Clark, J. Dunion, J. Fernandez-Partagas, P. Hungerford, C. Neumann, M. Zimmer, 2004: The Atlantic Hurricane Database Reanalysis Project: Documentation for 1851-1910 Alterations and Additions to the HURDAT database. Published in Murnane, R. J. and K.B. Liu, *Hurricanes and Typhoons: Past, Present and Future*, Columbia Press 2004. Landsea et. al contributed pgs 178- 221. This document is published on the Web at: http://www.aoml.noaa.gov/hrd/Landsea/rpibook-final04.pdf

Landsea, C., 2005: What is the complete list of continental U.S. landfalling hurricanes? *Atlantic Oceanographic and Meteorological Laboratory Hurricane Research Division,* Published on the Web at: http://www.aoml.noaa.gov/hrd/tcfaq/E23.html

Landsea, C., 2007: Record number of storms by basin. Table published on the Web through the Atlantic Oceanographic and Meteorological Laboratory, Hurricane Research Division at: http://www.aoml.noaa.gov/hrd/tcfaq/E10.html.

Landsea, C., C. Anderson, W. Bredemeyer, C. Carrasco, N. Charles, M. Chenoweth, G. Clark, J. Dunion, R. Ellis, J. Fernandez-Partagas, J. Gamache, D. Glenn, L. Hufstetler, C. Mock, C. Neumann, A. Santiago, D. Thomas, L. Woolcock, and M. Zimmer, 2008: Documentation of Atlantic Tropical Cyclones Changes in HURDAT. *Atlantic Oceanographic and Meteorological Laboratory,* Published on the Web at: http://www.aoml.noaa.gov/hrd/hurdat/metadata_19151920_new.html

Landsea, C., C. Anderson, W. Bredemeyer, C. Carrasco, N. Charles, M. Chenoweth, G. Clark, J. Dunion, R. Ellis, J. Fernandez-Partagas, S. Feuer, J. Gamache, D. Glenn, L.

Hufstetler, C. Mock, C. Neumann, R. Perez Suarez, R. Prieto, J. Sanchez-Sesma, A. Santiago, D. Thomas, L. Woolcock, and M. Zimmer, 2009: Documentation of Atlantic Tropical Cyclones Changes in HURDAT. Atlantic Oceanographic and Meteorological Laboratory, Hurricane Research Division, Re-Analysis Project. Published on the Web at: http://www.aoml.noaa.gov/hrd/hurdat/metadata_jun09.html

Larson, E., 1999: *Isaac's Storm.* Published by Crown Publishers, New York, New York. Copyright 1999. 323 pp.

Lawrence, M.B., 1978: Atlantic Hurricane Season of 1977. *Monthly Weather Review*, **106**, 534-565.

Lawrence, M, and H. Cobb, 2005: National Hurricane Center Tropical Cyclone Report on Hurricane Jeanne, updated January 7, 2005. Published on the Web at http://www.nhc.noaa.gov/pdf/TCR-AL112004_Jeanne.pdf.

Li, C.X., D.D. Fan, B. Deng, V. Korotaev, 2004: The coasts of China and issues of sea level rise. *Journal of Coastal Research*, Special Issue, Summer 2004, **43**, 36-49.

Lichtblau, S., 1958: Report on Tropical Storm Ella Sept. 3 to 6, 1958, in the Gulf of Mexico. Report published by the National Weather Bureau. Available on the Web at: http://www.nhc.noaa.gov/archive/storm_wallets/atlantic/atl1958/ella/preloc/pshnew.gif

Makino, M., 1992: On a risk analysis of storm surges. *Journal of Wind Engineering and Industrial Aerodynamics*, **44**, 2523-2534.

Manderson, E., (date of publication unknown): Florida's Historical Hurricanes, published online by the International Hurricane Research Center, found on the Web at: http://www.ihrc.fiu.edu/about_us/historical_hurricanes.htm

McDonald, W.F., 1935: The hurricane of August 31 to September 6, 1935. *Monthly Weather Review*, **63**, 269-272.

McTaggart-Cowan R., G.D. Deane, L.F. Bosart, C.A. Davis, T.J. Galarneau, Jr., 2008: Climatology of tropical cyclogenesis in the North Atlantic (1948-2004). *Monthly Weather Review*, **136**, 1284-1304.

Mestre, O., and S. Hallegatte, 2008: Predictors of Tropical Cyclone Numbers and Extreme Hurricane Intensities over the North Atlantic Using Generalized Additive and Linear Models. *Journal of Climate*, **22**, 633-648.

Mitchell, C.L., 1926: The West Indian Hurricane of September 14-22, 1926. *Monthly Weather Review,* **54** (10). Available on the Web at: http://www.aoml.noaa.gov/general/lib/lib1/nhclib/mwreviews/1926.pdf

Monthly Weather Review. Index of 1872-2006 data available through NOAA's Atlantic Oceanographic and Meteorological Laboratory at the following link: http://www.aoml.noaa.gov/general/lib/lib1/nhclib/mwreviews/

Mozeney, R.P., 1960: Tropical Low Report for June 23-24. Report published by the National Weather Bureau. Available on the Web at: http://www.nhc.noaa.gov/archive/storm_wallets/atlantic/atl1960/td1/preloc/pshcrp.gif

Murnane, R.J. and K-B. Liu, editors, 2004: *Hurricanes and typhoons, past, present and future.* Columbia University Press. Pages 178-221 publish research provided by Landsea, C.W., C. Anderson, N. Charles, G. Clark, J. Dunion, J. Fernandez-Partagas, P. Hungerford, C. Neumann, and M. Zimmer, titled, *The Atlantic Hurricane Database Re-analysis Project: Documentation for 1851-1910 Alterations and Additions to the HURDAT Database.* This publication is available on the Web at: http://www.aoml.noaa.gov/hrd/Landsea/rpibook-final04.pdf

Murty, T.S., R.A. Flather, R.F. Henry, 1986: The storm-surge problem in the Bay of Bengal. *Progress in Oceanography*, **16**, 195-233.

National Hurricane Center, Miami, Florida, 1979: Preliminary Report, Hurricane Bob, 9-16 July, 1979. Author only identified by initials, "GBC." Available on the Web at: http://www.nhc.noaa.gov/archive/storm_wallets/atlantic/atl1979-prelim/bob/prelim01.gif

National Hurricane Center, Miami, Florida, 1980: Report on Tropical Storm Danielle, 4-7 September 1980. Author unknown. Available on the Web at: http://www.nhc.noaa.gov/archive/storm_wallets/atlantic/atl1980-prelim/danielle/prelim02.gif

National Hurricane Center, Miami, Florida, 1980: Preliminary Report, Hurricane Jeanne, November 7-16, 1980. Author only identified by initials "JMP." Available on the Web at: http://www.nhc.noaa.gov/archive/storm_wallets/atlantic/atl1980-prelim/jeanne/prelim02.gif

National Hurricane Center, Miami, Florida, 1988: Preliminary Report, Hurricane Gilbert, 08-19 September 1988. Author only identified by initials, "GBC." Available on the Web at: http://www.nhc.noaa.gov/archive/storm_wallets/atlantic/atl1988-prelim/gilbert/prelim02.gif

National Hurricane Center, Miami, FL, Preliminary report on Hurricane Mitch, October 22- November 5, 1998. Published on the Web at http://www.nhc.noaa.gov/1998/mitch.html.

National Hurricane Center, Miami, Florida, 2002: The Saffir-Simpson Hurricane Scale (Text). Author: Unknown. Last Updated July 1, 2002. Published on the Web at: http://www.nhc.noaa.gov/aboutsshs_text.html

National Hurricane Center, Miami, Florida, 2004: Hurricane Charley Advisory Number 17…Correction. Forecaster: Lawrence. Advisory issued 11AM EDT, Friday, August 13, 2004. Published on the Web at: http://www.nhc.noaa.gov/archive/2004/pub/al032004.public.017.shtml?

National Hurricane Center, Miami, FL, Tropical Cyclone Report on Hurricane Katrina, 23-30 August 2005. Published on the Web at: http://www.nhc.noaa.gov/pdf/TCR-AL122005_Katrina.pdf.

National Hurricane Center, Miami, Florida, 2008: Hurricane Gustav Intermediate Advisory Number 27A. Forecaster: Beven. Advisory issued 7AM CDT, Sunday, August 31, 2008. Published on the Web at: http://www.nhc.noaa.gov/archive/2008/al07/al072008.public_a.027.shtml?

National Hurricane Center, Miami, Florida, 2009: Archive of Hurricane Seasons. Tropical cyclone reports available on the Web at: http://www.nhc.noaa.gov/pastall.shtml

National Oceanic and Atmospheric Administration (NOAA), 1999: NOAA releases century's top weather, water and climate events. Published on the Web at: http://www.noaanews.noaa.gov/stories/s334.htm.

National Oceanic and Atmospheric Administration (NOAA), Earth System Research Laboratory- Physical Sciences Division, 2010: Sea Surface Temperature (SST) data available through the Atlantic Multidecadal Oscillation (AMO) index, published on the Web at: http://www.esrl.noaa.gov/psd/data/timeseries/AMO/

National Oceanic and Atmospheric Association, Climate Program Office, Regional Integrated Sciences and Assessments Website, as of February 23, 2010, found at http://www.climate.noaa.gov/cpo_pa/risa/

National Oceanic and Atmospheric Administration (NOAA), Tides and Currents Website. Data available through tabular and graphical form at the following Web site: http://tidesandcurrents.noaa.gov/

National Public Radio, 2005: Deadly Hurricanes No Strangers to Gulf Coast. Author Unknown. Published on the Web at: http://www.npr.org/templates/story/story.php?storyId=4821848

National Weather Bureau, 1959: Preliminary report on Tropical Storm Beulah, June 15-18, 1959. Author unknown. Available on the Web at: http://www.nhc.noaa.gov/archive/storm_wallets/atlantic/atl1959/beulah/prenhc/prelim1.gif

National Weather Bureau, September 1969: Preliminary Report on Hurricane Camille. Author unknown, document published on the Web at: http://www.nhc.noaa.gov/archive/storm_wallets/atlantic/atl1969-prelim/camille/TCR-1969Camille.pdf.

National Weather Service, Brownsville, TX, 2009: Regional tropical cyclone history, published on the Web at: http://www.srh.noaa.gov/bro/

National Weather Service, Corpus Christi, TX, 2009: Regional tropical cyclone history, published on the Web at: http://www.srh.noaa.gov/crp/

National Weather Service Houston/ Galveston, TX, 2009: Regional tropical cyclone history, published on the Web at: http://www.srh.noaa.gov/hgx/

National Weather Service Key West, FL, 2009: Regional tropical cyclone history, published on the Web at: http://www.srh.noaa.gov/key/

National Weather Service Lake Charles, LA, 2009: Regional tropical cyclone history, published on the Web at: http://www.srh.noaa.gov/lch/

National Weather Service, Lake Charles, LA, 2003: Louisiana Hurricane History: Late 19th Century. Published on the Web at http://www.srh.noaa.gov/lch/research/lalate19hu4.php.

National Weather Service, Lake Charles, LA, 2003: Texas Hurricane History: Late 20th Century. Published on the Web at: http://www.srh.noaa.gov/lch/research/txlate20hur.php.

National Weather Service, Lake Charles, Louisiana, 2009: Louisiana Hurricane History. Author unknown. Available on the Web at: http://www.srh.noaa.gov/lch/research/lalate20hur2.php

National Weather Service, Lake Charles, LA, 2009: Louisiana Hurricane History. Author unknown. Available on the Web at: http://www.srh.noaa.gov/lch/research/lalate20hur3.php

National Weather Service Miami-South Florida, FL, 2009: Regional tropical cyclone history, published on the Web at: http://www.srh.noaa.gov/mfl/

National Weather Service Mobile/ Pensacola, 2009: Regional tropical cyclone history, published on the Web at: http://www.srh.noaa.gov/mob/

National Weather Service New Orleans/Baton Rouge, LA, 2009: Regional tropical cyclone history, published on the Web at: http://www.srh.noaa.gov/lix/

National Weather Service, Southern Region Headquarters, Available on the Web at: http://www.srh.noaa.gov/images/mfl/events/

National Weather Service Tallahassee, FL, 2009: Regional tropical cyclone history, published on the Web at: http://www.srh.noaa.gov/tlh/

National Weather Service Tampa Bay, FL, 2009: Regional tropical cyclone history, published on the Web at: http://www.srh.noaa.gov/tbw/

Neumann, C.J., B.R. Jarvinen, C.J. McAdie, J.D. Elms, 1993: *Tropical cyclones of the North Atlantic Ocean.* U.S. Department of Commerce, prepared by the National Climate Data Center, Asheville, North Carolina, 193 pp.

New Mexican, Santa Fe, New Mexico, Tuesday, June 6, 1995. Author unknown.

Nott, J., and M. Hayne, 2000: How high was the storm surge from Tropical Cyclone Mahina? North Queensland, 1899. *The Australian Journal of Emergency Management*, **15**, 11-13.

Panama City News-Herald, Panama City, Florida, September 27, 1953. Author unknown.

Parisi, F., and R. Lund, 2008: Return Periods of Continental U.S. Hurricanes. *Journal of Climate*, **21**, 2, 403-410.

Pasch, R.J., 1996: Preliminary Report, Hurricane Allison, 3-6 June 1995. Report published at the National Hurricane Center, Miami, Florida. Available on the Web at: http://www.nhc.noaa.gov/1995allison.html

Pasch, R.J., Florida, 1997: Preliminary Report, Tropical Storm Josephine, 4-8 October 1996. Report published at the National Hurricane Center, Miami, Florida. Available on the Web at: http://www.nhc.noaa.gov/1996josephin.html

Pasch, R.J., D.P. Brown, and E.S. Blake, 2004: Tropical Cyclone Report, Hurricane Charley, 9-14 August 2004. Available on the Web at: http://www.nhc.noaa.gov/pdf/TCR-AL032004_Charley.pdf

Pasch, R.J., D.P. Brown, and E.S. Blake, 2005: Tropical Cyclone Report, Hurricane Charley, 9-14 August 2004. Revised edition. Report produced by the National Hurricane Center, Miami, Florida, and published on the Web at: http://www.nhc.noaa.gov/pdf/TCR-AL032004_Charley.pdf

Raja, R., S.G. Chaudhuri, N. Ravisankar, T.P. Swarnam, V. Jayakumar, R.C. Srivastava, 2009: Salinity status of tsunami-affected soil and water resources of South Andaman, India. *Current Science,* **96**, 152-156.

Rappaport, E.N., 1994: Preliminary Report, Tropical Storm Alberto, 30 June – 7 July 1994. Report published at the National Hurricane Center, Miami, Florida. Available on the Web at: http://www.nhc.noaa.gov/archive/storm_wallets/atlantic/atl1994/alberto/prenhc/prelim03.gif

Rappaport, E.N, and J. Fernandez-Partagas, 1995: The deadliest Atlantic tropical cyclones, 1492-1994. *NOAA Technical Memorandum NWS NHC-47*, National Hurricane Center, Pgs. 1-41.

Rego, J.L., and C. Li, 2009: On the importance of the forward speed of hurricanes in storm surge forecasting: A numerical study. *Geophysical Research Letters*, 36, L07609.

Roberts, N.C., 1969: *Extreme Hurricane Camille, August 14th through 22nd, 1969*. Copyright: N.C. Roberts, 1969. 135 pp.

Ropelewski C.F., and P.D. Jones, 1987: An extension of the Tahiti-Darwin Southern Oscillation Index. *Monthly Weather Review*, **115**, 9, 2161-2165.

Saunders, M.A., and A.R. Harris, 1997: Statistical evidence links exceptional 1995 Atlantic hurricane season to record sea warming. *Geophysical Research Letters*, **24**, 1255-1258.

Saunders, M.A., R.E. Chandler, C.J. Merchant, and F.P. Roberts, 2000: Atlantic hurricanes and NW Pacific typhoons: ENSO spatial impacts on occurrence and landfall. *Geophysical Research Letters*, **27**, 8, 1147-1150.

Schencking, J.C., 2008: The Great Kanto Earthquake and the culture of catastrophe and reconstruction in 1920s Japan. *The Journal of Japanese Studies*, **34**, 295-331.

Simpson, R. H., A.L. Sugg, and Staff at National Hurricane Center, 1970: The Atlantic hurricane season of 1969. *Monthly Weather Review,* **98**, 293-306.

Smith, J.M., M.A. Cialone, T.V. Wamsley, T.O. McAlpin, 2010: Potential impact of sea level rise on coastal surges in southeast Louisiana. *Ocean Engineering*, **37**, 1, pgs. 37-47.

Solar Influences Data Analysis Center (SIDC), Brussels, Belgium. Monthly sunspot data available at the following Website: http://sidc.oma.be/sunspot-data/

Sparks, P., E.J. Baker, J. Belville, D.C. Perry, 1991: Hurricane Elena, Gulf Coast, August 29- September 2, 1985. Published in *Natural Disaster Studies, Volume Two*, National Academy Press, Washington D.C. Prepared for the Committee on Natural Disasters, Division of Natural Hazard Mitigation, Commission on Engineering and Technical Systems, National Research Council.

Spennemann, D.H.R., 1996: Nontraditional settlement patterns and typhoon hazard on contemporary Majuro Atoll, Republic of the Marshall Islands. *Environmental Management,* **20**, 337-348.

Sugg, A.L., 1967: The Hurricane Season of 1966. *Monthly Weather Review*, **95** (3), 131-142.

Sugg, A.L. and P.J. Hebert, 1969: The Atlantic Hurricane Season of 1968. *Monthly Weather Review*, **97** (3), pp. 225-255.

Sugg, A.L., and J.M. Pelissier, 1968: The hurricane season of 1967. *Monthly Weather Review*, **96**, 242-259.

Sumner, H.C., 1941: Hurricane of October 3-12 and Tropical Disturbance of October 18-21, 1941. *Monthly Weather Review*, October 1941. Available on the Web at: http://www.aoml.noaa.gov/general/lib/lib1/nhclib/mwreviews/1941.pdf

Tampa Tribune, Tampa, Florida, October 19, 1959. Author unknown.

Tannehill, I.R., 1944: *Hurricanes*. Princeton University Press. 269pp.

Texas Advanced Computing Center, 2007: From Katrina forward: Producing better storm surge forecasts. Published on the Web at: http://www.tacc.utexas.edu/research/users/features/dawson.php.

Times-Picayune, New Orleans, Louisiana, September 19, 1957. Author unknown.

Turpin, R.J.B, Lieutenant Commander, Royal Navy Exchange, 1982: Analysis of the Tropical Cyclone Threat at Key West. Published as section 3 of 5 in *Hurricane Havens Handbook for the North Atlantic Ocean*, available on the Web at: http://www.nrlmry.navy.mil/~cannon/tr8203nc/keywest/text/frame.htm

Unisys Weather, 2009: Hurricane Data Website, found on the Web at: http://www.weather.unisys.com/hurricane/index.html

USA Today, Texas Hurricane History. Date unknown. Author unknown. Published on the Web at: http://www.usatoday.com/weather/hurricane/history/whtexas.htm

U.S. Army Corps of Engineers, 1972: *History of Hurricane Occurrences along Coastal Louisiana*. U.S. Army Engineer District, New Orleans Corps of Engineers, New Orleans, Louisiana. 43 pp. text, 20 maps.

U.S. Army Corps of Engineers, Jacksonville District, 2006: *Herbert Hoover Dike Vs. New Orleans Leeves* [title misspelled]*: comparison information*. This fact sheet is published on the Web at: http://www.saj.usace.army.mil/Divisions/Everglades/Branches/HHDProject/DOCS/HHD/HHDFactSheet_ComparisonWeb.pdf

United States Geologic Survey (USGS), 2008: Largest and Deadliest Earthquakes by Year, Updated July 16, 2008. Published on the Web at: http://earthquake.usgs.gov/eqcenter/eqarchives/year/byyear.php.

Walton, T.L., 2005: Short term storm surge forecasting. *Journal of Coastal Research*, **21**, 421-429.

Wang, Y.H., I.H. Lee, D.P. Wang, 2005: Typhoon induced extreme coastal surge: A case study at northeast Taiwan in 1994. *Journal of Coastal Research*, **21**, 548-552.

Wilks, D.S., 1993: Comparison of three-parameter probability distributions for representing annual extreme and partial duration precipitation series. *Water Resources Research,* **29**, 10, 3543-3549.

Wilks, D.S., and R.P. Cember, 1993: *Atlas of Precipitation Extremes for the North-eastern United States and South-eastern Canada.* Publication No. RR 93-5, Ithaca, New York: North-east Regional Climate Center, 40 pp.

Williams, J.M., and I.W. Duedall, 1997: *Florida hurricanes and tropical storms, revised edition.* University of Florida Press, copyright 1997 by Florida Sea Grant Program, 146 pp.

Williams, J.M., and I.W. Duedall, 2002: *Florida hurricanes and tropical storms, 1871-2001*. University of Florida Press. 167 pp.

Wyss, W., and S. Yim, 1996: Vulnerability and adaptation of Hong Kong to hazards under climatic change conditions. *Water, Air and Soil Pollution,* **92**, 181-190.

Zebrowski, E., and J. Howard, 2005: *Category 5: The story of Camille, lessons unlearned from America's most violent hurricane*. The University of Michigan Press. 276 pp.

Zerger, A., 2002: Examining GIS decision utility for natural hazard risk modeling. *Environmental Modelling & Software*, **17**, 287-294.

APPENDIX A: STORM SURGE DATABASE SOURCES

A.1: Government publications utilized for historical storm surge research.

Source and Location	Data Date(s)	Publication Date(s)
National Hurricane Center, Archive of Hurricane Seasons (Website)	1958-2009	Current
Monthly Weather Review (Index available on Website)	1872-2006	Current
National Oceanic and Atmospheric Administration (NOAA) Tides and Currents (Website)	Depends on tidal gauge	Current
HURDAT Re-analysis (until 1925) See Landsea (2009)	1851-1925	2009
HURDAT Re-analysis (until 1920) See Landsea (2008)	1851-1920	2008
HURDAT Re-analysis (until 1910) See Landsea (2004)	1851-1910	2004
Harris, D.L., Characteristics of the Hurricane Storm Surge Technical Paper No. 48 (Weather Bureau)	1926-1961	1963
Hurricane Elena, Gulf Coast, August 29- September 2, 1985; Prepared by Peter Sparks et al (1991)	1985	1991
Turpin, R.J.B., Analysis of the Tropical Cyclone Threat at Key West. Published in *Hurricane Havens Handbook for the North Atlantic Ocean*, through the Royal Navy Exchange	Variable	1982
U.S. Army Corps of Engineers, *History of Hurricane Occurrences along Coastal Louisiana*	1559-1971	1972

National Weather Service Southern Region Headquarters	Variable	Current
National Weather Service Brownsville, TX	Variable	Current
National Weather Service, Corpus Christi, TX	Variable	Current
National Weather Service Houston/ Galveston, TX	Variable	Current
National Weather Service Lake Charles, LA	Variable	Current
National Weather Service New Orleans/ Baton Rouge, LA	Variable	Current
National Weather Service Mobile, AL/ Pensacola, FL	Variable	Current
National Weather Service Tallahassee, FL	Variable	Current
National Weather Service Tampa Bay, FL	Variable	Current
National Weather Service Miami-South Florida, FL	Variable	Current
National Weather Service Key West, FL	Variable	Current

A.2: Books and online resources utilized for historical storm surge research.

Source	Publication Date
Baker et al., *The Social Impact of Hurricane Eloise on Panama City, Florida*	1976
Barnes, *Florida's Hurricane History, second edition*	2007
Cline, *Tropical Cyclones*	1926
Clyburn et al., *A Furious Form of Wind: Hurricanes and Their Impact on Two Texas Coastal Cities*	1989
Dunn and Miller, *Atlantic Hurricanes*	1960
Elsner, *Hurricanes of the North Atlantic: climate and society*	1999
Keim and Muller, *Hurricanes of the Gulf of Mexico*	2009
Manderson, *Florida's Historical Hurricanes*, published online by the International Hurricane Research Center	Unknown
Murnane and Liu, *Hurricanes and Typhoons, Past, Present, and Future*	2004
National Public Radio, Deadly Hurricanes No Strangers to Gulf Coast (Website)	2005
Roberts, N.C., *Extreme Hurricane Camille, August 14th through 22nd, 1969*	1969
Tannehill, *Hurricanes*	1944
USA TODAY, Texas Hurricane History (Website)	Unknown
Williams and Duedall, *Florida Hurricanes and Tropical Storms, Revised Edition*	1997
Williams and Duedall, *Florida Hurricanes and Tropical Storms, 1871-2001, Expanded Edition*	2002
Zebrowski and Howard, *Category 5: The story of Camille, lessons unlearned from America's most violent hurricane.*	2005

A.3: Newspapers utilized for historical storm surge database. These periodicals were ordered from libraries along the Gulf coast through the Interlibrary Loan program at Louisiana State University. This list does not include newspapers located online, such as the *New Mexican*, through websites such as www.newspaperarchive.com. Such periodicals were randomly found and seldom referenced, as they reported syndicated national stories. For a list of every source utilized to construct this database, please see the associated metadata file.

Periodical Title	Location
The Brownsville Herald	Brownsville, TX
The Corpus Christi Caller	Corpus Christi, TX
The Galveston Daily News	Galveston, TX
The Beaumont Enterprise	Beaumont, TX
The Lake Charles Daily Press	Lake Charles, LA
The Times-Picayune	New Orleans, LA
The Daily Herald	Biloxi, MS
The Mobile Register	Mobile, AL
The Pensacola Journal	Pensacola, FL
The Panama City News-Herald	Panama City, FL
The Saint Petersburg Times	Saint Petersburg, FL
The Tampa Tribune	Tampa, FL
The Fort Myers News-Press (or *Tropical News)*	Fort Myers, FL
The Naples Daily News	Naples, FL
Collier County News	Naples, FL
The Key West Citizen	Key West, FL

APPENDIX B: STORM SURGE DATABASE

B.1: The height and location of peak storm surges observed along the U.S. Gulf of Mexico coast, 1880-2009.

Rank	Surge (m)	Name	Year	Max Surge City/ Point/ Region	State
1	8.47	Katrina	2005	Pass Christian	MS
2	7.5	Camille	1969	Pass Christian	MS
3	6.1	“Labor Day”	1935	Long Key	FL
3	6.1	“Galveston”	1900	Galveston	TX
5	5.64	Carla	1961	Port Lavaca	TX
6	5.55	Eloise	1975	Dune Allen Beach	FL
7	5.49	Beulah	1967	South Padre Island	TX
8	5.33	Ike	2008	Chambers County	TX
9	5.18	“New Orleans”	1915	Southeastern LA, S of New Orleans	LA
10	4.88	Unnamed	1919	Corpus Christi (W shore Nueces Bay)	TX
10	4.88	“Cheniere Caminada”	1893	Cheniere Caminada (W of Grand Isle)	LA
12	4.72	“Galveston”	1915	GLS seawall (Galveston?)	TX
13	4.66	Frederic	1979	Gulf State Park	AL
14	4.63	Betsy	1965	Pointe a la Hache	LA
15	4.57	Rita	2005	Cameron	LA
15	4.57	Ivan	2004	Destin, FL to Mobile, AL	FL/ AL
15	4.57	Unnamed	1945	Port Lavaca	TX
15	4.57	Unnamed	1910	Key West	FL
15	4.57	“Grand Isle”	1909	Terrebonne Bay/ Bayou Portage (N of	LA/ MS

				Pass Chris)	
15	4.57	“Indianola”	1886	Indianola	TX
21	4.48	Unnamed	1942	Matagorda and Port Lavaca	TX
22	4.27	Opal	1995	Florida Panhandle	FL
22	4.27	Unnamed	1947	Chandeleur Light	LA
22	4.27	“Great Miami”	1926	Bagdad	FL
22	4.27	Unnamed	1919	Cow Key	FL
22	4.27	Unnamed	1906	Galt, Santa Rosa County	FL
27	4.24	Audrey	1957	west of Cameron	LA
28	4.11	Donna	1960	Upper Matecumbe Key	FL
29	3.96	Gustav	2008	Southeast LA, near Bay Gardene	LA
29	3.96	Wilma	2005	SW Florida	FL
29	3.96	Flossy	1956	Ostrica Lock	LA
29	3.96	Unnamed	1933	S Padre Island	TX
33	3.85	Alicia	1983	San Luis Pass (between Freeport and Galveston)	TX
34	3.81	Terrebonne Parish	1926	Terrebonne Parish	LA
35	3.75	Lili	2002	Crewboat Channel (Calumet)	LA
36	3.66	Allen	1980	Port Mansfield	TX
36	3.66	Unnamed	1944	Naples	FL
36	3.66	"Great Miami"	1926	Fort Myers and Punta Rosa	FL

36	3.66	Unnamed	1886	Johnson's Bayou	LA
40	3.63	Georges	1998	Fort Morgan	AL
41	3.54	Unnamed	1916	Mobile	AL
42	3.47	Unnamed	1949	Houston Ship Channel (Harrisburg)	TX
43	3.35	Kate	1985	Cape San Blas	FL
44	3.32	Unnamed	1888	Southeastern LA	LA
45	3.2	“Tampa Bay”	1921	Tampa Bay	FL
46	3.05	Elena	1985	Apalachicola	FL
46	3.05	Alma	1966	New Port Richey to Cedar Key	FL
46	3.05	“Velasco”	1909	Galveston and Velasco	TX
46	3.05	Unnamed	1903	Apalachicola	FL
46	3.05	Unnamed	1896	Cedar Key	FL
46	3.05	Unnamed	1896	Fort Walton Beach	FL
46	3.05	Unnamed	1894	Big Bend region of FL Panhandle	FL
53	3.02	Unnamed	1941	Sargent	TX
54	2.83	Josephine	1996	Suwannee	FL
55	2.8	Celia	1970	Port Aransas Beach	TX
55	2.8	Unnamed	1916	Corpus Christi	TX
57	2.74	Dennis	2005	Apalachee Bay	FL
57	2.74	Betsy	1965	North Key Largo	FL
57	2.74	King	1950	Bahia Honda (bridge), E of Big Pine Key	FL
57	2.74	Unnamed	1910	S Padre Island	TX

57	2.74	Unnamed	1888	Cedar Key	FL
62	2.68	Unnamed	1929	Key Largo	FL
63	2.53	Isidore	2002	Rigolets, LA and Gulfport Harbor, MS	LA/ MS
64	2.44	Bret	1999	Port Mansfield Pass	TX
64	2.44	Frances	1998	Matagorda Locks	TX
64	2.44	Earl	1998	Northwest FL- Big Bend area E of Apalach	FL
64	2.44	Allison	1995	Wakulla through Dixie Counties	FL
64	2.44	Andrew	1992	Cocodrie	LA
64	2.44	Juan	1985	Cocodrie	LA
64	2.44	Danny	1985	South Central LA Coast	LA
64	2.44	Edith	1971	Vermillion & Cote Blanche Bays	LA
64	2.44	Easy	1950	Clearwater to Sarasota	FL
64	2.44	Unnamed	1941	St. Marks	FL
64	2.44	Unnamed	1923	Biloxi	MS
64	2.44	Unnamed	1901	Port Eads and Mobile	LA/ AL
76	2.41	Debra	1959	Morgan Point	TX
77	2.38	Hilda	1964	Cocodrie	LA
77	2.38	Unnamed	1917	Fort Barrancas	FL
79	2.29	Unnamed	1921	West Bay (N side of W Galveston Island)	TX
80	2.26	Flossy	1956	Laguna Beach	FL

81	2.13	Charley	2004	Sanibel and Estero Islands	FL
81	2.13	Erin	1995	just west of Navarre Beach	FL
81	2.13	Andrew	1992	Goodland	FL
81	2.13	Jerry	1989	Baytown	TX
81	2.13	Chantal	1989	High Island	TX
81	2.13	Delia	1973	Galveston Bay	TX
81	2.13	Agnes	1972	Cedar Key and Port St. Joe	FL
81	2.13	Ethel	1960	Quarantine Bay	LA
81	2.13	Florence	1953	Panacea	FL
81	2.13	Unnamed	1942	High Island	TX
81	2.13	Unnamed	1934	Galveston Island	TX
81	2.13	Unnamed	1929	Seadrift	TX
81	2.13	Unnamed	1918	Creole	LA
81	2.13	Apalachicola	1915	Carrabelle	FL
81	2.13	Unnamed	1909	S Padre Island	TX
81	2.13	Unnamed	1886	Sabine Pass	TX
97	1.99	Ida	2009	Bay Gardene	LA
97	1.99	Danny	1997	HWY 182W, b/t Gulf Shores & Fort Morgan	AL
99	1.98	Gladys	1968	Homosassa	FL
99	1.98	Unnamed	1932	Mobile	AL
99	1.98	Unnamed	1931	Frenier	LA
102	1.95	Unnamed	1940	Frenier	LA
103	1.92	Bob	1979	Gulfport and Harrison County CD	MS

104	1.83	Alberto	2006	Homosassa	FL
104	1.83	Cindy	2005	SE LA, MS, Lakes Borgne & Pont	MS/ LA
104	1.83	Frances	2004	Pinellas County	FL
104	1.83	Claudette	2003	Matagorda Island (just E of Port O'Connor)	TX
104	1.83	Georges	1998	Florida Keys	FL
104	1.83	Lili	1996	Florida Keys	FL
104	1.83	Keith	1988	Bradenton and Fort Meyers	FL
104	1.83	Gilbert	1988	S Padre Island	TX
104	1.83	Florence	1988	Bayou Bienvenue	LA
104	1.83	Chris	1982	Cameron Parish	LA
104	1.83	Carmen	1974	South Central LA Coast	LA
104	1.83	Fern	1971	Freeport	TX
104	1.83	Debbie	1965	Industrial Canal in New Orleans	LA
104	1.83	TS #1	1965	Apalachicola (in vicinity)	FL
104	1.83	Dora	1964	Yankeetown	FL
104	1.83	TS Brenda	1955	Shell Beach	LA
104	1.83	How	1951	Fort Myers Beach	FL
104	1.83	Unnamed	1948	Key West	FL
104	1.83	Unnamed	1948	MS Coast	MS
104	1.83	Unnamed	1946	Punta Gorda to Bradenton	FL
104	1.83	Unnamed	1943	Chef Menteur	LA

104	1.83	Unnamed	1936	Fort Walton Beach, Panama City, Valparaiso	FL
104	1.83	Unnamed	1929	Panama City to Apalachicola	FL
104	1.83	Unnamed	1920	Lake Borgne and Mississippi Sound	MS/ LA
104	1.83	Unnamed	1912	Point Isabel	TX
104	1.83	Unnamed	1909	S Padre Island	TX
104	1.83	Unnamed	1897	Sabine Pass	TX/ LA
104	1.83	Unnamed	1886	Indianola	TX
132	1.78	Matthew	2004	Frenier	LA
133	1.74	Debra	1978	Atchafalaya Bay to Vermillion Bay	LA
134	1.71	Abby	1968	Everglades City	FL
135	1.69	Bill	2003	Bayou Bienvenue	MS
136	1.68	Beryl	1988	Bayou Bienvenue	LA
136	1.68	Anita	1977	Port Isabel Coast Guard Station/ S. Padre Is.	TX
136	1.68	Baker	1950	Pensacola	FL
136	1.68	Unnamed	1947	Everglades City	FL
136	1.68	Unnamed	1936	Everglades City	FL
141	1.58	Bonnie	1986	Sabine Pass	TX
142	1.55	Hanna	2002	Gulfport Harbor	MS
142	1.55	Gabrielle	2001	Charlotte County	FL
144	1.52	Fay	2008	Everglades City	FL
144	1.52	Rita	2005	Key West	FL
144	1.52	Emily	2005	S Padre Island	TX

144	1.52	Arlene	2005	Walton County	FL
144	1.52	Gordon	2000	Tampa Bay to Cedar Key	FL
144	1.52	Alberto	1994	Okaloosa Island to Destin	FL
144	1.52	Claudette	1979	Sabine Coast Guard Station	TX
144	1.52	Babe	1977	Southeastern LA	LA
144	1.52	Inez	1966	Big Pine Key	FL
144	1.52	Alma	1966	Fort Myers Beach	FL
144	1.52	Isbell	1964	Key West	FL
144	1.52	Esther	1957	MS Coast	MS
144	1.52	TS Hazel	1953	Everglades City	FL
144	1.52	Unnamed	1945	Key Largo	FL
144	1.52	Unnamed	1945	Tampa (Garcia Avenue Bridge)	FL
144	1.52	"Labor Day"	1935	Cedar Key	FL
144	1.52	Unnamed	1933	South Padre Island	TX
144	1.52	Unnamed	1933	Port Isabel	TX
144	1.52	“Freeport”	1932	Galveston	TX
144	1.52	Unnamed	1920	Tampa	FL
164	1.48	Humberto	2007	Texas Point TCOON Tide Gage	TX
165	1.43	Bertha	1957	west end of Vermillion Bay	LA
165	1.43	TS #1	1956	Biloxi	MS
167	1.4	Cindy	1963	Galveston	TX
168	1.37	Candy	1968	Palacios (Matagorda County)	TX

168	1.37	Gladys	1955	S Padre Island to Corpus Christi	TX
168	1.37	Unnamed	1924	Cedar Key	FL
168	1.37	Unnamed	1901	Galveston	TX
172	1.34	Unnamed	1912	Mobile	AL
173	1.25	Unnamed	1941	Everglades City	FL
174	1.22	Dolly	2008	S Padre Is., Port Mansfield, Brownsville	TX
174	1.22	Katrina	2005	Extreme SW FL	FL
174	1.22	Mitch	1998	Lower Florida Keys	FL
174	1.22	Gordon	1994	Upper FL Keys	FL
174	1.22	Arlene	1993	South and Central Texas Coast	TX
174	1.22	Floyd	1987	Lower and Middle Keys	FL
174	1.22	Jeanne	1980	South Texas Coast	TX
174	1.22	Abby	1964	Matagorda to Freeport	TX
174	1.22	Irene	1959	Cedar Key	FL
174	1.22	Ella	1958	Texas and Louisiana Coasts	TX/ LA
174	1.22	Debbie	1957	Apalachee Bay	FL
174	1.22	Unnamed	1947	Tampa; Anna Maria Island	FL
174	1.22	Unnamed	1947	Galveston (entrance of Galveston Channel)	TX
174	1.22	Unnamed	1943	Galveston	TX
174	1.22	Unnamed	1938	Cameron and Vermillion Parishes	LA

174	1.22	Unnamed	1934	Port O'Connor to Freeport	TX
174	1.22	Unnamed	1923	Apalachicola	FL
174	1.22	Unnamed	1916	Mobile	AL
174	1.22	Unnamed	1902	Central TX Coast	TX
174	1.22	Unnamed	1899	Carrabelle	FL

VITA

Hal Needham was born in October 1974, to Harold and Nancy Needham in Allentown, Pennsylvania. He was raised in Whitehall, Pennsylvania, and graduated from Whitehall High School in June 1993. He attended the Pennsylvania State University, where he received a Bachelor of Science degree in geography in May 1997. After graduation, he worked in Casablanca, Morocco, for several years in the field of cross-cultural education. He then worked as a geospatial technologist for both the Penn State University and the University of Alaska Fairbanks for several years before commencing graduate studies at Louisiana State University in August 2008. He is expected to receive his Master of Science degree in geography in May 2010.